TIP Channel Sounder Program Results Summary Report

mmWave Networks Project Group

Authors and Contributors

David Lai
NIST
chiehping.lai@nist.gov

Zahid Aslam
SIRADEL
ZAslam@siradel.com

Yoann Corre
SIRADEL
YCorre@siradel.com

Ioannis Chondroulis
Athens Information Technology (AIT)
icho@ait.gr

Fabian Undi
Fraunhofer HHI
fabian.undi@hhi.fraunhofer.de

Emmeric Tanghe
Ghent University – IMEC
emmeric.tanghe@ugent.be

Brecht De Beelde
Ghent University – IMEC
brecht.debeelde@ugent.be

Wout Joseph
Ghent University – IMEC
wout.joseph@ugent.be

Julius Kusuma
Facebook
jkusuma@fb.com

Ketaki Mangalmurti
Facebook
ketakipm@fb.com

Abhimanyu Gosain
Institute for the Wireless Internet of Things
at Northeastern University
agosain@coe.neu.edu

Sara Garcia Sanchez
Institute for the Wireless Internet of Things
at Northeastern University
garciasanchez.s@husky.neu.edu

Lorenzo Bertizzolo
Institute for the Wireless Internet of Things
at Northeastern University
bertizzolo@ece.neu.edu

Leonardo Bonati
Institute for the Wireless Internet of Things
at Northeastern University
bonati@ece.neu.edu

Michele Polese
Institute for the Wireless Internet of Things
at Northeastern University
m.polese@northeastern.edu

Halit Bugra Tulay
The Ohio State University
tulay.1@osu.edu

Tom Barratt
Blu Wireless
tom.barratt@bluwireless.com

Halit Bugra Tulay
The Ohio State University
tulay.1@osu.edu

Seth Goldstein
Telecom Infra Project
seth.goldstein@telecominfraproject.com

Anatolij Zubow
Technische Universität Berlin
anatolij.zubow@tu-berlin.de

Table of Contents

1 Executive Summary

This report is an output of the Channel Modeling subgroup within the Telecom Infra Project (TIP) mmWave Networks Project Group. It's the result of a collaboration between TIP members —academic institutions, operators, and equipment vendors—to contribute to the global knowledge base of millimeter wave channel characteristics through a set of detailed, controlled experiments. This report is a compilation of point-to-point measurement results from the Channel Sounder Program participants. Each participant explains the scope of their tests, including the topologies and test setup, measurement results, and conclusions.

1.1 Introduction to TIP Channel Sounder Program

The TIP Channel Sounder Program was launched in 2018 to support the characterization of the mmWave radio channel. This program supports the overall goals of the mmWave Networks Project Group to help facilitate the deployment of high-speed applications, such as Fixed Wireless Access, Smart City Connectivity, and Small Cell Backhaul with a focus on 60GHz spectrum and 802.11ad/802.1ay technologies for outdoor transmission at street-level.

Applicants to the program submitted proposals describing experiments that could be done to characterize the mmWave radio channel. Financial grants were made available to academic institutions to assist in offsetting costs associated with performing the channel measurements.

1.2 Program Details

The program provided V-Band 802.11ad/802.11ay-based "Channel Sounder Kits" to academic institutions and vendors for performing and collecting radio channel measurements. The kits were provided free of charge to qualified academic institutions that agreed to perform a standard set of measurements along with their own proposed unique set of tests. Program participants contributed the data to the National Institute of Standards and Technology (NIST) database, an open forum that can be freely accessed by the public.

The primary activities of the program included:

- Creating a reliable outdoor propagation model at 60GHz for Terragraph that could be an input to network planning tools
    - ✓ At varying terrain heights—street level, pole level, and roof level, considering obstructions at each height
- Understanding behavior of 60GHz link in different environmental conditions
    - ✓ Through free space, foliage, weather, natural and TG designed reflectors, and other naturally occurring environmental obstructions

- Understanding multipath, channel impulse response and delay spread
    - ✓ In indoor settings, urban canyons, and other reverberative conditions
- Explore new use-cases for V-band 802.11ad/ay

1.3 Program Participants

The participants in the program are (in alphabetical order):

- Athens Information Technology (AIT)
- Blu Wireless Technologies
- Deutsche Telekom (DT)
- Fraunhofer Institute for Telecommunications, Heinrich Hertz Institute (Fraunhofer HHI)
- Ghent University (UGent)
- National Institute of Standards and Technology (NIST)
- Northeastern University
- The Ohio State University (OSU)
- Siradel
- Technische Universität Berlin (TU Berlin)

1.4 About Telecom Infra Project (TIP)

The Telecom Infra Project (TIP) is a global community of companies and organizations that are driving infrastructure solutions to advance global connectivity. Half of the world's population is still not connected to the internet, and connectivity is often insufficient for those who are. This limits access to the multitude of consumer and commercial benefits provided by the internet, thereby impacting global GDP growth. However, a lack of flexibility in the current solutions—exacerbated by a limited choice in technology providers—makes it challenging for operators to efficiently build and upgrade networks.

Founded in 2016, TIP is a community of diverse members that includes hundreds of companies—from service providers and technology partners, to systems integrators and other connectivity stakeholders. We are working together to develop, test, and deploy open, disaggregated, and standards-based solutions that deliver the high-quality connectivity the world needs—both now and in the decades to come. Read more: www.telecominfraproject.com

2 Equipment, Measurements, and Data

2.1 Equipment

The V-Band 802.11ad/802.11ay-based Channel Sounder Kits distributed to participants included two retrofitted Terragraph radio nodes, called channel sounders, calibrated and loaded with firmware and software that enables the measurement of channel impulse response (CIR) and beam-scan path loss measured at different Tx–Rx beam-scan angles and combinations.

The Sounder in a Box is a customized pair of Terragraph (TG) nodes designed for measurement and modeling of 60GHz channels. The sounder is capable of measuring 60GHz characteristics such as the directional path loss and channel impulse response. Sounder technical specifications are listed below.

Max. EIRP	45dBm	
No. of Tx antennas	36x8	Individual on-off control
No. of Rx antennas	36x8	Individual on-off control
MCS	1–12	802.11ad
RF channel	1–3	802.11ad 58.32/60.48/62.64 GHz
Scanning range	-45° to 45°	Azimuth only
Min. beam width	2.8°	

Terragraph nodes are individually calibrated prior to shipping. Transmitter calibration ensures accurate EIRP over process and temperature variations. Receiver calibration translates the reported RSSI into the receive incident power and ensures stability over process and temperature variations.

Contact mmWave-info@telecominfraproject.com for more information about the equipment used.

2.2 Measurement modes

- Path loss
- Multipath characterization through pathloss over beam-scan angles
- Channel impulse response (CIR)

2.3 Access to data

NIST established the 5G mmWave Channel Model Alliance to promote fundamental research to better understand the characterization of millimeter-wave channel propagation channels in 2015. The alliance explores usage scenarios, parameters, frequencies, and architectures. It identifies gaps in channel measurement and modeling to promote new and improved channel measurement and modeling methodologies.

A summary of the Alliance's activities can be found here: https://www.nist.gov/ctl/5g-mmwave-channel-model-alliance

Where available, data and model measurements can be downloaded from the NIST 5G mmWave Channel Model Alliance (https://5gmm.nist.gov/), a NIST-hosted repository.

3 Test Cases and Scenarios of Interest

Tests were conducted in a number of settings, including:

- **Transmission in dense indoor environments** – Characterization of propagation in highly reflective, multipath settings such as industrial sites and operations in office environments.
- **Transmission loss through foliage** – Characterization of transmission loss through various types of foliage having varying moisture levels (dry, fresh, wet), at various distances, and with varying depth of foliage. Path loss is highly dependent on relative alignment between foliage and the transceivers, so averaging multiple measurements per test configuration provides the most accurate data.
- **Transmission loss in bad weather** – Characterization of transmission loss through adverse weather conditions (e.g., fog, rain, snow) should be comprehensively characterized. Care should be taken to isolate losses due to wetness at the surface of the transceivers from losses due to the environment in the transmission channel.
- **Reflection loss through natural reflectors** – Characterization of reflecting a transmitted signal off of buildings, walls, and other reflectors that exist naturally in urban environments. For this scenario, the line of sight (LOS) should be blocked to emphasize the reflected paths in the results. Reflection from multiple materials (e.g., wood, brick, concrete, glass, wet and dry) at multiple angles of incidence should be considered.
- **Reflection loss through artificial reflectors** – Characterization of the performance of intentionally-placed artificial reflectors in the urban environment to overcome losses due to foliage and other common blockers. One such example is a parabolic mirror, which can be placed on buildings and street fixtures to increase field of view and create alternate transmission paths.
- **Transmission loss through natural obstructions** – Characterization of transmission loss through different types of naturally occurring obstructions in outdoor environments, such as (but not limited to) various automobiles, traffic lights, poles, and billboards.
- **Transmission over different elevations** – Characterization of propagation when the transmitter and receiver are placed at different heights. In this case, emphasis is placed on understanding the multipath effect that may result from the link geometry.

Measurements campaigns were conducted in a variety of settings, as follows.

3.1 Indoor propagation

- AIT, BWRC, NIST, TU Berlin, OSU performed measurements in their labs to validate channel sounder kit performance [sections 4.1, 4.2, 4.6, 4.9, and 4.10]
- UGent – In dense industrial settings with machineries and significant multipath [section 4.5]
- NIST – In office settings, including reflection off- and propagation through glass [section 4.6]

3.2 Urban propagation

- AIT – In a university campus having tall buildings—including testing links off NLOS reflections, penetration through glass, and elevated (tilted) propagation [section 4.1]
- HHI, includes explorations of LOS and NLOS propagation when the path is obstructed by foliage and walls [section 4.4]
- DT/Siradel – In urban canyons in Deutsche Telekom's Berlin campus [section 4.8]

3.3 Suburban settings

- Blu Wireless – Measured propagation on streetlamp posts over time and quantified long-term variability due to weather conditions [section 4.3]
- DT/Siradel – In residential parts of Berlin, including parked vehicles and street signs [section 4.8]
- AIT – In a suburban residential setting where it emulated the use of wireless backhaul to connect from a legacy macro cellular site to a small, street-level cellular site. [section 4.1]

3.4 Rural propagation

- The Ohio State University (OSU) – Exploring LOS, NLOS, and blockage in agriculture settings, silos, and farm equipment. [section 4.9]

3.5 Mobility

- Northeastern PAWR – Includes user mobility and use of drone platforms to provide coverage enhancements. [section 4.7]

4 60GHz WiGig Measurements

4.1 Athens Information Technology (AIT)

AIT is a recognized non-profit scientific center of excellence in Greece. It has already proved its excellence and capabilities through its record number of attracted funds, research publications, and honors awarded to its staff. AIT has participated in more than 60 EU and national projects, very often in the role of scientific coordinator.

Broadband Wireless & Sensor Networks Research Group (B-WiSE)

The activities of AIT's Broadband Wireless & Sensor Networks (B-WiSE) Research Group are directed toward the design, study, and demonstration of smart, spectrally and energy-efficient wireless communications systems and networks ranging from body area to sensor to wide area and satellite networks. The group has hosted over three dozen researchers and graduate students since its inception in 2002. It's comprised of a research lab equipped with several wireless testbeds and software tools, including its own.

The group is active in many research communities and corresponding literature (with a large output of scientific journal/conference papers, books, and book chapters). Also, the group has run and participated in several collaborative research projects (mostly funded from the European Commission but also via national and industrial grants), collaborates with a large number of universities and companies (primarily in Europe), and has been internationally recognized as a recipient of number of honors and awards.

4.1.1 Test scope

Phase 1 Initial Measurements	**Phase 2** Outdoor Measurements at AIT facilities	**Phase 3** Outdoor Measurements at Cosmote facilities
Initial TIP indoor measurements were conducted by AIT in May – June 2019 at its office space to validate the get familiar with the TIP hardware and software and assess its proper operation.	The second measurement phase took place at AIT's Monumental Plaza facilities in July – August 2019. Several outdoor and indoor/outdoor scenarios were implemented to replicate the nodes' operation in an urban environment. A number of parameter sets were used, including a wide range of distance, angle, and gain values, as well as different antenna masks and reflection surfaces.	The third measurement phase involved the extension of outdoor measuring scenarios and was performed at Cosmote's premises in October 2019. Using its facilities and equipment, the nodes were placed at broad distances and heights to replicate a suburban environment.

4.1.2 Test setup

4.1.2.1 Phase 1 (indoor)

The first phase of measurements consisted of validation measurements conducted in AIT's meeting room for the distances of 2, 4, and 6m between the nodes as well as an additional indoor scenario with the nodes placed at AIT's main corridor at a distance of 20m from one another. Values of 5, 10, 15, and 20dB were used for the measured Tx gain levels. Two antenna mask configurations were used: the all-active mask, where all 36 columns are active (abbreviation: fff|fff|fff), and the middle-active mask, were the middle 12 columns are active (abbreviation: 000|fff|000). Both nodes were deployed as Tx and Rx for all scenarios.

The measurements' setup is shown in the pictures below:

Setup 1: 2 meters	Setup 2: 4 meters	Setup 3: 6 meters	Setup 4: 20 meters
		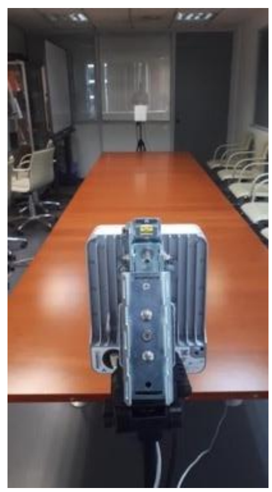	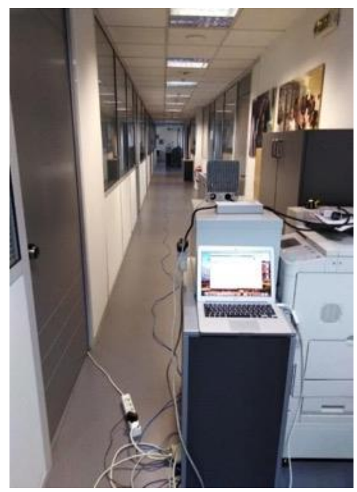

4.1.2.2 Phase 2 (urban, Smart City)

The second measurement phase consisted of several outdoor scenarios. The measurements were conducted at AIT's facilities to replicate mmWave communication scenarios in an urban environment. The team explored the vertical dimension, path loss through glass, and use of both LOS and N-LOS propagation. The goal was to exploit environment materials/surfaces as well as interference factors of a real-world setup. The deployed antenna masks are the ones previously used (all-active, middle-12-active), plus one where only the middle column (out of 36) is active (abbreviation: 000|020|000). Most measurements were conducted using 20 dB gain at the Tx, apart from the setups using the widest available beam where the Tx gain was set at 30 dB.

The scenarios implemented are listed below, followed by detailed descriptions for each one:

- Scenario 1: Building alley, equal height placement, LOS
- Scenario 2:
  - ✓ Setup 1: First floor to ground, window presence, LOS
  - ✓ Setup 2: First floor to ground, window presence, NLOS
- Scenario 3: Pole to different lampposts and tripod, LOS
- Scenario 4: Terrace to 1st floor, window presence, LOS
- Scenario 5:
  - ✓ Set 1: Building plaza, fountain between nodes, LOS
  - ✓ Set 2: Building plaza, obstacles between nodes, NLOS

Scenario 1: Building alley, equal height placement, LOS

Parameter	Description
	Basic scenario physical parameters
Indoor/ Outdoor	Outdoor
Shape	Open – alley
Dimensions/Site map	Alley total length: 100m, width: 10m
	
Node 1 location	On a pole, beside building C
	Height: 3.5m, pointing angle: toward node 2, scanning axis: azimuth (default)
Node 2 location	On a tripod, beside building C
	Height: 3.5m, pointing angle: toward node 1, scanning axis: azimuth (default)
Transmitter – receiver separation	Distance between nodes: 55m, direct path
	LOS
	Basic scenario materials

Description of walls in surrounding environment (if any)	Glass, marble
	8-story buildings
Ceilings	Open sky
Floors	Granite pavement
	Smooth level
Obstructions	Light pedestrian traffic below scanning level
Architectural details	Glass windows (with mirror effect), glass doors, marble columns and walls, metallic poles
	Reflective surrounding materials, smooth glass, dry pavement
Photographs	
 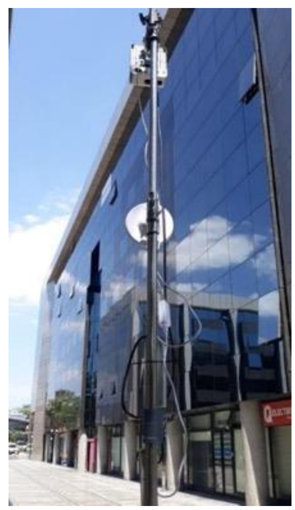	
Scene overview 	

Scenario 2: Floor to ground, window presence, LOS and NLOS

Setup 1: Floor to ground, window presence, LOS

Parameter	Description	
Basic scenario physical parameters		
Indoor/Outdoor	Node 1: Indoor, Node 2: Outdoor	
Shape	Node 1: First floor office room	Node 2: Open – Alley
Dimensions/ Site map	Node 1: On a tripod sitting on a 0.8m height bench, window dimensions: 1.5m (h) x 1.7m (w)	Node 2: Alley total length: 100m, width: 10m
	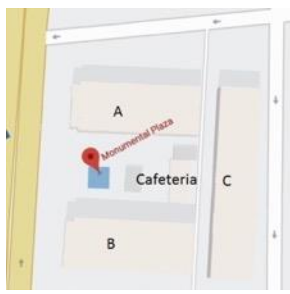	
Node 1 location	On a tripod sitting on a bench	
	Total height: 2m from the floor (tripod and bench), on the first floor, about 3.5m from the ground, pointing angle: through the window toward node 2, scanning axis: elevation	
Node 2 location	On a tripod, beside the cafeteria building	
	Height: 2.5m, pointing angle: toward node 1 on the first floor, scanning axis: elevation	
Transmitter – receiver separation	Distance between nodes: approx. 10m, direct path	
	LOS (through a glass window)	
Basic scenario materials		
Description of walls in surrounding environment (if any)	Node 1: plasterboard walls	Node 2: Glass, marble
	Node 1: wall height: 2.4m	Node 2: 8-story buildings
Ceilings	Node 1: cardboard paneled ceiling	Node 2: open sky

Floors	Node 1: Plastic floor	Node 2: Granite pavement
	Smooth level	
Obstructions	Glass window	
Architectural details	Node 1: Office environment	Node 2: Glass windows (with mirror effect), glass doors, marble columns and walls, metallic poles
	Node 1: Glass windows	Node 2: Reflective surrounding materials, smooth glass, dry pavement

Photographs

Scene overview

Setup 2: Floor to ground, window presence, NLOS

Parameter	Description
Basic scenario physical parameters Same as Set 1, apart from the nodes' pointing angle and Node 2 height	
Node 1 location	On a tripod sitting on a bench
	Total height: 2m from the floor (tripod and bench), on the first floor, about 3.5m from the ground, pointing angle: through the window toward the ground, scanning axis: elevation
Node 2 location	On a tripod, beside the cafeteria building
	Height: 1m, pointing angle: toward the ground, scanning axis: elevation
Transmitter – receiver separation	Distance between nodes: approx. 10m, ground reflection path
	NLOS (through a glass window)
Photographs	
	 

Scenario 3: Pole to different lampposts and tripod, LOS

Parameter	Description
Basic scenario physical parameters	
Indoor/ Outdoor	Outdoor
Shape	Open – alley
	Alley total length: 100m, width: 10m

Dimensions/ Site map	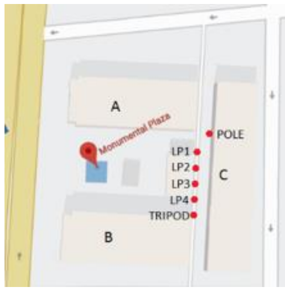
Node 1 location	On a pole beside building C
	Height: 2.7m, pointing angle: toward lamppost 2 (fixed alignment), scanning axis: azimuth (default)
Node 2 location	On four side-by-side poles and a tripod beside the cafeteria
	Height: 2.7m, pointing angle: toward node 1, scanning axis: azimuth (default)
Transmitter – receiver separation	Distance from Tx to each pole: 10, 15, 22, 30, 40m (approx.), direct path
	LOS
Basic scenario materials	
Description of walls in surrounding environment (if any)	Glass, marble
	8-story buildings
Ceilings	Open sky
Floors	Granite pavement
	Smooth level
Obstructions	Light pedestrian traffic below scanning level
Architectural details	Glass windows (with mirror effect), glass doors, marble columns and walls, metallic poles
	Reflective surrounding materials, smooth glass, dry pavement

<table>
<tr><th colspan="2">Photographs</th></tr>
<tr><td>Node 1
</td><td>Node 2
</td></tr>
<tr><td>
</td><td></td></tr>
<tr><td colspan="2">Scene overview

</td></tr>
</table>

Scenario 4: Terrace to 1st floor, window presence, LOS

<table>
<tr><th>Parameter</th><th colspan="2">Parameter description</th></tr>
<tr><td colspan="3">Basic scenario physical parameters</td></tr>
<tr><td>Indoor/Outdoor</td><td colspan="2">Node 1: Outdoor, Node 2: Indoor</td></tr>
<tr><td>Shape</td><td colspan="2">Node 1: Open – Terrace, Node 2: Office room on the first floor</td></tr>
<tr><td rowspan="2">Dimensions/Site-map</td><td>Node 1: On a short pole on a 1-story terrace (cafeteria)</td><td>Node 2: On a tripod sitting on a 0.8m height bench, window dimensions: 1.5m (h) x 1.7m (w)</td></tr>
<tr><td colspan="2">
</td></tr>
<tr><td rowspan="2">Node 1 location</td><td colspan="2">On a short pole on the edge of a terrace</td></tr>
<tr><td colspan="2">Pole height: 0.4, Terrace height: 2.5m, pointing angle: toward node 2, scanning axis: azimuth</td></tr>
<tr><td rowspan="2">Node 2 location</td><td colspan="2">On a tripod sitting on a bench</td></tr>
<tr><td colspan="2">Total height: 2m from the floor (tripod and bench), on the first floor about 3.5m from the ground, pointing angle: through the window toward node 2, scanning axis: azimuth</td></tr>
<tr><td rowspan="2">Transmitter – receiver separation</td><td colspan="2">Distance between nodes: approx. 12m, direct path</td></tr>
<tr><td colspan="2">LOS (through a glass window)</td></tr>
<tr><td colspan="3">Basic scenario materials</td></tr>
<tr><td rowspan="2">Description of walls in surrounding environment (if any)</td><td>Node 1: Glass, marble</td><td>Node 2: Plasterboard walls</td></tr>
<tr><td>Node 1: 8-story buildings</td><td>Node 2: Wall height: 2.4m</td></tr>
<tr><td>Ceilings</td><td>Node 1: Open sky</td><td>Node 2: Cardboard panels ceiling</td></tr>
<tr><td rowspan="2">Floors</td><td>Node 1: Granite floor</td><td>Node 2: Plastic floor</td></tr>
<tr><td colspan="2">Smooth level</td></tr>
<tr><td>Obstructions</td><td colspan="2">Glass</td></tr>
</table>

Architectural details	Node 1: Cafeteria terrace with granite floor	Node 2: Office environment
	Node 1: Glass windows (with mirror effect), glass doors, marble columns and walls, metallic poles, glass windows	Node 2: Reflective surrounding materials, smooth glass, dry pavement
Photographs		

Scene overview

Scenario 5

Setup 1: Building plaza, fountain between nodes, LOS

Parameter	Description
Basic scenario physical parameters	
Indoor/Outdoor	Outdoor
Shape	Open – Plaza
Dimensions/Site map	Alley total length: 50m, width: 35m

	
Node 1 location	On a lamppost beside building B
	Height: 3m, pointing angle: toward node 2, scanning axis: elevation
Node 2 location	On a tripod, beside building A
	Height: 3m, pointing angle: toward node 1, scanning axis: elevation
Transmitter – receiver separation	Distance between nodes: 24m, direct path and water reflection path
	LOS
Basic scenario materials	
Description of walls in surrounding environment (if any)	Glass, marble
	8-story buildings
Ceilings	Open sky
Floors	Granite pavement, water surface of fountain
	Smooth level pavement, calm and moving water surface
Obstructions	Light pedestrian traffic below scanning level
Architectural details	Glass windows (with mirror effect), glass doors, marble columns and walls, metallic poles
	Reflective surrounding materials, smooth glass, dry pavement, fountain

Photographs
Node 1 
Scene overview 

Setup 2: Building plaza, Obstacles between nodes, NLOS

Parameter	Description
Basic scenario physical parameters	
Indoor/Outdoor	Outdoor
Shape	Open – Plaza
Dimensions/Site map	Alley total length: 50m, width: 35m

	
Node 1 location	On a lamppost beside building B
	Height: 3m, pointing angle: toward node 2, scanning axis: azimuth
Node 2 location	On a tripod, beside building A
	Height: 3m, pointing angle: toward node 1, scanning axis: azimuth
Transmitter – receiver separation	Distance between nodes: 35m, direct path
	NLOS
Basic scenario materials	
Description of walls in surrounding environment (if any)	Glass, marble
	8-story buildings
Ceilings	Open sky
Floors	Granite pavement, water surface of fountain
	Smooth level pavement, calm and moving water surface
Obstructions	Cafeteria equipment: Over 3m umbrellas, foliage, objects below scanning level: metallic tables and chairs, flowerpots, etc.
Architectural details	Cafeteria plaza: glass windows (with mirror effect), glass doors, marble columns and walls, metallic poles
	Reflective surrounding materials, smooth glass

Photographs
 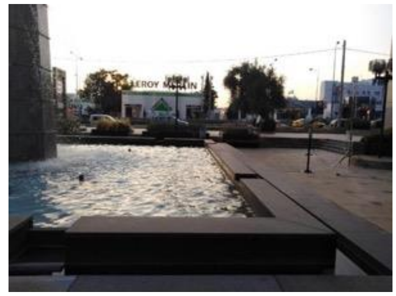
Scene overview 

4.1.2.3 Phase 3 (suburban, small cell backhaul)

The third measurement phase involved outdoor scenarios in a suburban environment, specifically a Cosmote facility parking lot. The Node 2 Tx was placed at 15 m. height on Cosmote's telecom mast. The Node 1 Rx was mounted on the roof of an SUV. Measurements were conducted over a range of 40–100m. Tx gain was set at 20 dB for all measurements. The antenna masks used the all-active configuration for the Tx and the middle-12-active for the Rx. Those were the first AIT outdoor measurements conducted in a cloudy, highly humid—with occasional light drizzle—environment.

Parameter	Description
Basic scenario physical parameters	
Indoor/Outdoor	Outdoor
Shape	Open – Parking lot
Dimensions/Site map	Measurement path length: 100m

	
Node 1 location	On the roof of an SUV
	Height: 2m, pointing angle: toward node 2, scanning axis: azimuth
Node 2 location	On a mast, approx. at the center of the lot
	Height: 15m, pointing angle: toward measurement path, scanning axis: azimuth
Transmitter – receiver separation	Distance between nodes: 40–100m, direct path
	LOS
Basic scenario materials	
Description of walls in surrounding environment (if any)	Glass windows
	Office buildings
Ceilings	Open sky
Floors	Concrete ground
Obstructions	N/A
Architectural details	Cars, trees, buildings
	Reflective surrounding materials, smooth glass

Photographs	
Node 1 	Node 2 
Scene overview  	

4.1.3 Results

Phases 1 and 2

Setup 1 (Free space path loss – 2m. (dB):74.09)

	Direction	Tx_Gain (dB)	n_stat	Antenna Mask	Path Loss Measured (dB)	Incident Power (dBm)	Post-EQ SNR
a	1 to 2	5	1	fff|fff|fff	72.31	−50.09	19
b	2 to 1	5	1	fff|fff|fff	73.46	−50.04	19
c	1 to 2	5	3	000|fff|000	70.56	−55.37	17
d	2 to 1	5	1	000|fff|000	69.23	−54.43	17

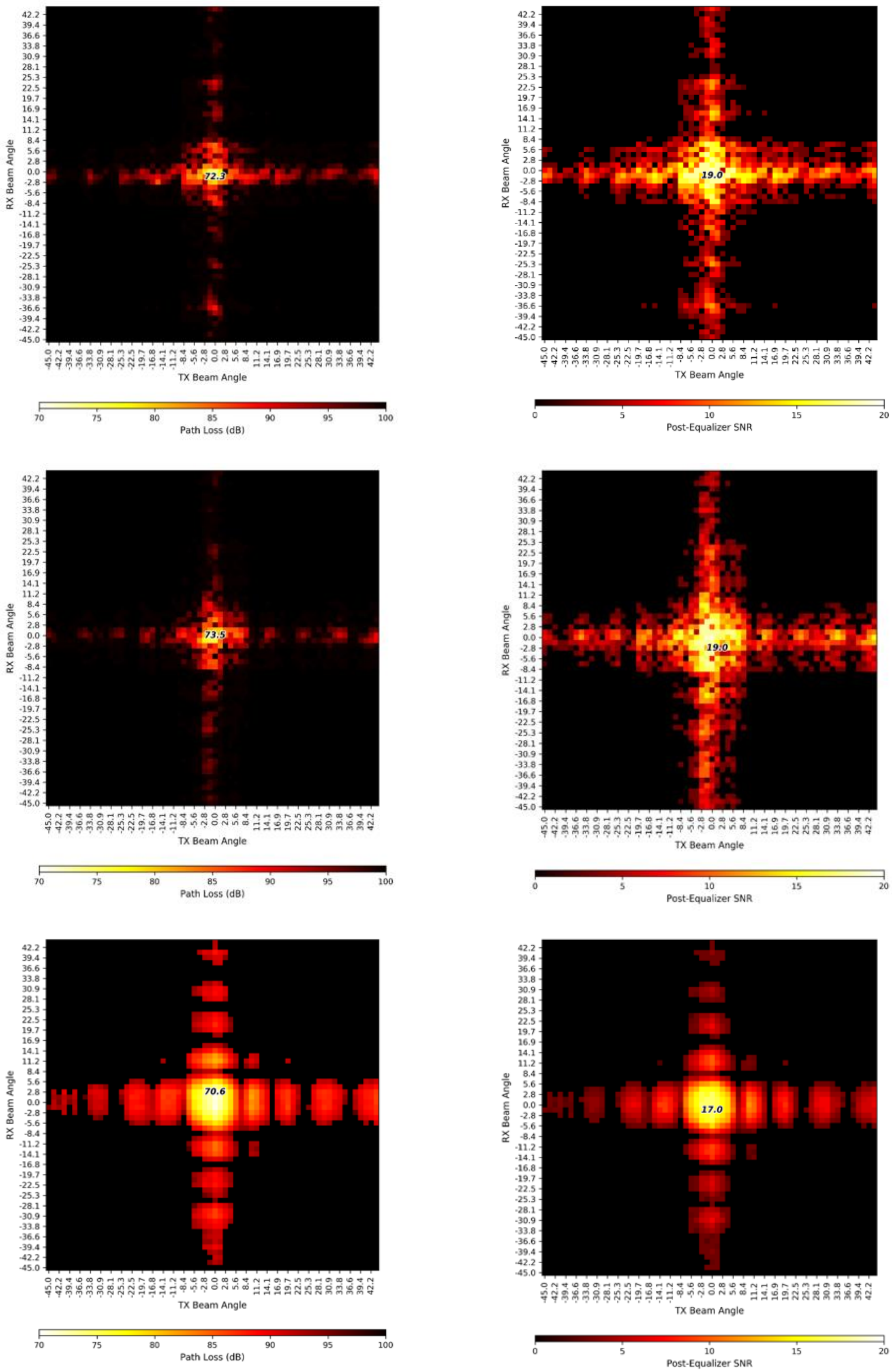
RX Beam Angle
TX Beam Angle
72.3
Path Loss (dB)
70 75 80 85 90 95 100
19.0
Post-Equalizer SNR
0 5 10 15 20
73.5
19.0
70.6
17.0

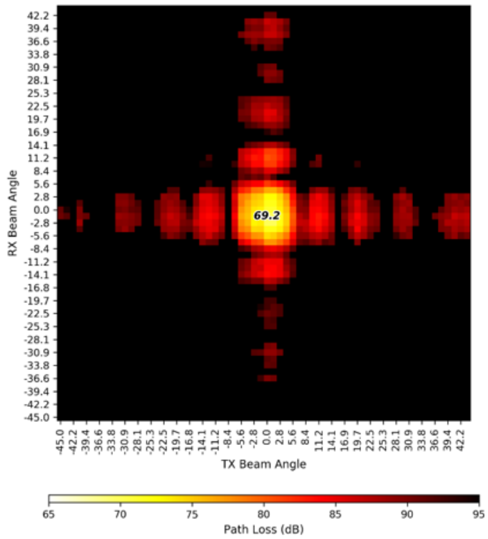

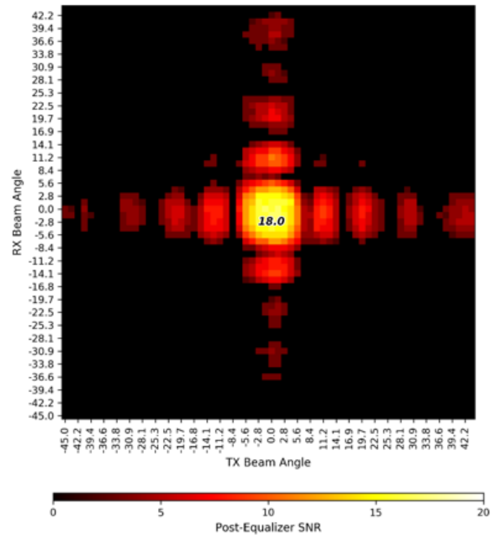

Setup 2 (free space path loss – 4m. (dB):80.11)

	Direction	Tx_Gain (dB)	n_stat	Antenna Mask	Path Loss Measured (dB)	Incident Power (dBm)	Post-EQ SNR
a	1 to 2	5	1	fff|fff|fff	77.65	−55.63	18
b	1 to 2	15	5	fff|fff|fff	79.49	−46.33	17.8
c	2 to 1	5	1	fff|fff|fff	78.04	−54.42	19
d	2 to 1	15	5	fff|fff|fff	78.45	−44.48	18
e	1 to 2	5	3	000|fff|000	75.52	−60.67	19
f	1 to 2	15	5	000|fff|000	76.57	−50.63	18.2
g	2 to 1	5	1	000|fff|000	76.26	−61.67	12
h	2 to 1	15	5	000|fff|000	76.13	−51.31	17.8

Phase 3

Setup 3

Both channel sounder nodes are oriented to scan vertically instead of horizontally. Node 2 is mounted on a cellular tower at 15m AGL; Node 1 is mounted on top of a vehicle as shown.

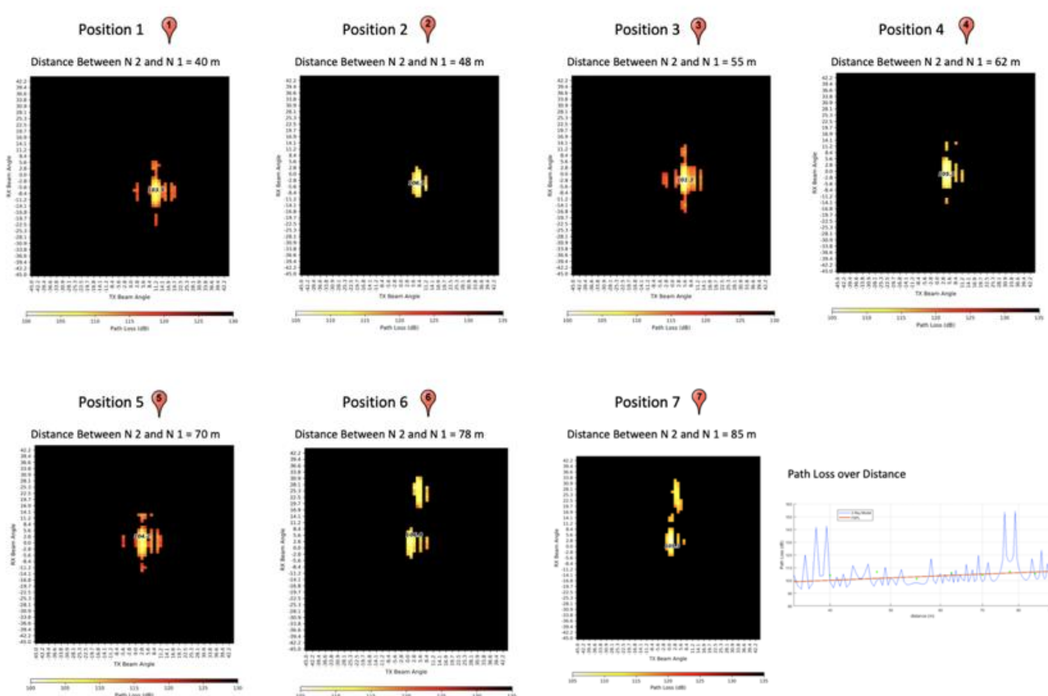

4.1.4 Findings

Phase 1

The initial measurement's goal was successfully achieved. The results were satisfying, as the path loss and received power levels approximate the results of the respective measurements conducted at Telefar. In some cases, the presence of constructive interference (produced by reflections) resulted in path loss values below the free space path loss mark.

As observed in results of setups 1 – 3, the cross-like formation in the heatmaps is due to the relatively short distance between the nodes. This effect occurs when the central beam of the Tx matches a wide set of Rx beams and vice versa. Reflection marks also are formed at the corners of the heatmaps; they're justified due to the reflective materials of the environment. The glass windows at the sidewall of the meeting room, as well as reflective objects on the interior bookcase, often result in double reflections (where Tx side beams match the Rx side beams across, and vice versa).

Saturation is another characteristic of short distance measurements. The signal is often saturated at the Rx for the direct path beam combinations, especially when higher gain levels are used.

For the 20m corridor measurements, resulting heatmaps were much more spread out when narrower beams were deployed—due to reflections produced by glass windows in the corridor. Compared to the heatmaps of previous setups, their irregular direction resulted in scattered reflection marks, due to a longer distance between nodes. In measurements where the wider beam configuration was used, Tx side beams were unable to reach the Rx and resulted in much more compact heatmaps.

Phase 2

The second measurement phase was an experimental real-world setup. In Scenario 1, a long-distance node communication in an urban environment was implemented. An optimal beam configuration for outdoor, long-distance measurements was established. Using the all-active mask with the narrowest beams for the Tx and the middle-12-active mask for the Rx, the lowest path loss values among the mask configurations was achieved. Moreover, successful links using the widest possible beams at the Rx were established. Due to the distance between nodes, high Tx gain levels were available for this configuration without exceeding the radiated power limits applied by the software. Buildings on each side of the alley caused the heatmap reflection marks.

An indoor-to-outdoor communication scheme was deployed in Scenario 2. Using the setup's environment, the extra path loss caused by window attenuation was measured, calculated at approximately 20dB. In the NLOS setup, the reflection path was strong enough to establish a link, with a loss of 4dB in the post-equalization SNR values and a 3 – 5dB loss in path loss values.

The third scenario implements a scheme where a fixed Tx successfully transmitted to multiple Rxs. With the Tx direction fixed toward the Rx on pole 2, all five Rx locations were served. Here an antenna mask combination was used, the Rx using the narrowest beam and the Tx using a wider beam. High path loss values were observed; these were approximately 20 dB higher than the free space path loss (FSPL) due to saturation. Taking the Tx–Rx distance into account, better path loss values can be achieved by decreasing Tx gain. However, the saturation effect didn't cause an impact to the SNR measurement, where high values were achieved (15 – 18 dB).

A real-world, fixed-wireless-access, Smart City communication scheme was implemented in scenario 4. Much like scenario 2, a window obstacle was deployed that produced similar deviation in path loss values. The outdoor node was placed on a terrace, with both nodes deployed as Tx and Rx in rotation. Successful links were established for both direct path and reflection path configurations.

In the last scenario of phase 2, the nodes were placed at the building complex plaza. In the fountain setup, the effect of turbulent water is portrayed on the heatmaps. Reflection marks on the calm water heatmaps are clearly smoother than on their turbulent water counterparts. In the second setup, certain beam combinations produced successful links, although high path loss and low SNR values were observed. The results were satisfying, considering that the NLOS setup included obstacles such as metallic furniture (tables, chairs, umbrellas) and foliage.

Phase 3

The third measurement phase took place in a suburban environment, where distance between nodes is usually larger than urban environments. The use of Cosmote's equipment (telecom mast, SUV) permitted node placement a range from 40 – 80 meters. The nodes were rotated by 90° to safely match Tx and Rx beams during the measurements, thus scanning the elevation axis (the beams were unable to be properly matched when scanning the azimuth due to the angle of the node positioning in the elevation). The path loss values approximately measured the FSPL values and high SNR values were produced for most cases.

4.2 Berkeley Wireless Research Center (BWRC)

Our focus at the Berkeley Wireless Research Center (BWRC) has been to understand how interference affects mmWave mesh network capacity. Our past work has been based in simulation and mathematical modeling. Availability of Terragraph nodes has given us the ability to perform measurements in the real-world.

Here we report preliminary experiments using Terragraph nodes inside the BWRC, followed by baseline experiments taking measurements in a relatively reflection-free outdoor environment. For the latter we used an active link and an interferer, measuring how the interferer affected the link's SNR quality. Future measurements will take place in outdoor environments using reflectors and scatterers—more typical of urban settings.

We observed two interesting and unexpected phenomena in our interference measurements:

- The active link degraded independent of where the interferer was electronically steered
- The active link's performance improved with interference present

These two phenomena have motivated us to substitute a custom node for the Terragraph receivers in future measurements.

Preliminary measurements – Indoor

Our preliminary indoor measurement experiments helped us gain experience with the set up and operation of Terragraph sounders. Being positioned close to a highly reflective glass divider panel, a node pair was configured in the BWRC common area as is shown in Figure 1.

Figure 1 – BWRC test setup

The standard Terragraph channel sounding software measures path loss by sweeping the receiver through its full steering range for each transmitter angle. Figure 2 shows a typical result of running the standard channel sounding script in our environment. As expected, both the LOS signal and reflected paths are apparent from the plot, as well as the reflection side lobes.

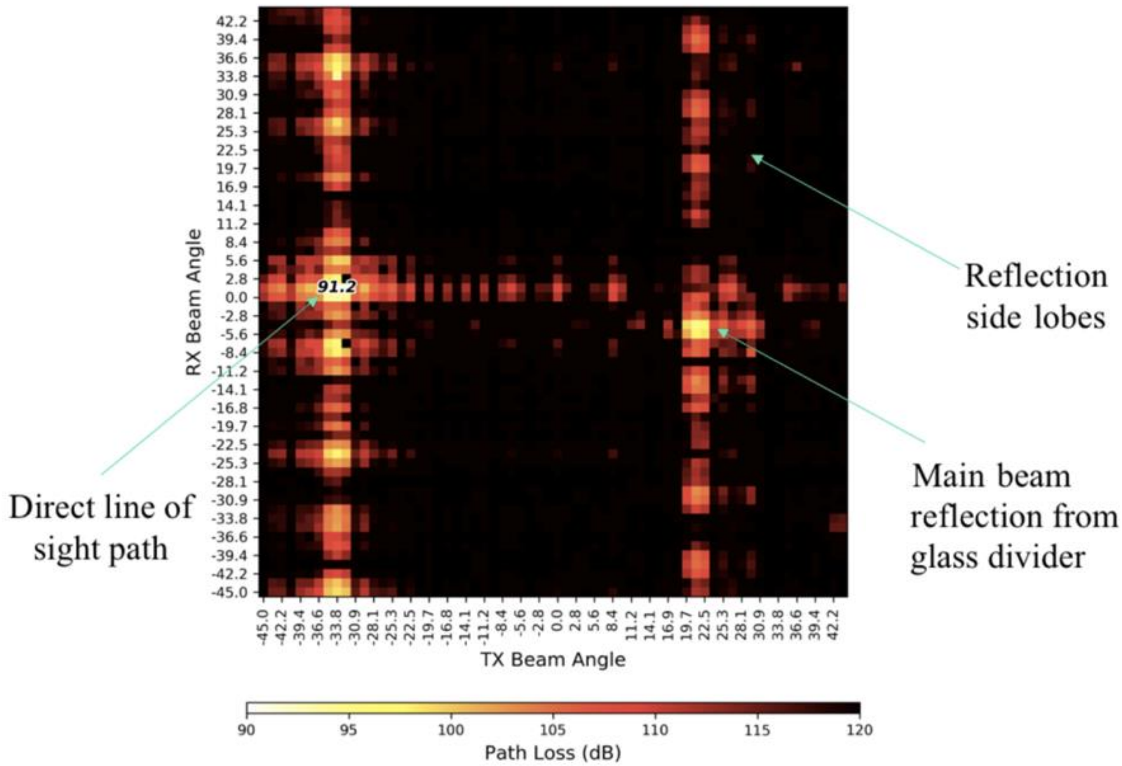

Figure 2 – Typical output of standard channel sounding script

Indoor measurements were taken when we didn’t yet have full understanding of node operation in terms of reported values and beam patterns. In hindsight we now understand that they were unfortunately taken with the power set too high. Even though the reported values were below saturation, there are problems when the RF gain index is equal to zero, leading to non-monotonicity. In addition, we discovered the beam patterns weren’t calibrated on a per node basis, but instead used a golden calibration. We only became aware of these issues later in an anechoic chamber, where we calibrated each node’s beam pattern and took measurements to ensure we understood which patterns we were actually using.

Baseline setup – Outdoor

For the baseline outdoor experiments, we sought a location free of physical features that could create reflections. An open field at the Richmond Field Station, a University of California research and storage facility, met these criteria. The site has no buildings, trees, or other features, thereby limiting possible reflections to the ground only.

Figure 3 – BWRC outdoor test site

Using telescoping tripods, the nodes were placed approximately 25 feet into the air to emulate real-world Terragraph deployments. Each pole consists of a Terragraph node and a Wi-Fi module (2.4 GHz) control network.

The test network configuration comprised three nodes placed one hundred feet from each other. Two acted as the intended link's transmitter, LinkTx, and the link's receiver, LinkRx, while a third served as an interfering transmitter. For all configurations, LinkRx was oriented to point to LinkTx, while Interferer and LinkTx were both pointed at LinkRx. To emulate a variety of configurations and geometric situations typical of real Terragraph deployments, measurements were taken at 45 degrees and 90 degrees between LinkTx <> LinkRx and Interferer <> LinkRx. They were obtained by physically moving the position of the latter.

Calibration

For each measurement angle, three sets of measurements were performed using combinations of active nodes. To differentiate the origin of received packets, the two transmitters, LinkRx and LinkTx, were configured to use disparate modulation and coding schemes (MCS). Packets were first sent between LinkTx and LinkRx to establish a no interference case between the two nodes. For this case, the best LinkTx-steered direction was determined and then LinkRx swept its beam.

Next, packets were sent between Interferer and LinkRx to establish what the receiver could see when its intended transmitter, LinkTx, is not active. Both the Interferer and LinkRx's beam are swept for this scenario.

For the final scenario, all three nodes were active; LinkTx kept a fixed beam, transmitting packets to LinkRx, while Interferer and LinkRx sweep their beams. (Superposition cannot be used in this case due to various concerns with the radio non-linearity of the AGC and limited dynamic range.)

The experiments were controlled, with results being displayed via custom BWRC-developed scripts. Performance was reported using SNR values calibrated by BWRC at Nokia Bell Lab's anechoic chamber. Unlike the indoor measurements, the outdoor measurements were taken with individually calibrated nodes in relation to both SNR and beam patterns.

45-degree interference measurements

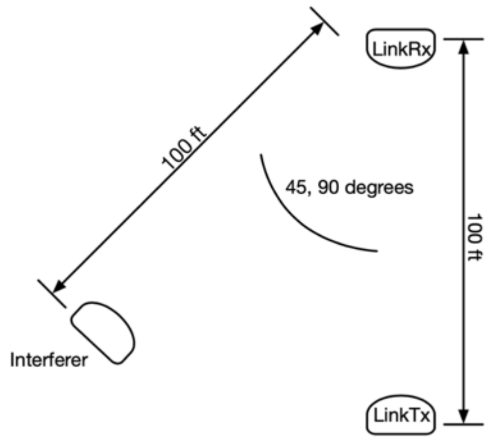

Figure 4 – 45° Test setup with Interferer

No interference

As expected, LinkTx to LinkRx has a nearly identical pattern as to the 90-degree case, as is apparent from Figure 5a. This result is to be expected, as neither of node moved and the rest of the environment remained relatively static.

Figure 5b shows packets being transmitted between Interferer and LinkRx. If superposition were to hold, we would expect interference to entirely follow the same cross pattern.

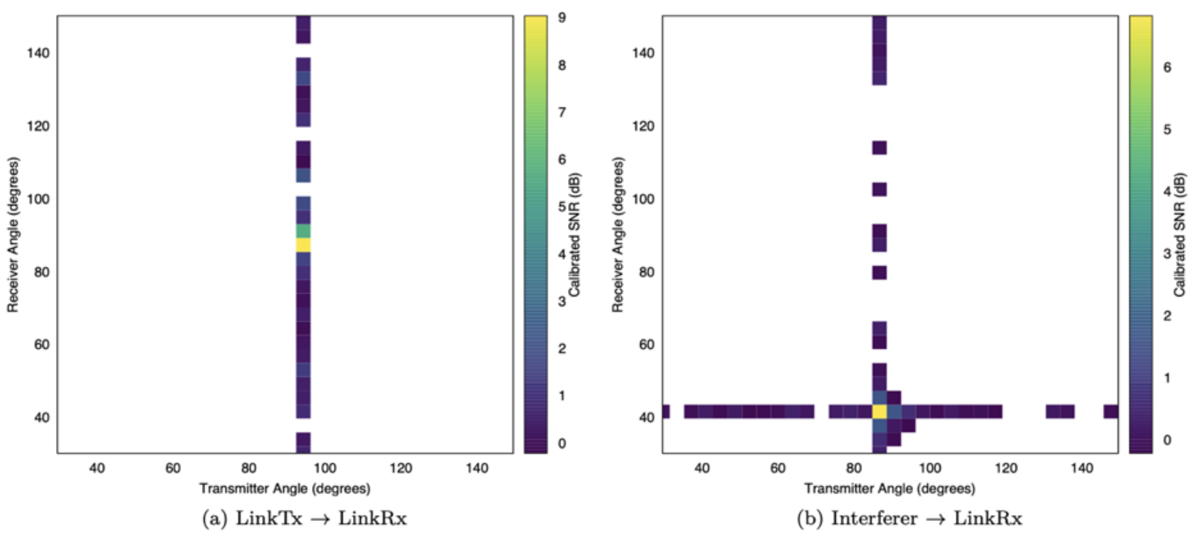

Figure 5 – 45°, one active link

With interference

For the interference case, we saw the same cross pattern—where either wrong packets would enter or packets would be corrupted due to SINR degradation (Figure 6b). However, with respect to the receiver, note there is a line near 90 degrees where the SINR and packet error rate improved by a small amount. It indicates that the link's quality actually improved with interference (Figure 7). This suggests that receiver functionalities such as gain control, phase resolution, and amplitude quantization can be sensitive to SINR degradation, thereby affecting measurement and link quality.

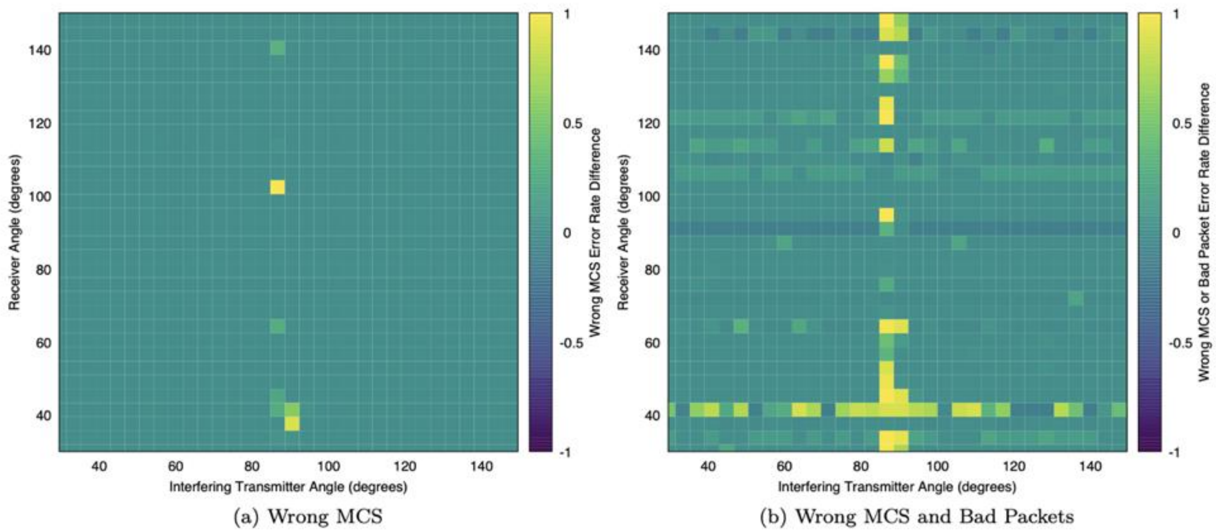

Figure 6 – 45°, bad MCS and corrupted packets

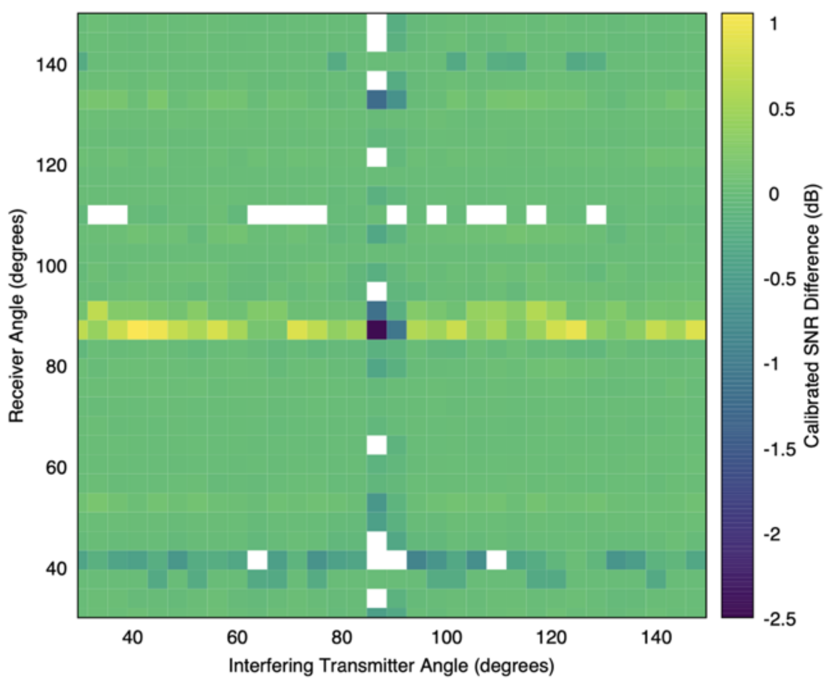

Figure 7 – 45°, SNR difference

4.3 Blu Wireless Technologies

Focused on developing solutions for gigabit connectivity using millimeter wave radio, Blu Wireless is a Bristol, UK-based SME. It has expertise in chip design as well as system solutions that solve technical challenges in carrier-grade mmWave applications. Blu Wireless currently has products in fixed-wireless access deployments for smart cities as well as mobility solutions providing wireless links to devices travelling at high speeds.

4.3.1 Test scope

The scope of the test was to investigate any mmWave link variations over time in an urban, smart city deployment providing wireless backhaul. The deployment test focused on using existing street fixtures—specifically lampposts. Also taking into account weather conditions over time, observed performance variations permitted a correlation between the two to be analyzed.

Each weather measurement was logged using the TGSounding application. We used DarkSky to capture the weather criteria that included humidity, temperature, and rainfall.

4.3.2 Test setup

Nodes 1 and 2 were both mounted on lampposts at 5 m above street level, with 105m separating them. Measurements were captured using channel 2 at a center frequency at 60.48 GHz.

The two nodes were deployed along the south side of an urban road having two lanes of traffic either side of it (Figures 8 and 9). The road has moderate traffic flow during busy times. Figure 10 shows a street level view from node 1 to node 2.

Figure 8 – Location of node 1 and node 2 mounted in Sheil Road (Liverpool, UK)

Figure 9 – The lamppost-mounted nodes on Sheil Road

Figure 10 – View from node 1 on the lamppost at left to node 2 in the center of the image two lampposts away

4.3.3 Results

A snapshot of the local weather station was captured alongside the channel sounder data. The weather station captured temperature, humidity, and precipitation over the measurement period. The weather data shows temperatures varied between a low of 1°C and high of 20°C, while humidity fluctuated each day between 34% – 98%. There was little rainfall, it reading over 1 mm/h for 1.2% of the measured data.

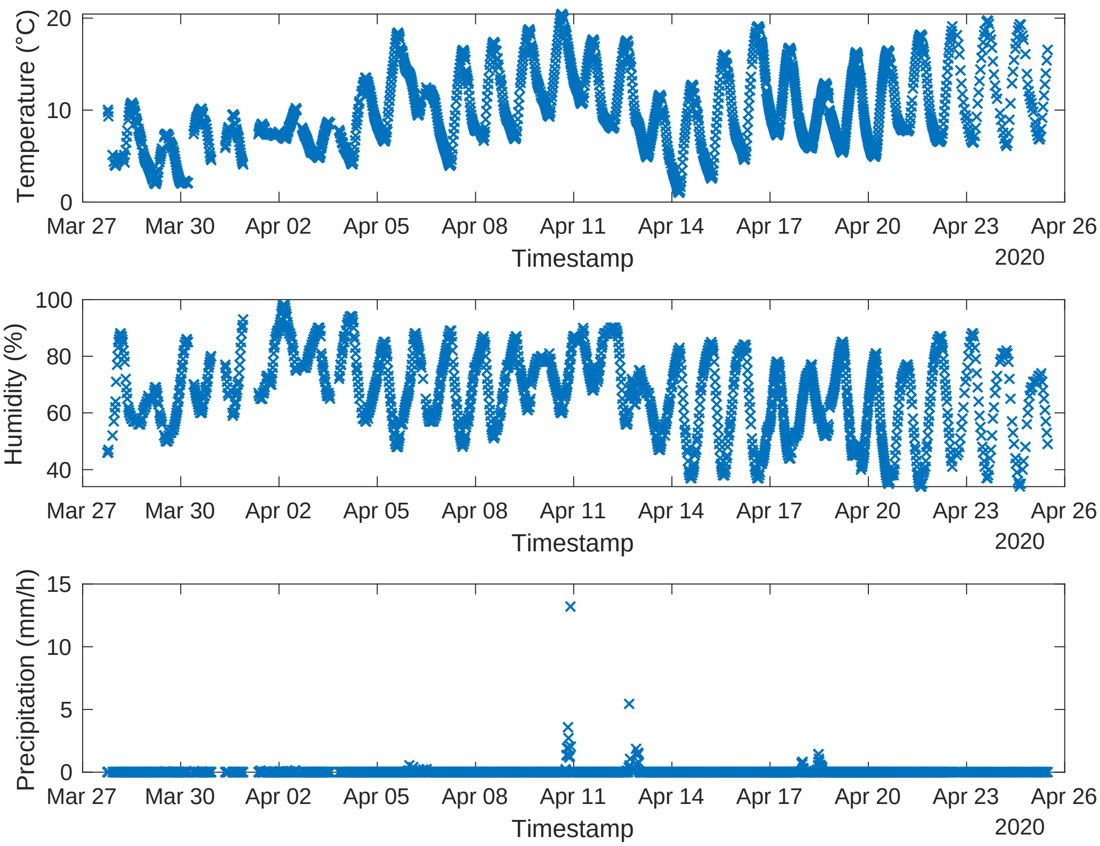

Snapshot 1

Figure 11 shows a scan of node 1 (Tx) and node 2 (Rx) in the azimuth plane. Measured data shows path loss on the left and delay spread on the right. Two distinct paths were present at Tx −1.4°, Rx 4.9°; the line of sight path had a reflection at Tx −8.4°, Rx 4.9°.

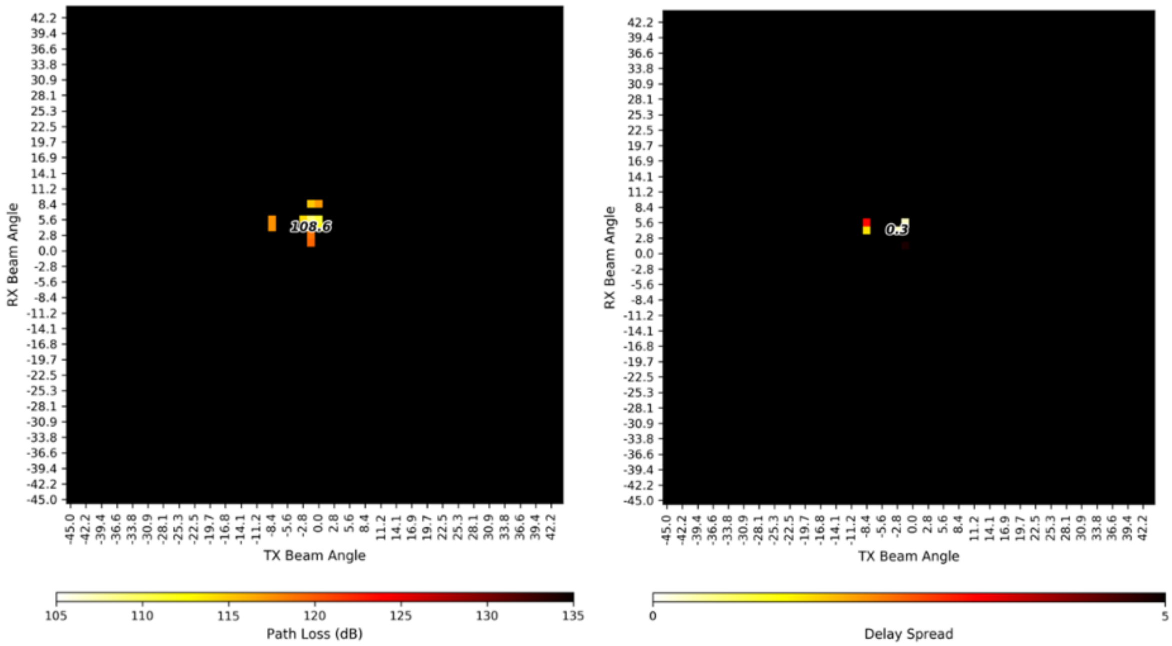

Figure 11 – A data snapshot on April 8th, 2020 at 2:16 pm local time during a sunny day with a temperature of 17.4°C and a 51% humidity

The channel impulse response (CIR) can be seen in Figure 12. The reflect path in (b) has an additional attenuation of 9dB in the path loss field compared to the LOS path.

(a) LOS path

(b) Reflected path

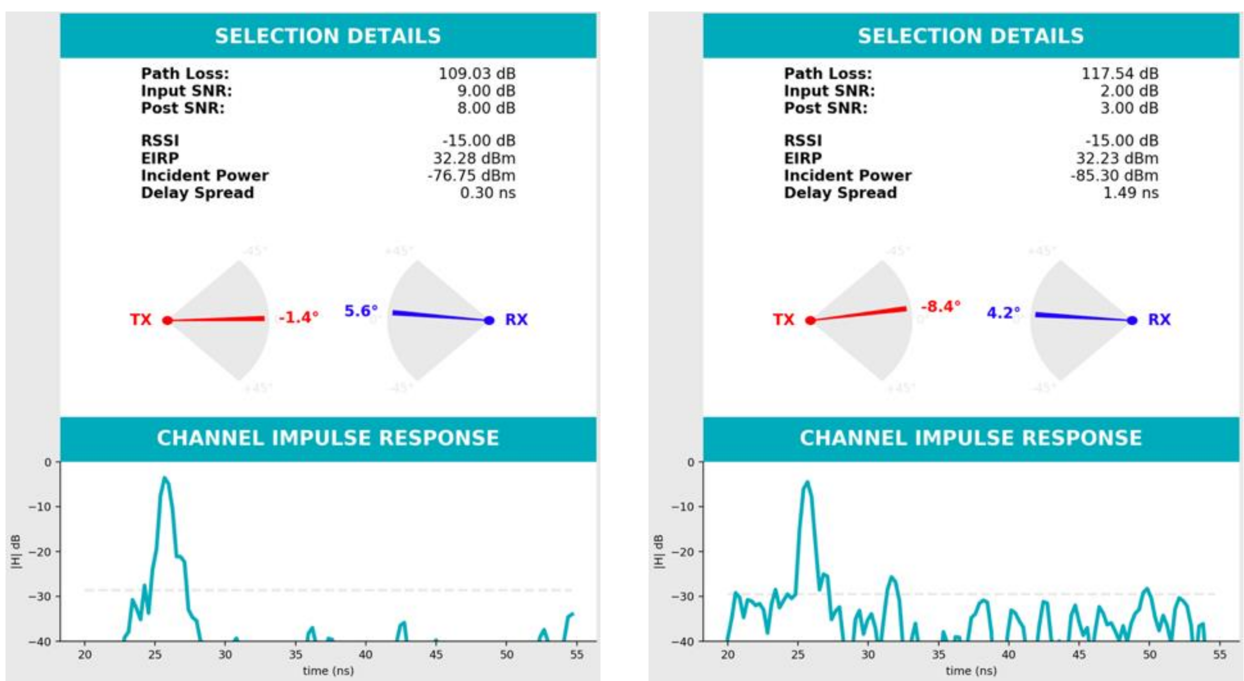

Figure 12 – Impulse response from April 8th, 2020 channel scan data

Snapshot 2

Figure 13 shows a second snapshot taken at 3:21 am on April 9th during heavy rain. The precipitation was 13mm/h with a temperature of 15°C and humidity of 79%. An additional 6 dB of attenuation, seen between snapshot 1 and snapshot 2 has caused the reflection seen in snapshot 1 which is attributed to the noise floor.

The CIR response for the LOS path is shown in Figure 14. There is little delta when comparing snapshots 1 and 2.

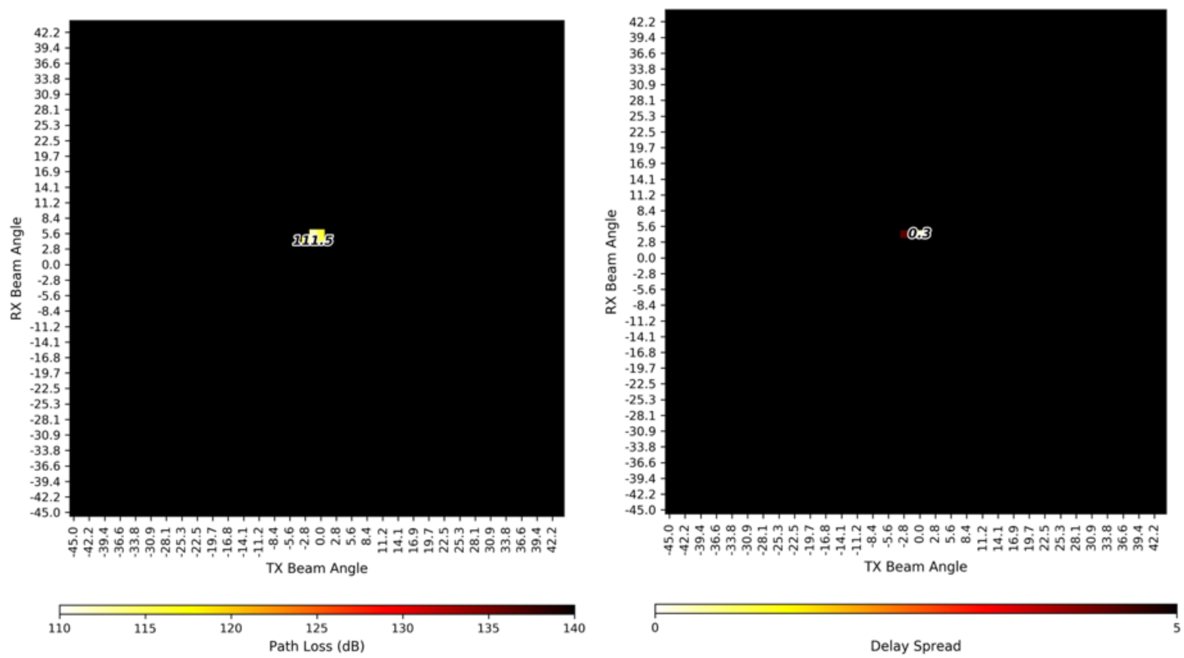

Figure 13 – April 9th snapshot: azimuth beam angles are varied with node 1 as Tx and node 2 as Rx

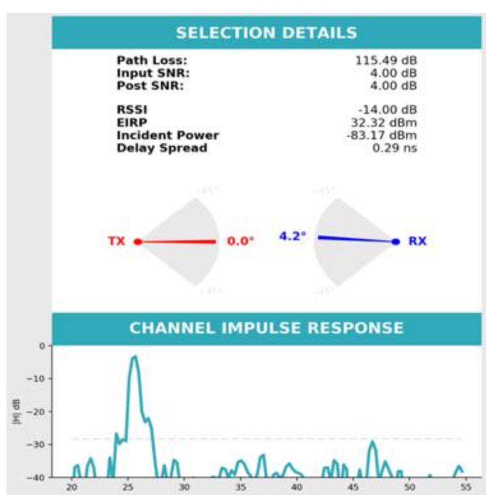

Figure 14 – The April 9th CIR

4.3.4 Findings

The focus has been on using the LOS path for variation; it has the least path loss and is therefore assumed to be picked from the sector level sweep.

Figure 15 shows a time comparison using Tx 0°, Rx 4.2°, with the path loss varying over the days captured. In Figure 15 (a) the path loss can be seen vary over the time period from 27th March to 23rd April.

(a) Path loss over time (b) CDF of the path loss

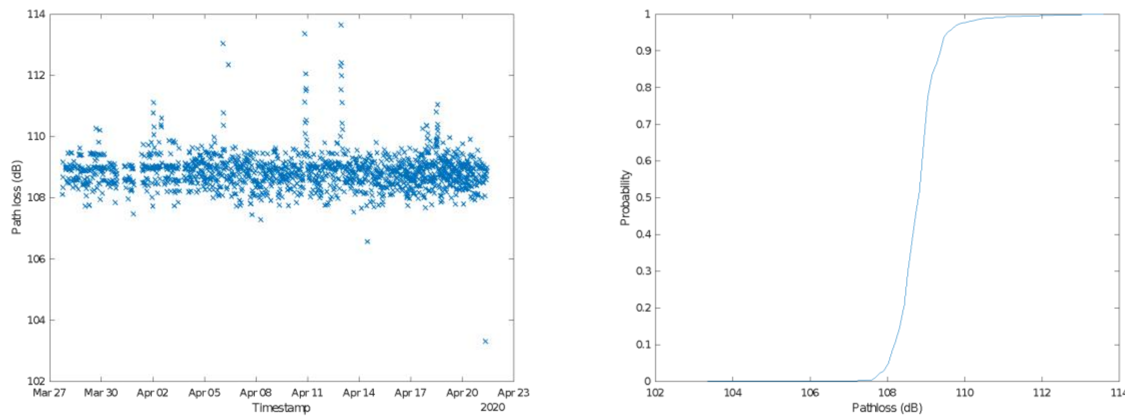

Figure 15 – The path loss capture between March 27th and April 23rd for Tx 0°, Rx 4.2

Considering that precipitation has a higher effect on path loss, a comparison on varying precipitation amounts is shown in Figure 16:

- Blue line – no precipitation (least path loss)
- Red line – an additional path loss can be seen when precipitation is less than 1mm/h
- Yellow line – there is a higher path loss when rainfall is over 1mm/h

Not much rainfall was recorded when the measurements were captured. Figure 13 depicts rainfall of 15mm/h. In Figure 16, a rainfall CDF shows that 90% of the time the path loss for no rainfall is ≥109.3 dB, for light rainfall (under 1 mm/h) the path loss is ≥110.3 dB, and the path loss is ≥112.3 dB for heavy rainfall (>2mm/h).

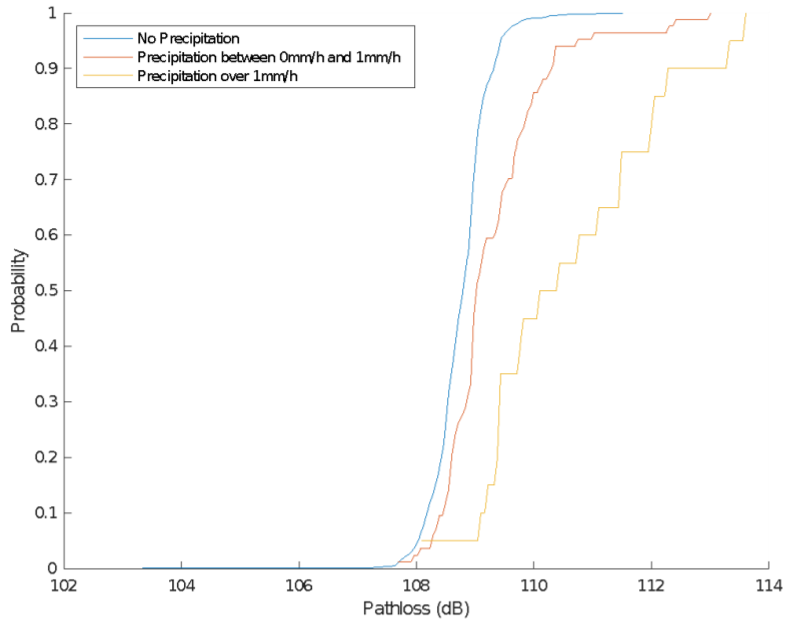

Figure 16 – A CDF showing a comparison on reported path loss for different rainfall amounts

4.4 Fraunhofer Institute for Telecommunications, Heinrich Hertz Institute

The Fraunhofer Institute for Telecommunications, Heinrich Hertz Institute (HHI) is a research institute on applied science in Berlin, Germany. Video and audio coding, photonic components and networks, and wireless networks are three main pillars of its research. Within its Wireless Communications and Networks department, the mmWave group—specializing in design, simulation, and implementation of mobile communication systems—has gained expertise in channel sounding and modeling.

Past activities include the development of channel sounder systems and conducting measurement campaigns for frequencies ranging from MHz up to THz domain—including 60 GHz. Recent activities focused on development and analysis of virtual antenna arrays for directional channel measurements.

4.4.1 Test topology

This measurement campaign was conducted at HHI's location in an urban environment, having buildings of varying heights surrounding the area in addition to scattered trees and bushes (Figures 17, 20 – 21). The tests were twofold: 1) to measure along an LOS path at distinct distances, and 2) measure various transition stages from LOS to NLOS (Figures 18 – 19).

Figure 17 – Measurement location at HHI

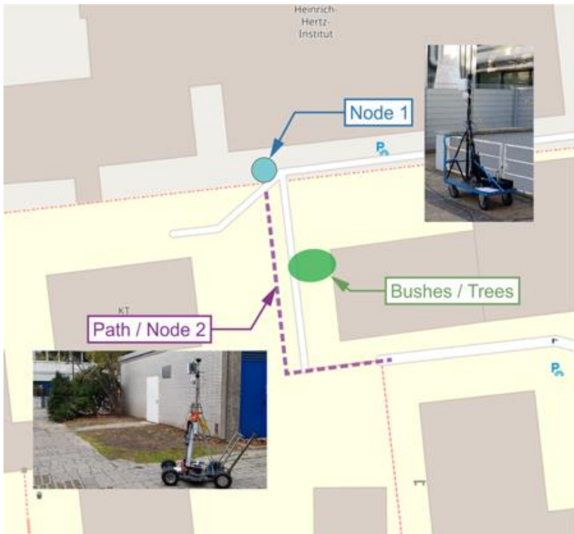

Figure 18 – Map highlighting environmental objects (buildings, bushes/trees), location of nodes, and measurement paths of LOS and LOS/OLOS/NLOS transition

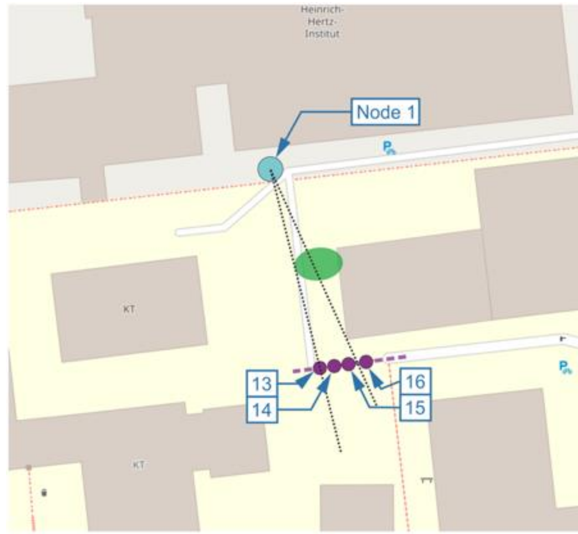

Figure 19 – A more detailed map of locations for LOS/OLOS/NLOS transition. Transition from LOS/OLOS/NLOS due to foliage (bushes/trees) at positions 13 – 15. Fully blocked NLOS by building at position 16

Figure 20 – Measurement scenario; node 1 is stationary (blue), whereas node 2 is a mobile platform (purple)

Figure 21 – Measurement scenario from another POV; node 1 is stationary (blue), while node 2 is a mobile platform (purple)

4.4.2 Measurement description

Both nodes were mounted at a height of 1.95 meters and aligned in elevation angle. Node 1 was put up on a stationary tripod, while node 2 was attached to a movable platform.

Two measurement scenarios were conducted—an LOS and a LOS to NLOS transition. Table 1 lists operation mode and settings (valid for both scenarios).

Table 1 – Sounder Parameters

Parameter	Settings
Antenna mask (Tx & Rx)	0xFFF, 0xFFF, 0xFFF (Full)
Tx gain index	Location specific; 0 / 10 / 20
Averaging (n_stat)	1
Beam scanning range (Tx & Rx)	Full (64x64 combinations)
Antenna height (Tx & Rx)	1.95 m

LOS

For LOS measurements, both nodes faced toward each other while node 2 was successively moved along the LOS path. Twelve positions, with distances from 4 m up to 25.5 m, were tested (Table 2, Figures 22 – 23).

In addition to extracting channel properties and multipath components, these results can be used to validate and determine system gain offset by comparing LOS path loss with the free space path loss.

Table 2 – LOS positions and corresponding distances between nodes 1 and 2

Pos.	Distance (m)	Pos.	Distance (m)
1	4.00	7	9.00
2	4.73	8	10.50
3	5.00	9	11.94
4	6.00	10	15.06
5	7.00	11	20.50
6	8.00	12	25.50

Figure 22 – LOS scenario

Figure 23 – LOS scenario, position 12

NLOS

The transition from LOS to NLOS (Figure 19) included multiple stages. It began with a clear LOS scenario (position 12), evolved to an OLOS and NLOS scenario due to foliage (bushes/ trees, positions 13 – 15, Figure 24), and finally to an NLOS scenario behind a solid building (position 16, Figures 25 – 26).

Figure 24 – Transition from LOS to NLOS due to foliage. Node 2 at measurement position 13

Figure 25 – NLOS scenario due to solid building. Node 2 at measurement position 16

Figure 26 – NLOS scenario due to solid building. Node 2 at measurement position 16

4.4.3 Results

LOS

Expecting the LOS path to correspond with the highest signal power (i.e., the lowest path loss), the minimum loss values across all Tx – Rx beam combinations have been extracted and plotted in Figure 27. The results follow the expected trend with an offset (of the linear fit) of −3.7 dB relative to the FSPL.

Illustration of path loss heatmaps are depicted in Figures 28 – 29. No distinct multipath components can be identified. This holds true even for measurement positions having greater distances between nodes (i.e., potentially more objects/surfaces within the covered beam area).

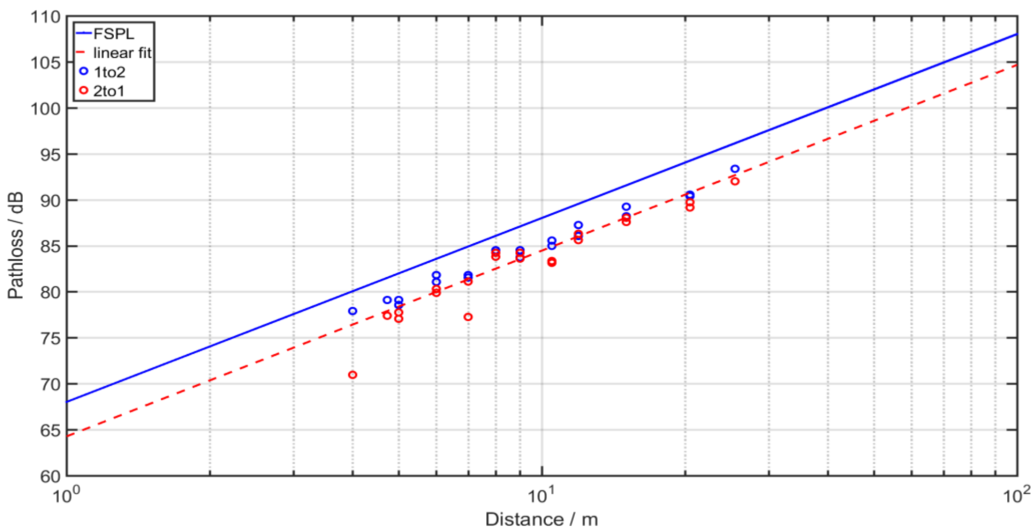

Figure 27 – Path loss for LOS scenario (circles o, 1 – 2 in blue color, 2 – 1 in red color), a linear fit on both link directions (red dashed line), and FSPL as reference (blue line)

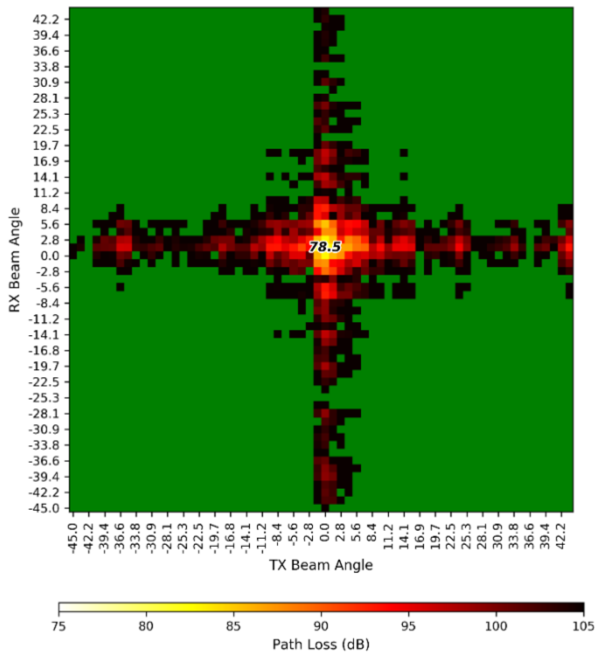

Figure 28 – Path loss heatmap for measurement position 3 with Tx gain index 10

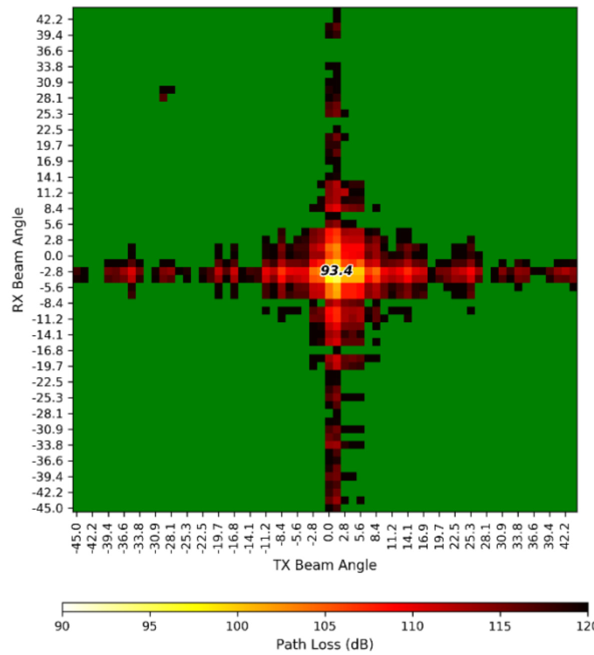

Figure 29 – Path loss heatmap for measurement position 12 with Tx gain index 20

NLOS

Foliage blocking leads to an increase in path loss (Figure 30), but the nodes weren't able to detect any signal in the NLOS scenario when node 2 was behind a building.

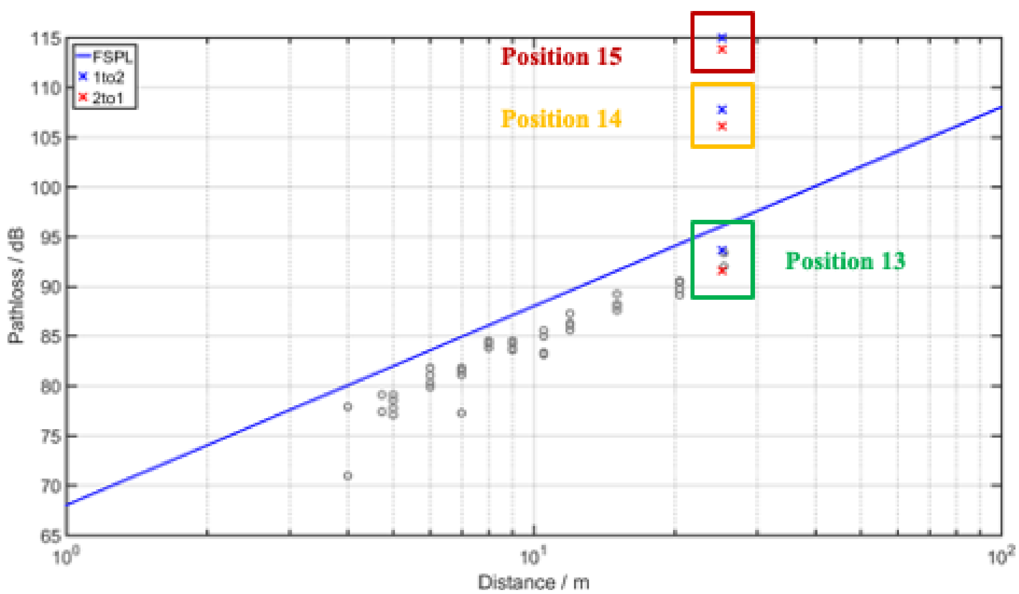

Figure 30 – Path loss increases during the LOS to NLOS (crosses x, position 13 – 15) transition. No signal was received in the NLOS scenario (node 2 behind a building)

Seen in the heatmaps in Figures 31 – 32, no additional multipath components can be identified with the received signal power.

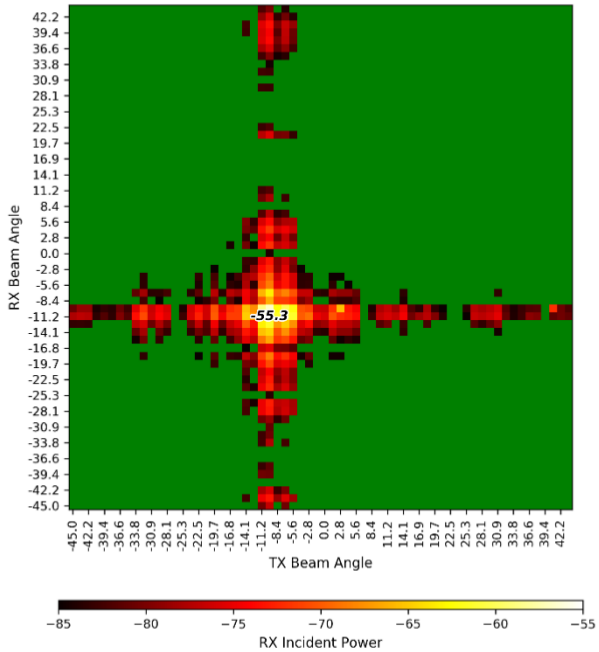

Figure 31 – Rx incident power heatmap for measurement position 13 with Tx gain index 20

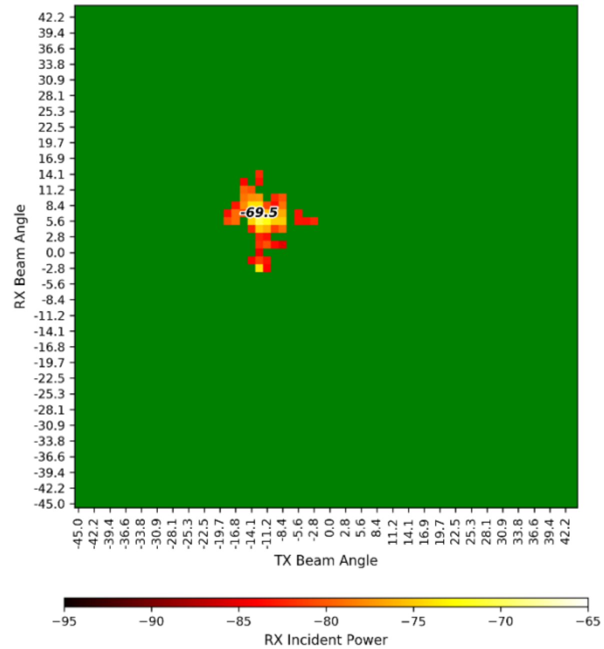

Figure 32 – Rx incident power heatmap for measurement position 14 with Tx gain index 20

4.4.4 Findings

A more in-depth analysis of multipath components in an NLOS scenario is desirable. Therefore, for nodes in such a scenario, multiple measurements with various (re-) alignments in azimuth domain are necessary to gain results for a full angular range of 360 degrees. Furthermore, Tx gain should be maximized given the anticipation of increased path loss.

4.5 Ghent University – IMEC

The UGent-WAVES research group, affiliated with IMEC, has about 15 years of experience in experimental characterization of wireless propagation. For this research, UGent-WAVES builds its own radio channel sounders. Historically, the group performed experiments with inexpensive, frequency-swept radio channel sounders built around a vector network analyzer and virtual antenna arrays. Today, the group has created a real-time sounder at 1.35 GHz with 16 × 16 spatial channels and sub-millisecond acquisition time (extensions to 6 GHz and massive MIMO are planned). UGent-WAVES uses maximum-likelihood algorithms, such as RiMAX, to estimate propagating plane waves and their parameters from sounding data.

In general, the group estimates propagation parameters from experimental data, analyzes their statistics, and uses them to create semi-deterministic propagation models. UGent-WAVES puts special focus on creating radio channel models for industrial (or otherwise highly metallic) propagation environments.

4.5.1 Test scope

This work assesses path loss at 60 GHz in the highly metallic environment of a freighter ship. The envisioned application is high data-rate wireless communication inside its engine room, with the goal of improving crew safety and efficiency.

Currently, all data collection and equipment tracking aboard ship is done by manually by writing in a logbook. Wireless connectivity would enable easy access to user manuals and notes during engine gear repair and maintenance. Moreover, high data-rate communication opens up the possibility of remote video monitoring of valve and engine operation, and of the ship's crew. The latter contributes to their safety, as an injured worker can be noticed faster.

4.5.2 Test setup

We performed 76 LOS measurements with the Terragraph sounder inside the engine room of a 200 m long bulk cargo ship. The various locations of the sounder's transmitter (Tx) and receiver (Rx) are shown on a blueprint of the ship's engine room (Figure 33). Here the combinations of Tx and Rx locations for which a measurement was taken are shown in the same color and share the same index number (1 – 5). The Tx location is fixed while the Rx is moved along the indicated track between measurements. For all measurements combined, we obtained path loss data for Tx – Rx distances between 1.50 m and 14.25 m in steps of 25 cm.

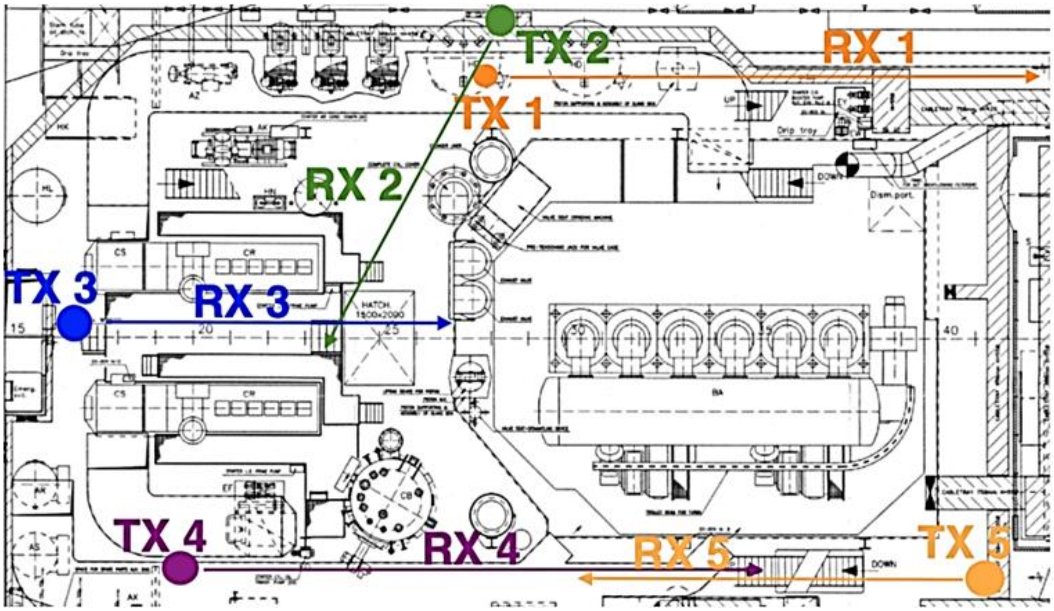

Figure 33 – Tx and Rx locations

Figures 34a and 34b offer a view of the engine room and its metallic content. They also show the Tx and Rx location along tracks 1 and 4, respectively.

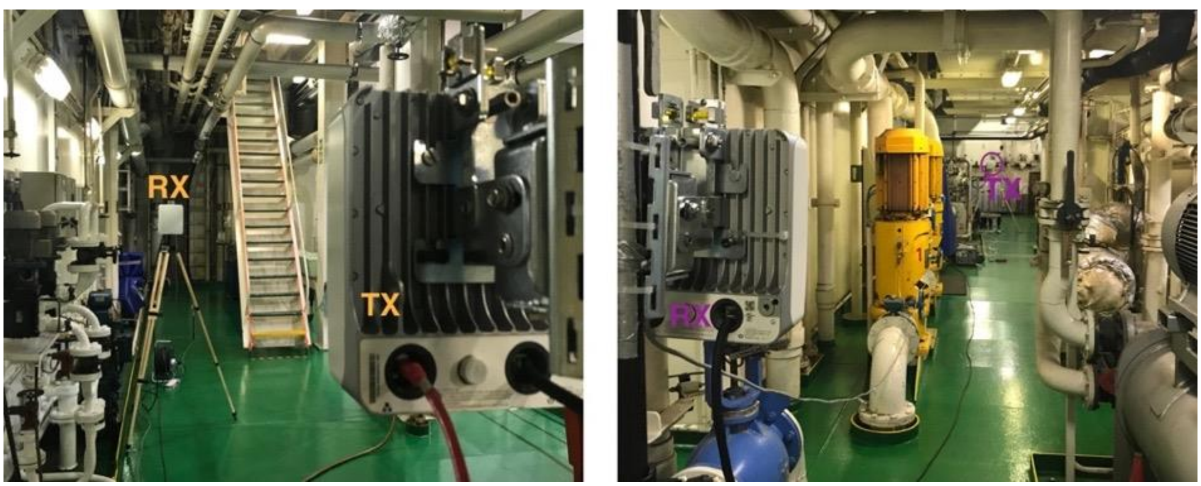

Figure 34 – Engine room, (a) Rx track 1, (b) Rx track 4

4.5.3 Results

Figure 35 presents measured path loss versus Tx – Rx distance for the five Rx tracks in Figure 33. Both the Tx and Rx make use of phased antenna arrays to generate narrow 2.8° beams that scan the radio channel in an azimuthal range between −45° and 45° with respect to an array's boresight. Measured path loss is for the Tx/Rx azimuthal beam directions registering the highest received power. The path loss samples were fitted to the well-known power-law decay model[1]:

$$PL(d) = PL(d_0) + 10n\, log_{10}\left(\frac{d}{d_0}\right) + \chi,$$

where $PL(d)$ is the path loss in dB at Tx – Rx distance d in m, n is the dimensionless path loss exponent, and $d_0 = 1.50$ m is an arbitrary reference distance. χ in dB is a random zero-mean normally distributed variable with standard deviation σ that expresses the deviation of the measured path loss from the median path loss dictated by the first two terms in the righthand side. Least-squares estimates of $PL(d_0)$ and n are 74.60 dB and 1.68, respectively. σ is found to be 3.48 dB.

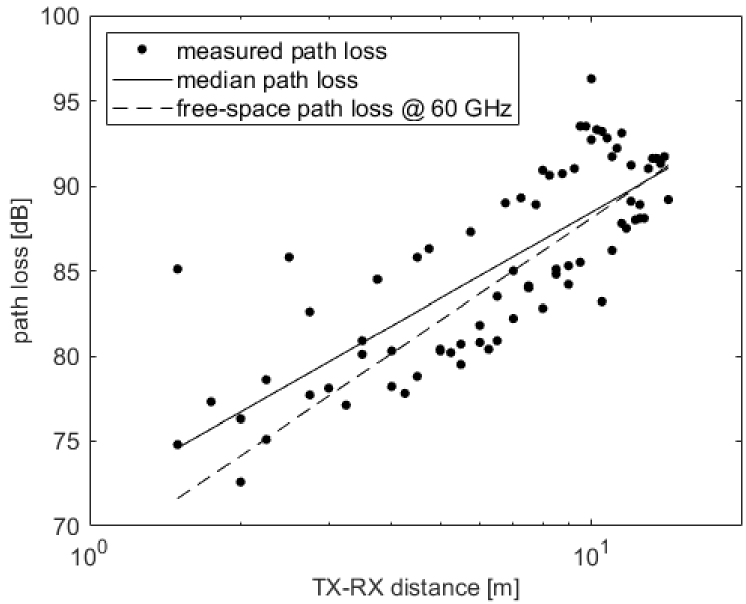

Figure 35 – Path loss versus Tx – Rx distance

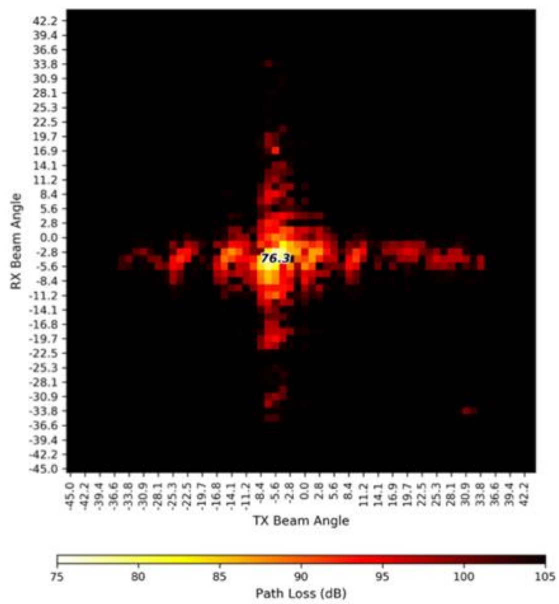

(a) LOS loc. 4, distance 2 m

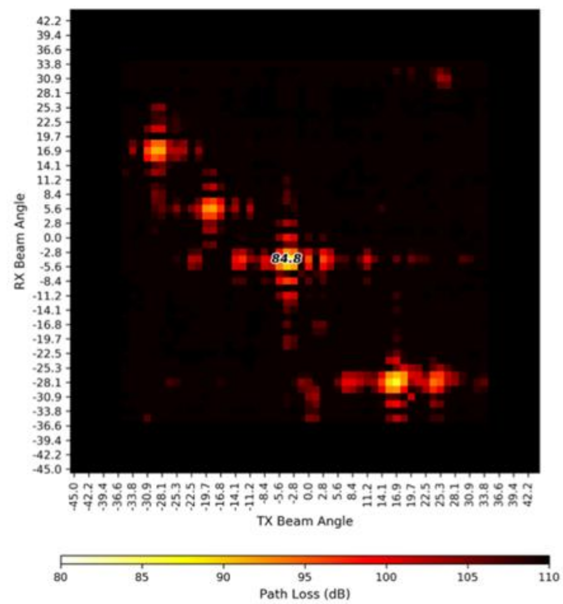

(b) LOS loc. 4, distance 8.5 m

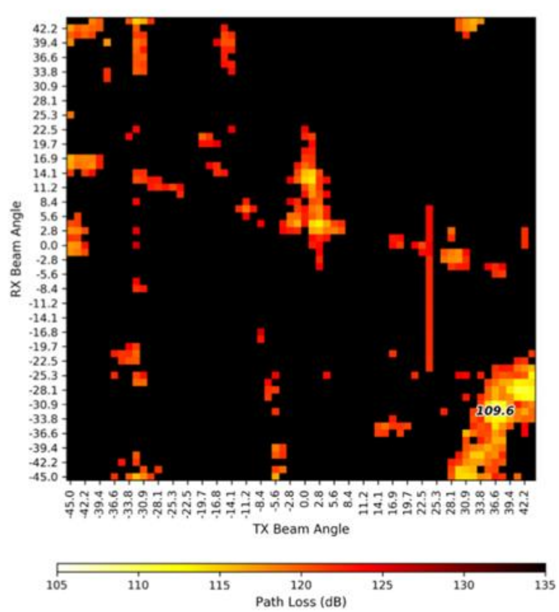

(c) OBS, distance 10 m

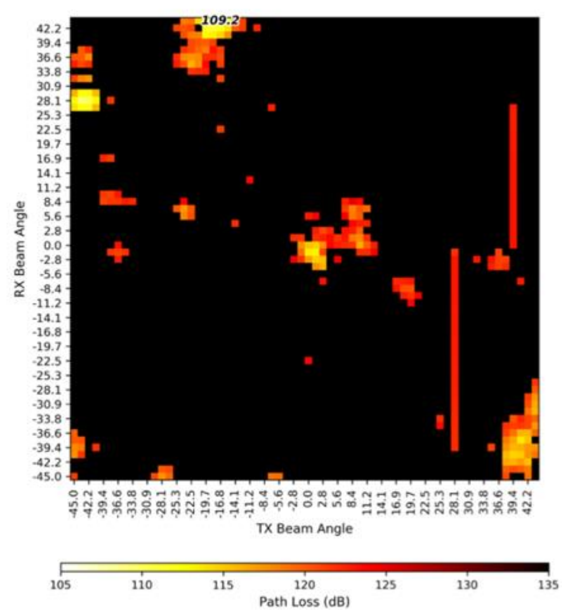

(d) OBS, distance 12 m

Figure 36 – Measured PL in function of Tx – Rx beam configuration

(a) Tx – Rx separation 2 m (b) Tx – Rx separation 8.5 m

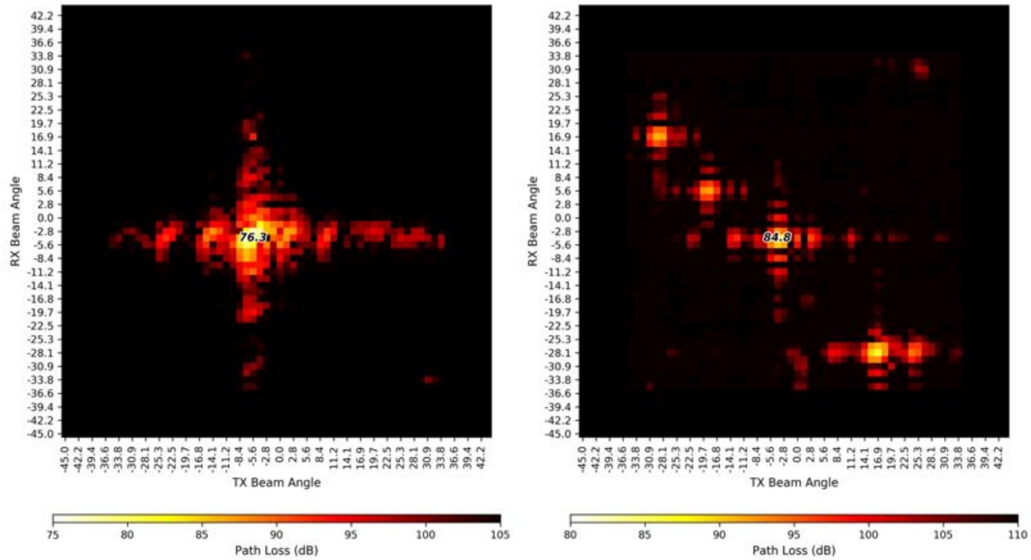

Figure 37 – Measured PL as a function of Tx – Rx beam configuration for LOS measurements at Tx4 – Rx4

(a) Tx-Rx separation 10 m (b) Tx-Rx separation 12 m

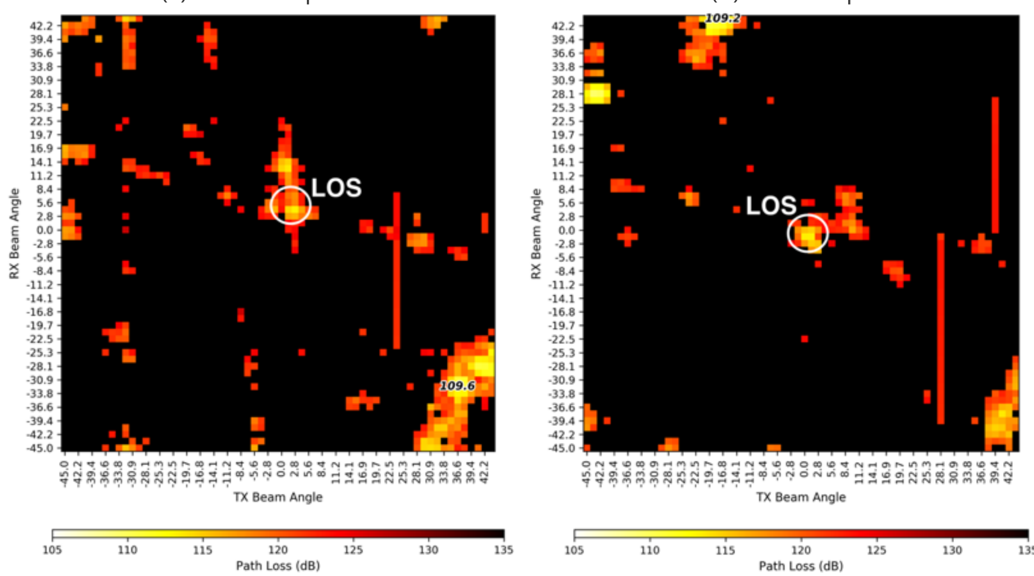

Figure 38 – Measured PL as a function of Tx – Rx beam configuration for OBS measurements in steering control room

4.5.4 Findings

We can observe from Figure 35 that the median path loss is close to the FSPL at 60 GHz. The path loss exponent is slightly smaller than the free-space exponent of 2, indicating a small waveguide effect in the engine room. Additionally, the standard deviation σ of χ hints at a limited shadowing effect for the LOS links— mainly caused by metallic piping that is sometimes present within the first Fresnel zone around the LOS link. For coverage and link budget calculations, we suggest adding a fading margin of ~5.72 dB (95th percentile of χ) to the median path loss to account for potential signal power reduction due to shadowing.

4.5.5 References

[1] S. R. Saunders, *Antennas and Propagation for Wireless Communication Systems*. Wiley and Sons, 1999.

4.6 NIST Communications Technology Lab (CTL)

NIST CTL's Wireless Networks Division works with industry to develop, deploy, and promote emerging technologies and standards that will dramatically improve the operation and use of wireless networks. Our team specializes in communications networks and protocols, as well as in digital communications technologies that make those networks possible.

In both of these areas, we perform both theoretical and empirical research to develop wireless channel models, simulation models, experimental testbeds, and proof-of-concept prototypes we use to 1) evaluate new technologies, and 2) refine existing standard specifications for wireless networks and systems.

Also, we define metrics and measurement methods to assess performance of many wireless system types. As part of our program planning activities, we continue our industry and stakeholders' outreach to identify additional measurements and metrology R&D gaps in support of wireless communication systems and standards development.

4.6.1 Test scope

The scope of this section is to evaluate the Terragraph sounder system in indoor and outdoor environments. To understand system functionality and performance, NIST designed several testing scenarios to compare theoretical and experimental results.

4.6.2 Test setup

This section describes the topologies and detailed descriptions of measurements taken.

4.6.2.1 Topologies

The measurement campaign was conducted on the NIST campus in Gaithersburg, Maryland. Two test locations are displayed in Figure 39—location A is between building 225 and building 101, where we performed short-distance path loss measurements, dielectric constant measurements, and tree propagation measurements; location B is inside a large parking lot for long-distance path loss measurements.

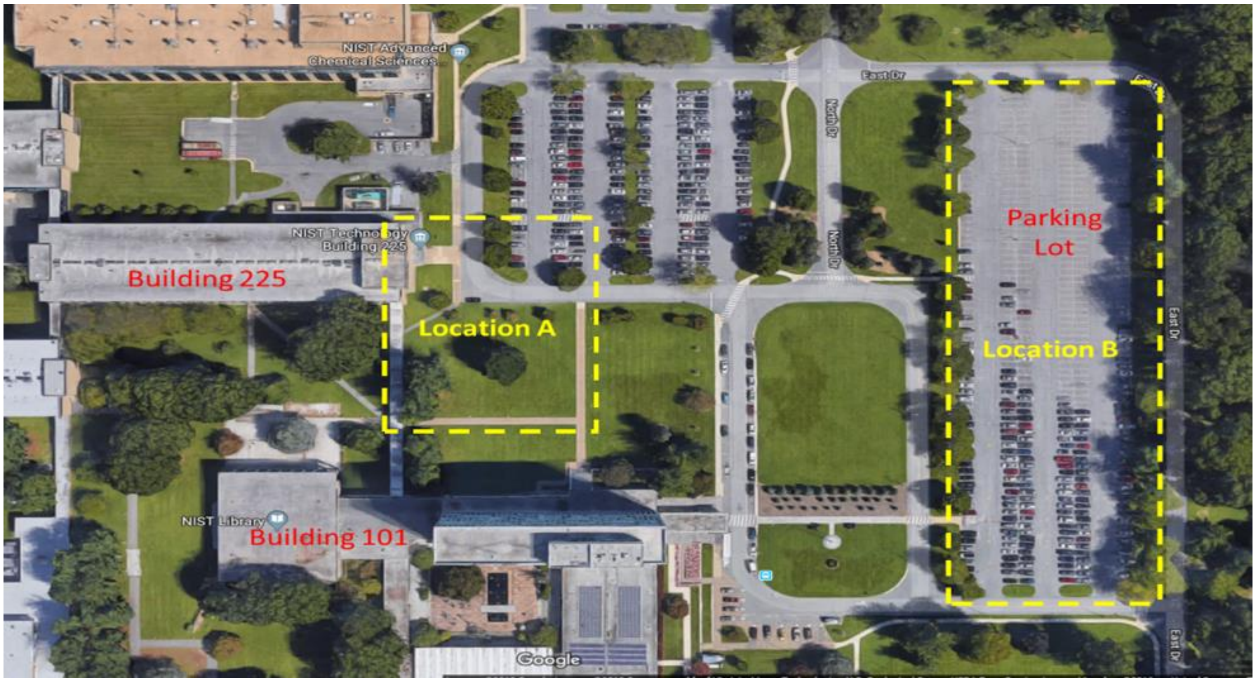

Figure 39 – NIST measurement test sites

4.6.2.2 Measurement description

Table 3 lists the operation mode and settings of the Terragraph sounder. Its antenna can actually scan ±45 degrees with 64 × 64 Tx – Rx beam combinations. To speed up the measurements, the field of view is reduced to ±30°, which still gives reliable results.

Table 3 – Terragraph sounder operation parameters

Radio Parameters	**Settings**	**Comments**
Radio Mode	Mode 2	Heat map
Antenna Mask	0×FFF	Full mask
Tx Gain Index	20	20 for outdoors
Antenna Array Gain	28 dbi	Maximum
Antenna Scanning Range (in angles)	±30°	32 × 32 Tx – Rx beam combinations
Antenna Pattern	28° @AZ 12° @EL	Fan beam
Tx Antenna Height	15 ft	
Rx Antenna Height		
Environment	Outdoors	

Outdoor path loss measurements

Short-distance path loss measurements

Short-distance measurements were performed at location A, which was mostly void of ambient reflectors (e.g., building walls, vehicles, trucks). It’s anticipated the future deployment for mmWave systems will have base stations mounted on street lampposts, the height of which generally ranges between 13 – 27 ft, with the most common range being 15 – 18 ft.

Accordingly, we set the antenna height to 15 ft for both the transmit (Tx) and receive (Rx) antennas for outdoor measurements. Figure 40 shows the test setup, where the longest distance between the Tx and Rx was 42 ft. Incremental distance steps started with 2.63 ft separation and doubled (exponentially) per step until the maximum distance was reached. The antennas were pointed so that their boresights were aligned in both azimuth and elevation.

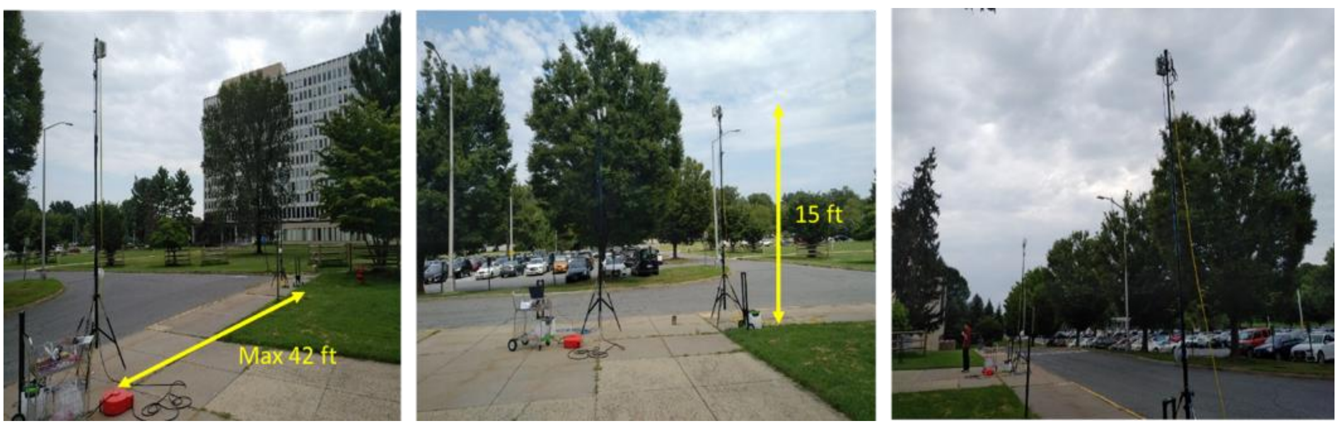

Figure 40 – Outdoor short-distance measurements of path loss

Long-distance path loss measurements

This measurement was conducted in the large parking lot (location B), shown in the right of Figure 41. The distance between Tx and Rx was measured as 663 ft (202 meters). The Tx antenna height was fixed at 15 ft, while the Rx antenna height was adjusted between 12 – 15 ft (to account for irregular terrain)—again so that the antennas boresights were aligned.

Figure 41 – NIST long-distance path loss setup

Dielectric constant measurements

Indoor dielectric constant measurements

The method to extract the dielectric constant from the double-directional path loss measurements is based on Fresnel equations.[2] Before doing so, the method was validated through indoor testing, as described in the sequel:

The Tx and Rx were pointed toward the glass wall/door (Figure 42). The glass is very smooth and the distance to the glass door is 7 ft for both Tx and Rx. The minimum path loss reported in the sounder-generated heat map was 87.3 dB, corresponding to the double-directional angle of the reflection from the glass panel of the door. The calculated dielectric constant from the method in[2] was 7.2, in close alignment with the window glass dielectric constant of the ITU-R and Microwave 101 reported as 6.5[3][4] (there is only a 10% difference between the two values).

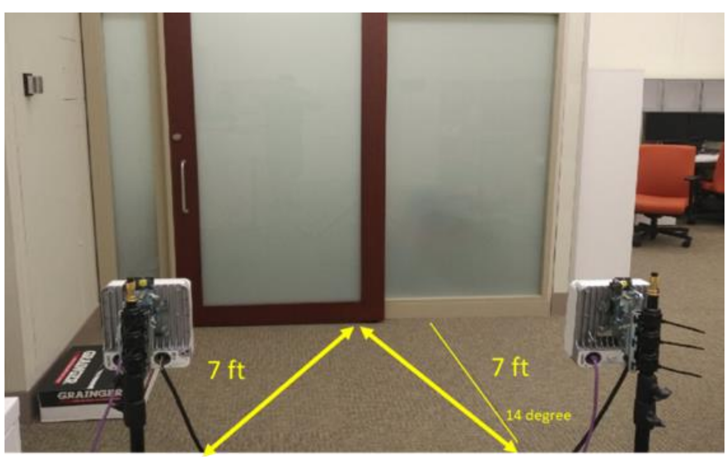

Figure 42 – NIST indoor setup for dielectric constant measurements

Outdoor dielectric-constant measurements

Outdoor objects under investigation included a car, a tree, and a brick wall. The Tx and Rx of the Terragraph sounder were set up in front of the test objects (Figure 43). The distances between the objects and antennas were 7 ft. The heights of the Tx and Rx antennas were adjusted per object, such that the elevation beam widths were aligned with the dominant reflection from the objects. The antenna heights were 4.5 ft for the car, while they were set to 8 ft. for the brick wall and the trees.

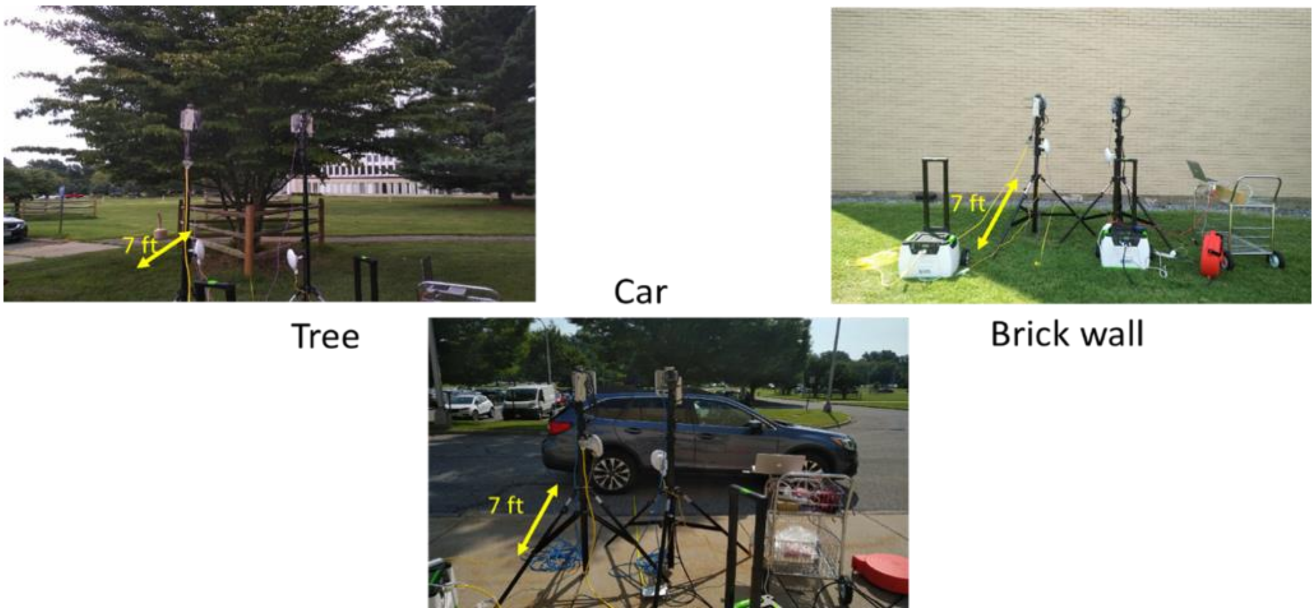

Figure 43 – NIST outdoor setup for dielectric constant measurements

Tree propagation loss measurements

To render comprehensive and reliable data for tree penetration loss, NIST designed a novel measurement approach—the Tx was fixed at one location in front of a tree, while 14 Rx locations were set up around the tree (Figure 44). This permitted both multiple Tx – Rx distances (20 – 55 ft) and penetration through varying tree cross sections.

Per Rx location, the Tx and Rx were adjusted in orientation and height such that their boresights were aligned in azimuth and elevation, respectively. It’s interesting to observe changes in propagation loss captured in the statistics as the Rx was moved around the tree.

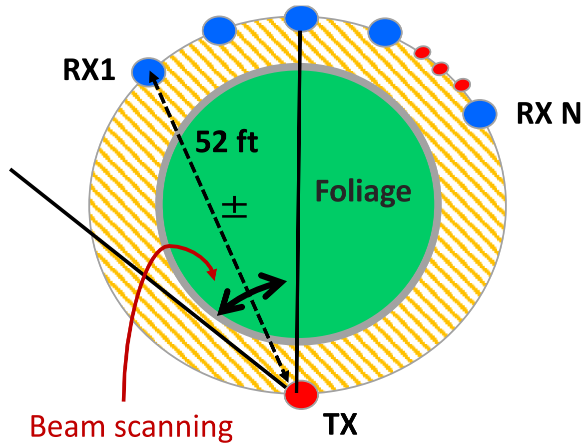

Figure 44 – NIST approach for tree propagation loss measurements

For most Rx locations, LOS was generally not available since tree leaves and tree strips/trunks blocked the Tx and Rx. There were some hollow spots between leaves that reduced the blockage category from *full* to *strong*. There are three levels of tree blockage, based on the visual inspection described in Table 4. Even in windy weather, we can assume such blockages always exist and maintain their own blockage levels.

Table 4 – Tree blockage level and definition

Blockage Level	Definition
Full	Full Tx antenna cannot be seen from the Rx view.
Strong	Strong blockage indicates that the corner or spot size of the Tx antenna can be seen from the Rx view with a lot of leaves and sticks between the nodes.
Medium	Medium blockage indicates that some parts of the Tx antenna can be seen from the Rx view with some leaves and sticks between the nodes.

Tx and Rx antenna heights were chosen as 15 ft, such that the fan beams laid comfortably within the tree foliage. This was also sufficiently high so that ground bounce was well within the side lobes of the fan beam (given the investigated range of Tx – Rx distance). However, it was sometimes necessary to lower the antenna height to collect valid data due to leave orientations, leave shapes, and sticks. Foliage presented less blockage near tree trunks.

Three different tree types (Figure 45)—typical of residential and commercial areas—were selected for this preliminary study. Foliage (branches and tree leaves) diameter was measured as 15 – 16 ft (using a tape measure).

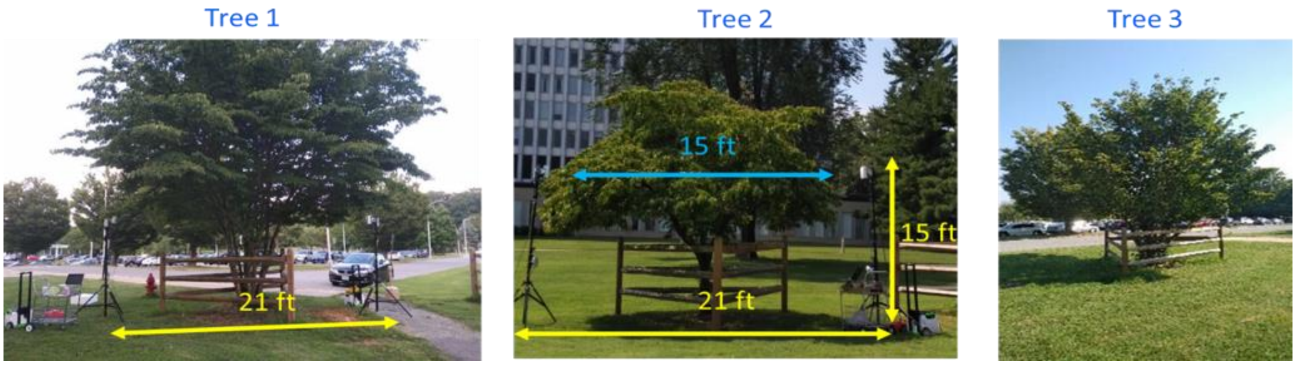

Figure 45 – NIST tree propagation loss measurements

4.6.3 Result

Outdoor path loss measurements

(a) Short-distance measurement

In the short-distance path loss measurement, the Tx – Rx distance is varied from 2.63 ft to 42 ft in Table 5. When the Tx – Rx distance was increased from 10 ft to 42 ft, the measured free-space path loss values were better than theoretical values resulting from the narrowband Friis transmission equation.[5] This is mainly due to the integration of the direct path with ambient paths, but may also be due to the wide bandwidth. When the Tx – Rx distance was less than 10 ft, the channel sounder consistently detected slightly higher path loss; this most likely had to do with greater beam misalignment at much shorter distances.

The SNR does not get significant better when the Tx – Rx distance is reduced to half. The received signal and SNR should both increase 6 dB when the path loss is simultaneously reduced 6 dB. According to the Facebook team, the reason is the reported SNR does not correlate well to distance changes after the auto-correlation process.

Table 5 – Outdoor free-space measurements in short distances

Distance (ft)	Measured PL (dB)	Theortical PL (dB)	Delta (dB)	Input SNR (dB)	Post SNR (dB)	Antenna Height (ft)
2.63	67.7	66.16	-1.54	25	18	15
5.25	73.9	72.16	-1.74	24	18	15
10.5	77.1	78.18	1.08	25	18	15
21	83.21	84.2	0.99	23	16	15
30	86.5	87.58	1.08	22	17	15
42	88.42	90.22	1.8	22	17	15

(b) Long-distance measurement

Measured path loss from a sounder is 111.4 dB and theoretical path loss is 114 dB. The delta between measured and theoretical is 2.6 dB. The EIRP is ~38 dBm (Tx gain index 18). The received power is -76.39 dBm. The thermal noise floor is -81.55 dBm. The measured noise figure of MCS 1 is 3 dB from the FB team. Post SNR is ~5 dB (i.e. -76.9-(-81.55)).

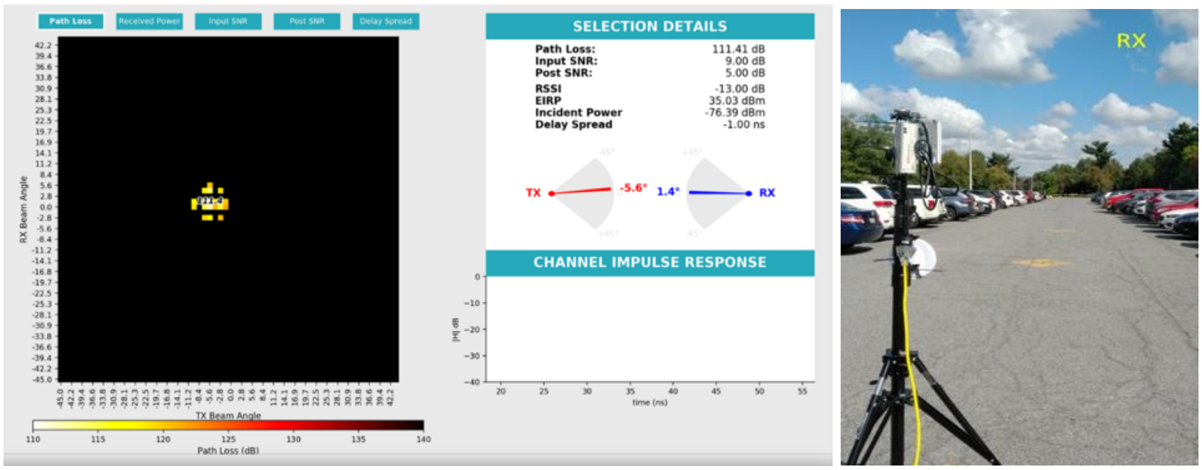

Figure 46 – Outdoor free-space measurements in long distances

Dielectric constant measurements

(a) Case 1: Tree

Tx and Rx were 7 ft distant from the center of the tree; their antenna height was 5.5 ft. Being the major reflections, the branches (bright spots) were used to estimate the dielectric constant of the tree. Leave path loss is around 10 dB down compared to the branch with bright colors.

Figure 47 – Tree dielectric constant measurements

(b) Case 2: Car

The Terragraph sounder only detected the signal when it scanned the side of the car. The sounder did not detect valid data from its front nor its back side. The estimated dielectric constant is 1.28 (car body and tires—not glass).

Figure 48 – Car dielectric constant measurements

The results of dielectric constant measurements are summarized in Table 6 and are compared to the ITU-R or theoretical dielectric constant values.

Table 6 – Measured dielectric constant and theoretical values

Object Type	Measured Dielectric Constant	ITU or theortical Dielectric Constant
Glass door (indoor)	7.2	3.7 to 10
Brick wall	4.9	4.5
Tree	1.43	1.2 to 2
Car (side)	1.28	1.5 to 5

Results of tree propagation loss measurements

NIST completed the measurement campaign of tree propagation loss according to the approach explained in the test setup. The weather during the measurement was stable, with a wind speed of less than 5 miles per hour. The outdoor temperature had to exceed 58 °F to collect valid data (without seeing the “too cold” message on the system). Additional measurement photos are shown in Figure 49.

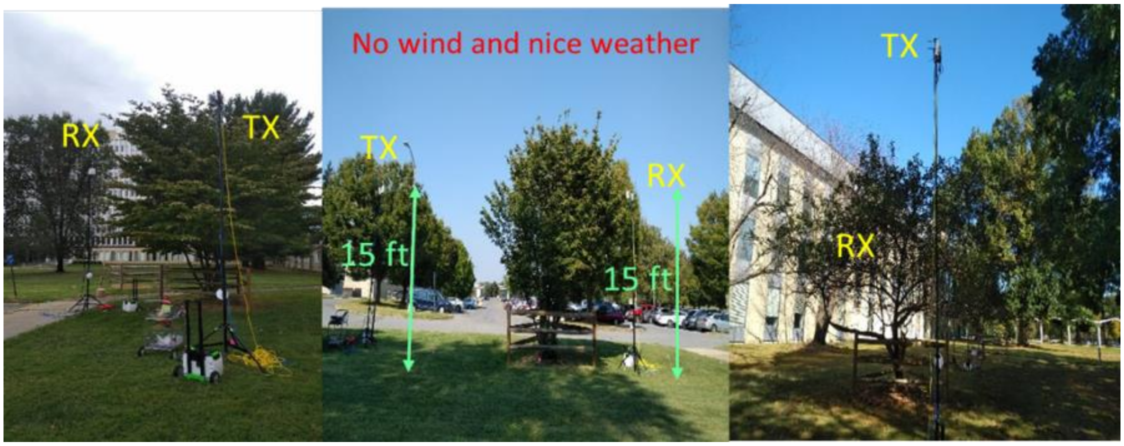

Figure 49 – Tree measurement campaign

(a) Leaf orientations

From the first few measurements, we observed that leaf orientations are very different and possibly impacted the propagation. Two orientations are shown in Figure 50: the first has fewer shades blocking the propagation of electromagnetic waves compared to the second.

To prove our assumptions, the same Tx – Rx separation distance (21 ft) and foliage diameter of each tree (15 ft) were used as parameters for the measurement setup in Figure 45. Leaf orientation 1 is for Trees 1 and 3; Leaf orientation 2 is for Tree 2. Figure 51 depicts different tree leaves commonly seen in the outdoor environment. Some cause higher propagation loss due to their orientation, wave incident angle, and shape.

The table in Figure 52 summarizes measurement results of tree propagation loss due to orientation differences. The Tree 1 loss is 6.4 dB, while Tree 3 has a loss of 20.25 dB. It being higher than 30 dB based on the maximum observed path loss of 120 dB, the propagation loss of Tree 2 is higher than Trees 1 and 2 with the same foliage diameter and antenna height.
To determine the propagation loss data from Tree 2, the antenna height was lowered to 6 ft. The leaf blockage was reduced by the visual inspection, with the propagation loss being around 14 dB with the new antenna height.

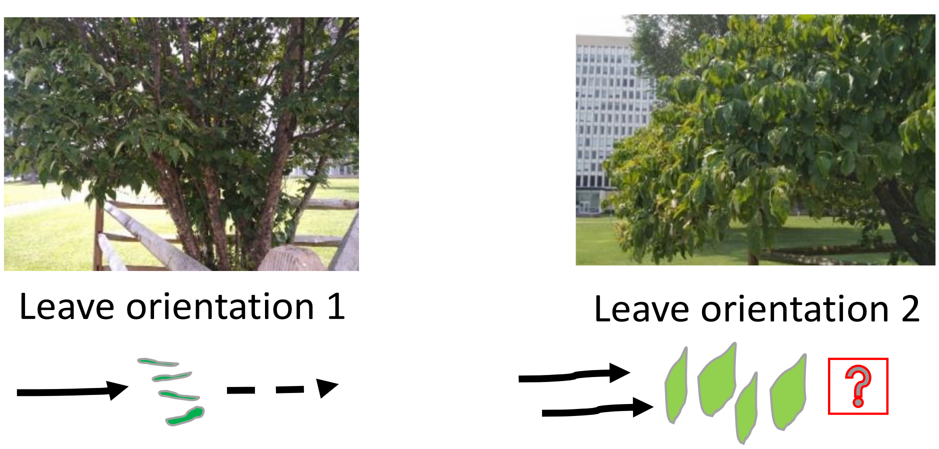

Figure 50 – Tree leave orientations

Figure 51 – Different tree leaves

Propagation Type	Leave Orientation	Antenna Height (ft)	Measured Path Loss (dB)	Delta to Theortical Free Space (dB)
Free Space	**-**	**15**	**83.21**	**-0.99**
Tree 1	**1**	**15**	**100.6**	**16.4**
Tree 2	**2**	**15**	**Not Available**	**>30**
Tree 2	**2**	**6**	**98.12**	**13.92**
Tree 3	**1**	**15**	**104.45**	**20.25**

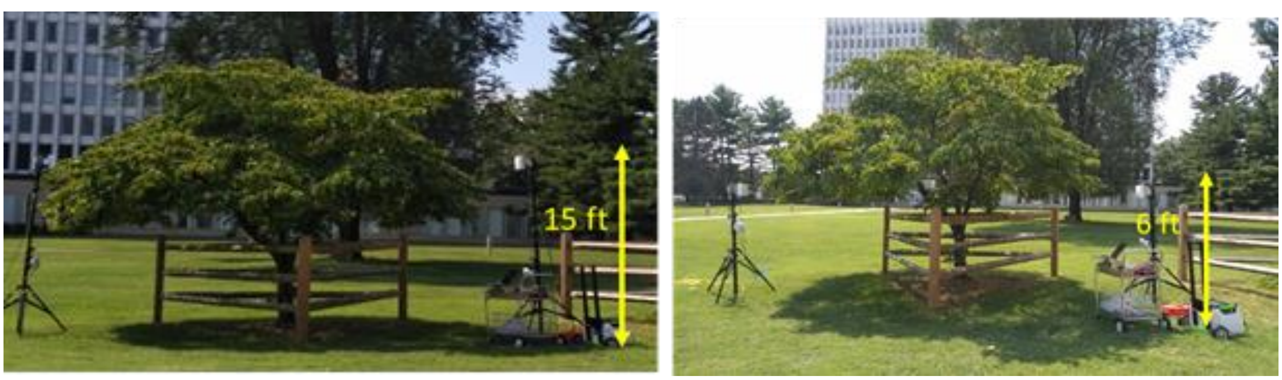

Figure 52 – Tree leave orientation measurement impact

(b) Tree propagation loss summary

Table 7 [provides a summary of measurement results based on multiple Rx locations per tree, for three select trees of medium size and density. The definition of tree blockage in the far-right column is based on the Table 4 definition and varies as full, strong, and medium (from worst to best). Penetration loss due to blockage was observed to vary in the range 14.8 – 29.7 dB, with a mean loss of 19.4 dB and 3.6 dB standard deviation of 3.6 dB (see empirical distribution in Figure 53).

Table 7 – Tree propagation loss based on NIST CTL measurement approach

Tree Type	Receiver	Meaured PL (dB)	FSPL (dB)	Tree Penetration Loss (dB)	Distance (ft)	Tree Blockage
Tree 1	RX1	111.8	91.7	20.1	50	Full
Tree 1	RX2	111.7	91.7	20.0	50	Full
Tree 1	RX3	105.7	90.2	15.5	42	Medium
Tree 1	RX11	115.1	89.5	25.6	39	Full
Tree 1	RX12	119.9	90.2	29.7	42	Full
Tree 2	RX1	110.8	91.7	19.1	50	Full
Tree 2	RX2	110.8	91.7	19.1	50	Full
Tree 2	RX13	108.3	91.6	16.7	49.5	Medium
Tree 2	RX14	108.9	92.0	16.9	52	Medium
Tree 2	RX16	109.3	91.7	17.6	50	Strong
Tree 3	RX1	112.0	91.7	20.3	50	Full
Tree 3	RX2	114.6	91.7	22.9	50	Full
Tree 3	RX3	107.8	90.2	17.6	42	Strong
Tree 3	RX4	107.9	88.8	19.1	36	Full
Tree 3	RX5	102.6	87.8	14.8	32	Strong
Tree 3	RX13	111.3	91.4	19.9	48.6	Full
Tree 3	RX14	109.0	91.2	17.8	47.3	Full
Tree 3	RX15	106.7	90.8	15.9	45.4	Strong

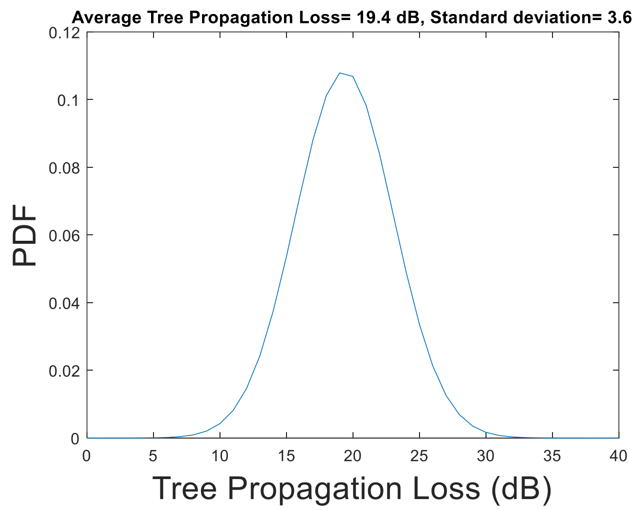

Figure 53 - PDF of tree propagation loss

4.6.4 Findings

NIST CTL has provided four types of outdoor measurements and results: short-distance path loss measurements, long-distance path loss measurements, dielectric constant measurements, and tree propagation measurements.

Path loss measurements confirm the Terragraph sounder's performance. It only has < 2 dB offset in short-distance measurements and 3 dB offset in long-distance measurements compared to theoretical path loss values. The object dielectric constants reported by NIST are close to ITU-reported values (measured in a lab environment). Finally, the tree propagation path loss is reported based on NIST CTL's approach. The mean tree path loss and standard deviation are reported.

4.6.5 References

[2] https://en.wikipedia.org/wiki/Fresnel_equations

[3] https://www.itu.int/dms_pubrec/itu-r/rec/p/R-REC-P.2040-1-201507-I!!PDF-E.pdf

[4] https://www.microwaves101.com/encyclopedias/miscellaneous-dielectric-constants

[5] https://en.wikipedia.org/wiki/Friis_transmission_equation

4.7 Northeastern University

4.7.1 Scope of work

The projects conducted at the Institute for the Wireless Internet of Things at Northeastern University targeted both measurement campaigns and novel mmWave applications for mobile networks.

An initial measurement phase was oriented to characterize the operational points and the performance of Terragraph sounders in a series of indoor/outdoor scenarios and in a number of setups—including different line-of-sight conditions, disparate surrounding objects and material, surrounding object mobility patterns, and varied weather conditions.

The initial measurement campaign was tailored to understand the performance, operational point, and channel characteristics under different deployment scenarios.

Afterward we put our expertise at work to test new uses of mmWave spectrum in mobile scenarios. We leveraged the unique UAV lab facility at the Kosta’s Research Institute Innovation Campus to design, prototype and test UAV-based mmWave communication solutions on Terragraph.

4.7.2 Measurements and outcomes

4.7.2.1 Measurement campaign

The goal of our experiments was to analyze some of the effects that typically occur in different scenarios at mmWave frequencies. To this extent, we used the Terragraph sounders, operating with the standard 802.11ad and configured at 60.48 GHz, to perform a measurement campaign in several indoor and outdoor scenarios—including an empty room, a rich scattering laboratory, and an outdoor bridge with reflecting metal walls. With the measurements collected, we analyzed different physical parameters of the communication link, such as path loss, delay spread and SNR post-equalization. Our analysis revealed relevant effects particular to environments in the 60 GHz band, which must be considered for real deployments.

4.7.2.1.1 Indoor

Effect of blockage: for this scenario we located the transmitter and receiver at a distance of 16.4 ft in an empty workbench (Figure 54). Then we placed two obstacles between them—a cardboard box and human body.

Figure 55 shows that, contrary to what was expected, we only observed a power drop of 3 dB for the former case, whereas Figure 56 shows how the human body greatly attenuated the signal , making transmission only feasible through wall reflections. Moreover, by analyzing the large delay spread of the signal blocked by the human body (Figure 57), we can infer the signal was scattered and arrived at the receiver from multiple delayed paths.

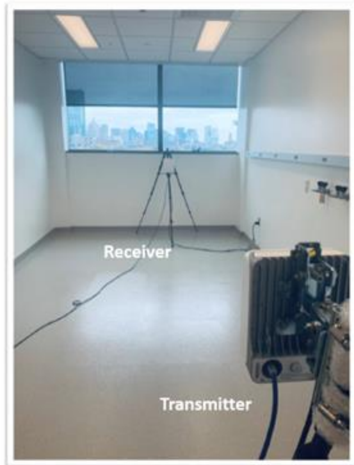

Figure 54 – Workbench setup

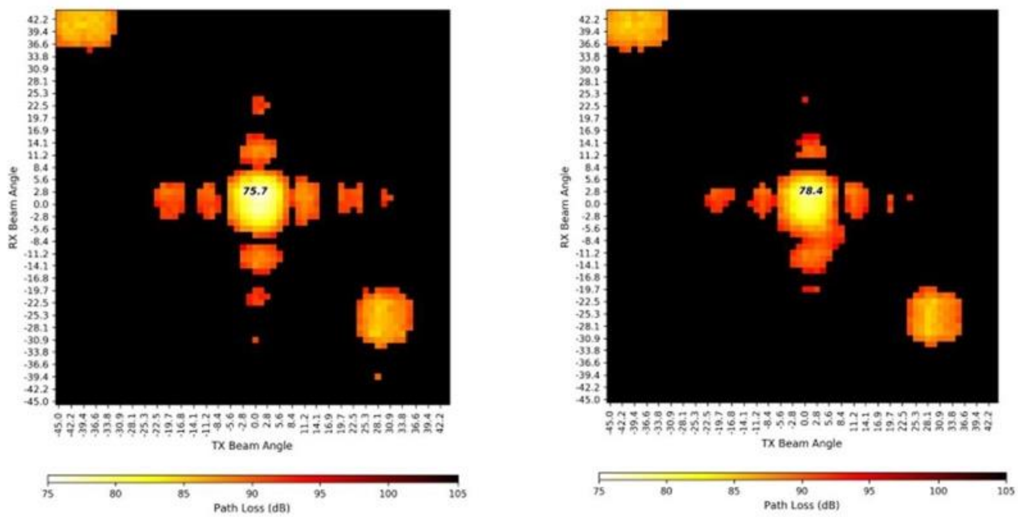

Figure 55 – Path loss for cardboard blockage

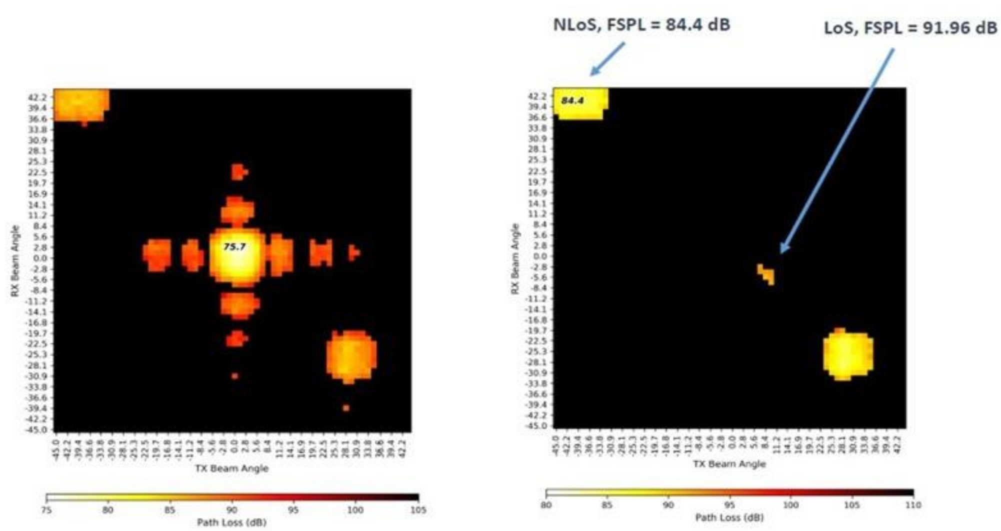

Figure 56 – Path loss for human body blockage

Reflections on different materials – We compared the path loss for the link reflected on the wall (Figure 56) to the path loss in Figure 58 (which corresponds to reflections on a glass surface). The collected data show that path loss for the same distance is 3.2 dB higher for the latter case, thus wall reflections may be preferred for transmission.

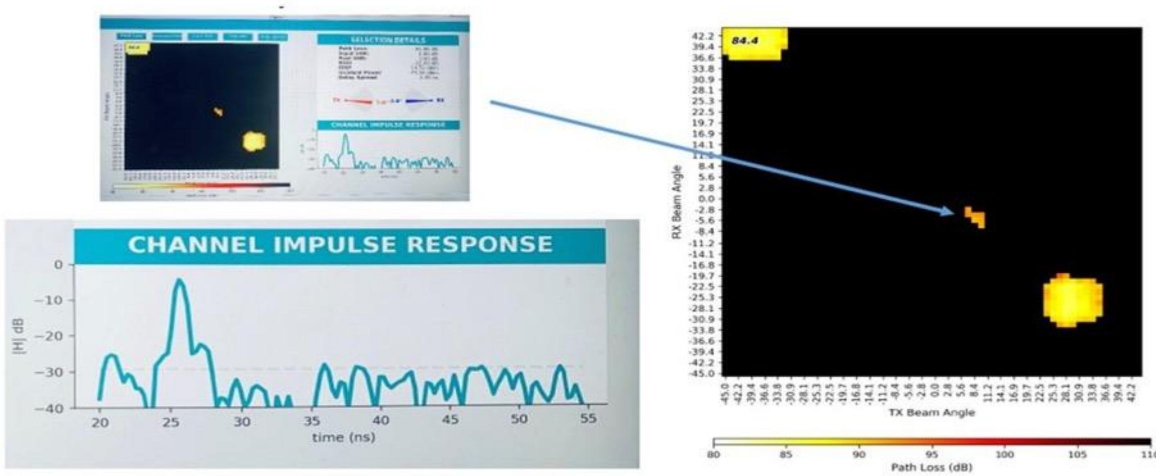

Figure 57 – Delay spread for human body blockage

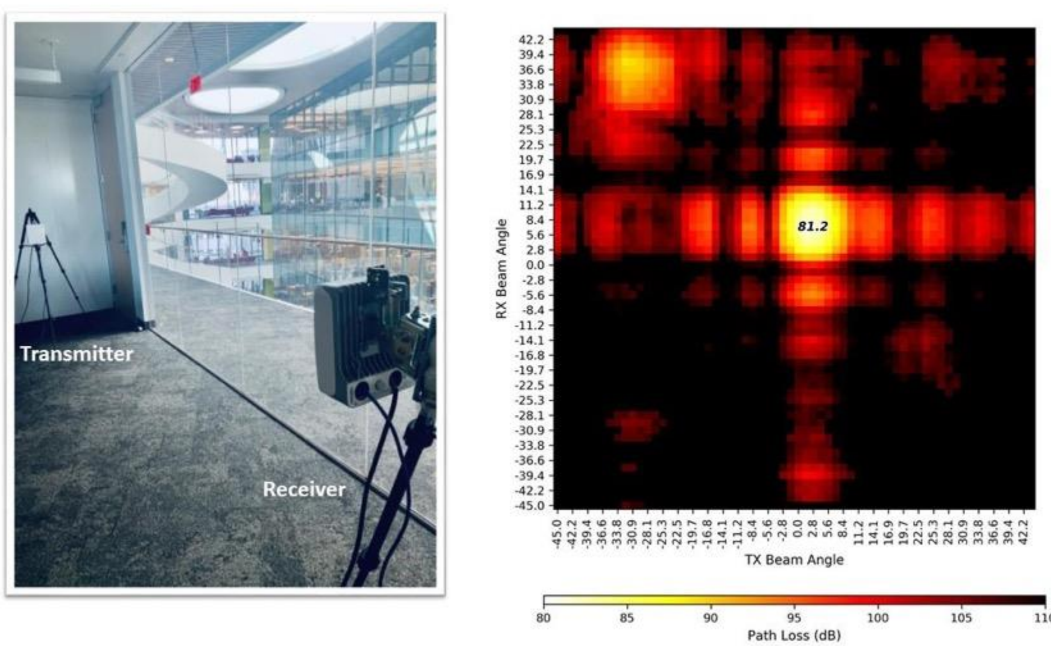

Figure 58 – Path loss for reflection on glass surface

Performance in rich scattering environments (laboratory with multiple scatterers) – Figure 59 shows that for a NLOS path, such as a metallic surface reflection, path loss drops 10 dB compared to the LOS) path. This highlights the possibility of using certain reflectors to overcome undesirable situations (e.g., strong blockage).

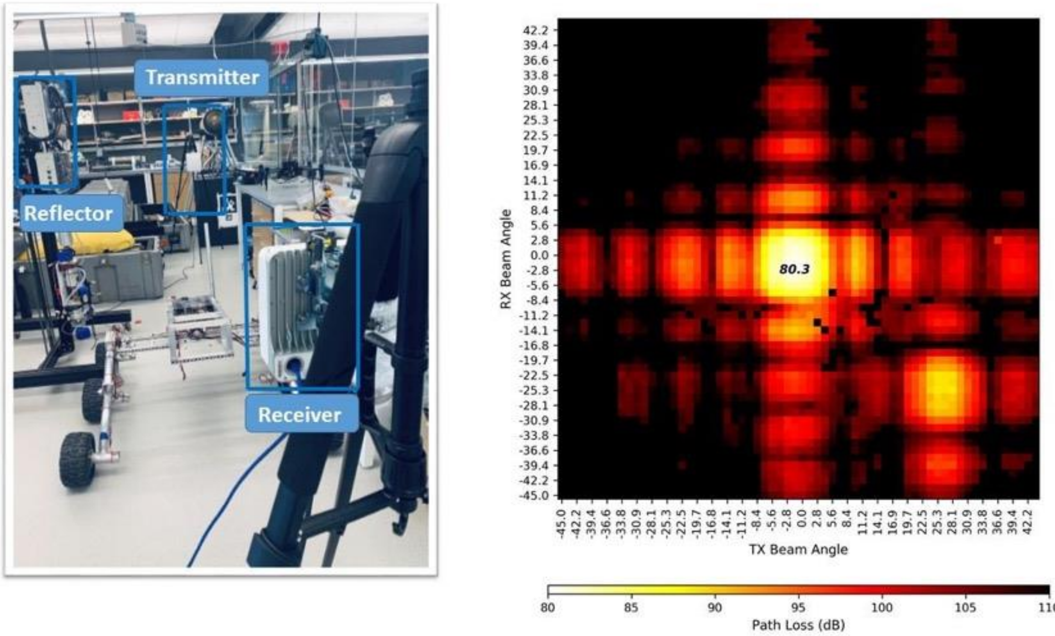

Figure 59 – Path loss in a rich scattering environment

4.7.2.1.2 Outdoor

We performed an outdoor measurement campaign to characterize the propagation as a function of the presence of natural reflectors. In particular, we considered a bridge with high metal walls (Figure 60a). We tested the sounder's default configuration, i.e., full transmit and receive mask with 64 beams at each endpoint, modulation and coding scheme 1. The main experiment consisted of a complete beam sweep at four distances ($d \in \{12.5, 25, 37.5, 50\}$ ft), for which we collected the path loss, STF and post-equalization SNR, and the received power. The following and additional results can also be found in [2].

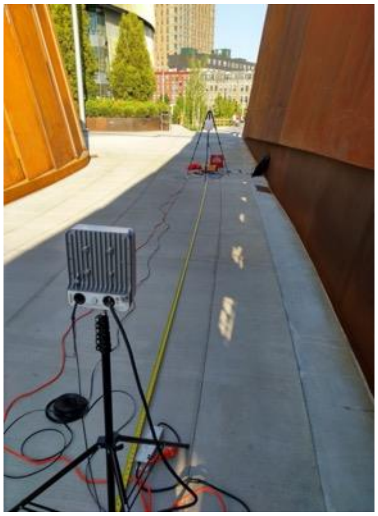

(a) Bridge

(b) Reflection test

Figure 60 – Outdoor test environment

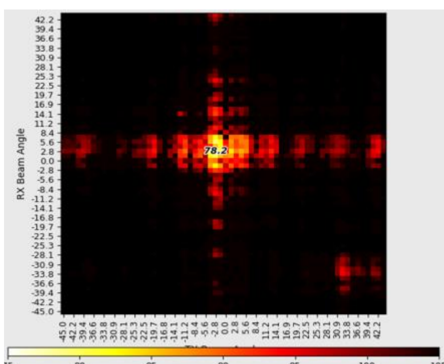

12.5 ft

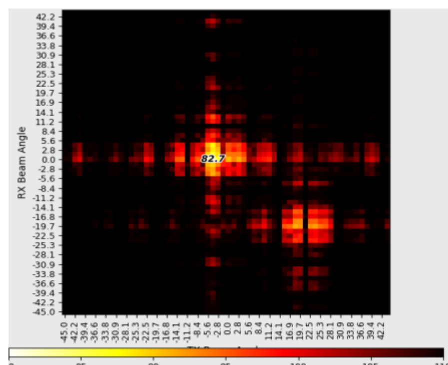

25 ft

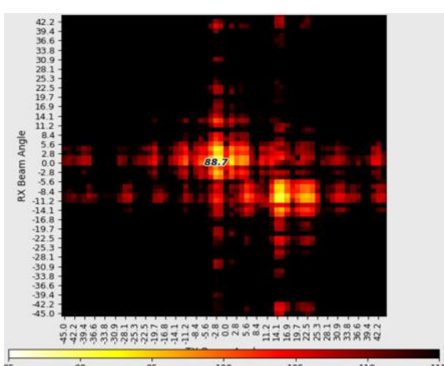

37.5 ft

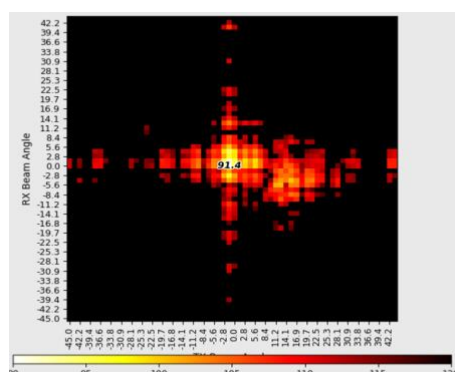

50 ft

Figure 61 – Path loss at different distances, for the complete scan in the Figure 60a scenario

Figure 62 shows path loss at the four measurement distances. As expected, given that the two radios are in LOS conditions, it’s possible to identify a clear cluster of directions that minimize the path loss. These correspond to the center of each figure, i.e., to the Tx and Rx beams steered toward the LOS direction at 0°. Moreover, path loss increases with distance.

However, the most interesting phenomenon is the presence of a reflected path over one of the metallic walls of the bridge, and the contributions it provides to path loss. Given that the distance between the radios and the metallic wall is constant, the reflection angle changes and becomes wider as distance between the sounders decreases. At larger distances the contribution of the reflected path is roughly equivalent to that of the LOS path; for $d = 12.5$ft the reflection is at least 10 dB worse than the LOS path. A similar behavior can be observed in Figure 63 for the received power.

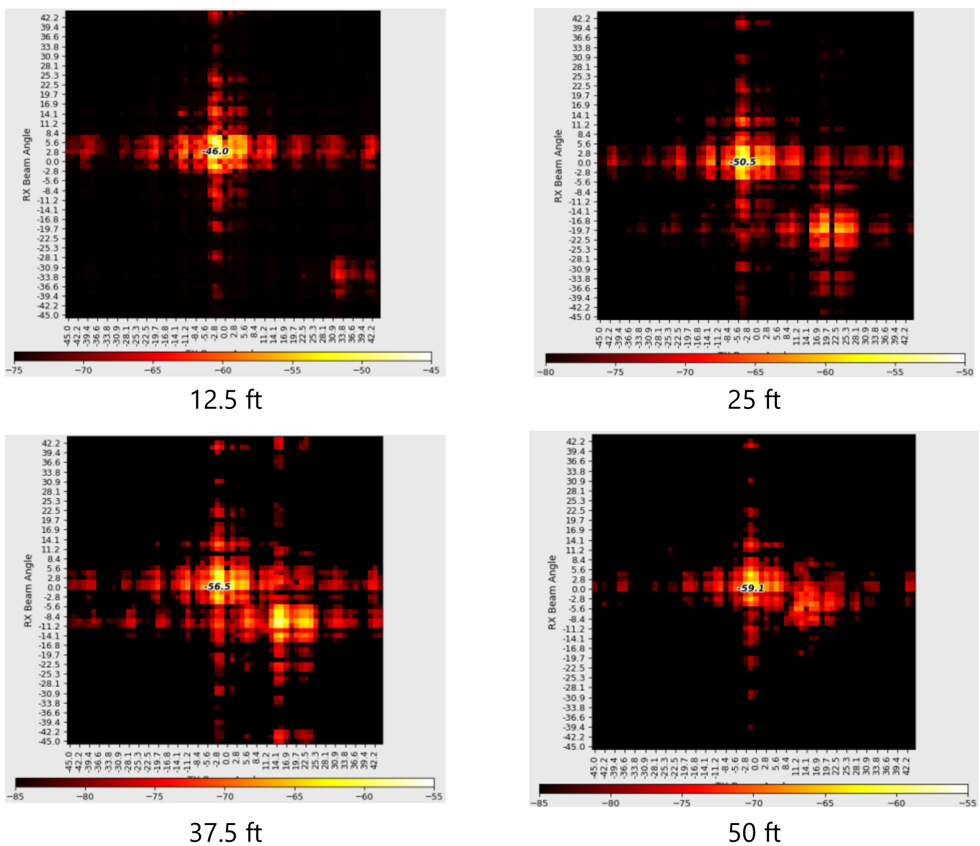

Figure 62 – Received power at different distances, for the complete scan in the Figure 60a scenario

Finally, we tested the setup shown in Figure 60b to understand if it's possible to receive a signal only through the reflection of the bridge metallic wall. The two radios were at a distance $d = 12.5$ ft from the wall, which is not directly facing them (it presents a slight curvature). Figure 64 depicts the received power for a full scan—around -75 dB for the strongest reflected path. However, only a few beam pairs received power in this setup.

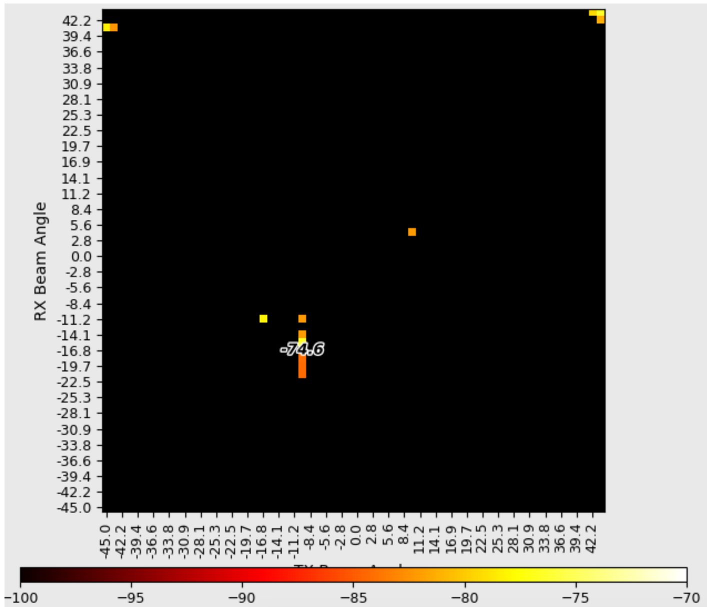

Figure 63 – Received power from a metallic reflection at 12.5 ft

4.7.2.2 Mobile wireless scenario

For this campaign we studied aspects of mmWave UAV-based communications. Here we deployed a DJI Matrice 600 (M600) Pro UAV, having mounted a 60 GHz mmWave Terragraph radio and an Intel NUC 7i7DNKE Mini PC to it.

The DJI M600 Pro is a hexacopter UAV for industrial applications. Its full dimensions are 1.67 × 1.52 × 0.73 m, it weighs 9.5 kg, and it can carry a 6 kg maximum payload. Its maximum speed is 64.8 km/h. It's equipped with six 4500 mAh TB47S batteries, guaranteeing a flight time of 16 minutes at full payload capacity.

As for embedded sensors, the drone is equipped with three inertial measurement units (IMUs, combining accelerometer, gyroscope, and magnetometer), and three global navigation satellite systems (GNSS) modules that permit a fine-grained localization of the UAV.

The UAVs sensors and motors interface with the ancillary A3 Pro DJI flight controller. The latter exposes an API to an onboard SDK; it enables drone control by uploading flying missions with specific GPS waypoints, as well as the monitoring of sensor readings (e.g., altitude and location).

We used an Intel NUC mini-PC (mounted on the drone) to operate the Terragraph radios and interface with the A3 flight controller. With an Intel Core i7 processor and 32 GB RAM, the small NUC (101.60 × 101.60 × 25.69 mm, 0.61 kg) has sufficient computational ability to manage the drone flight missions and interface with the Terragraph radios. It's powered by the UAV batteries through a DC – DC step-up power supply and interfaces with the A3 flight controller through a JTAG-USB cable and the 60 GHz radio through a 1 Gbps Ethernet cable.

We used Terragraph mmWave radios optimized for the 60 GHz frequency band; each was equipped with Tx and Rx arrays of 36 × 8 antenna elements. Each array covers an angular space of 90° with a total of 64 beam directions—each being as fine as 2.8°—while the radios have an EIRP of 45 dBm.

mmBAC: Location-aided mmWave backhaul management for UAV-based aerial cells

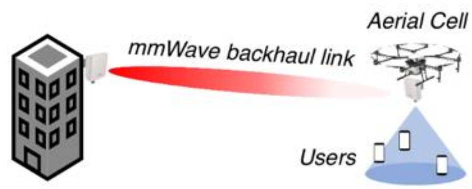

Employing the team's unmanned aerial system expertise, we developed mmBAC—an optimized beam management solution for mobile nodes with an air-to-ground mmWave backhaul link. It was first introduced at ACM mmNets 2019 and uses a point-to-point mmWave link, where one endpoint is aerial (e.g., a UAV-based cell) and the other is ground-based.

The problem mmBAC proposes to address is the following: 'How to optimize the mmWave beam management of such a system, where one endpoint is fixed, and the other frequently relocates—possibly never settling?"

We developed an algorithm that employs side information, e.g., relative positioning of the two endpoints to reinforce beam management procedures. At each UAV relocation, mmBAC derives its endpoint from its GPS data, thereby identifying a master beam pair used for refined beam analysis.

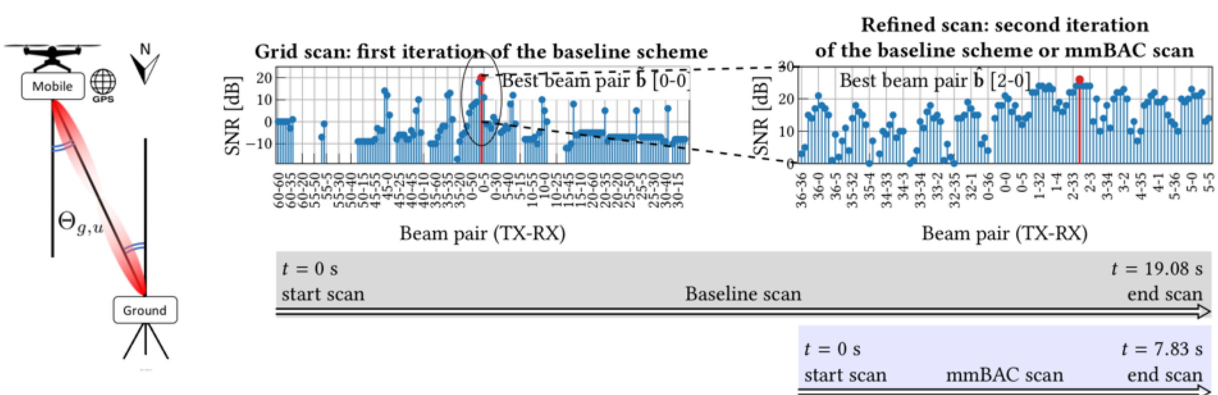

(a) Geometry.

(b) Example of beam scan patterns with baseline and mmBAC schemes.

Figure 64 – mmBAC beam analysis

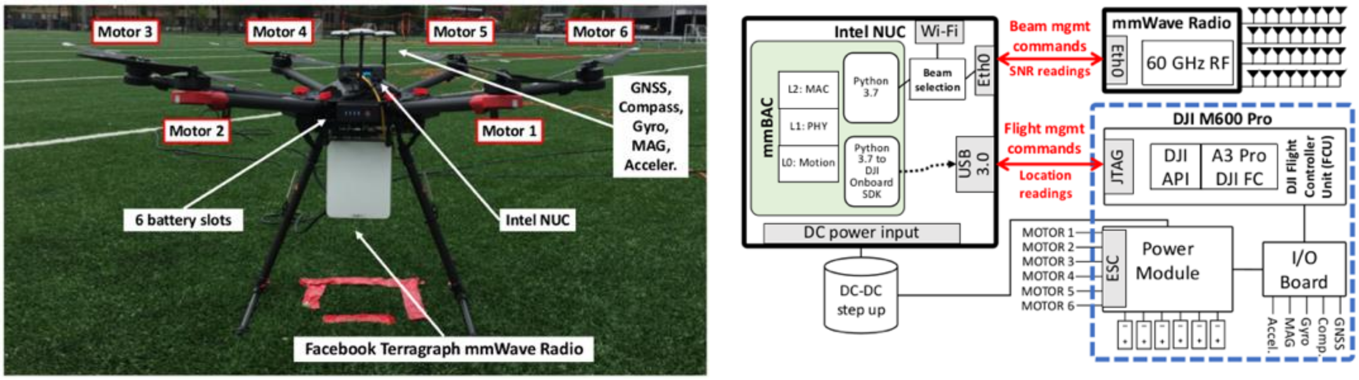

Figure 65 – UAV configuration

In evaluating mmBAC performance, we performed experiments where the aerial endpoint relocates at fixed time intervals, upon which a link set up phase occurs. We tested the mmBAC GPS-aided algorithm against a fast, multi-tier beam scan algorithm that samples one of every 25 beam pairs at regular angular intervals. It identifies a master beam pair to be used as the starting point for a refined search in a second phase. The considered measurement for both beam pair algorithms is their SNR.

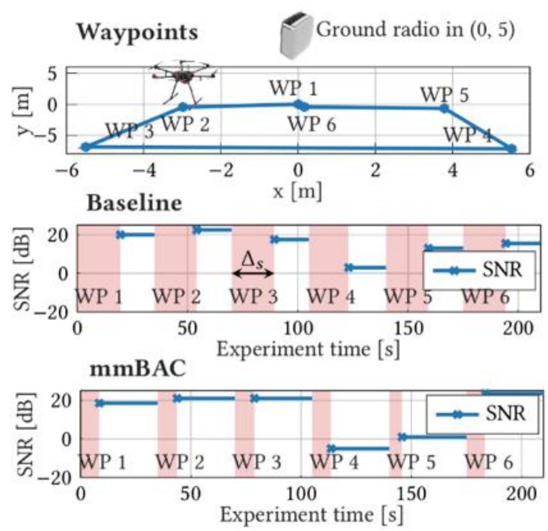

Figure 66 – mmBAC performance

Figure 66 shows mmBAC performance against the iterative beam scan procedure. The red columns show link establishment phase overhead, which identifies the best beam pair. The proposed GPS-aided beam tracking algorithm ensures a 66% overhead reduction in link establishment, compared to a state-of-the-art blind beam management scheme—all while guaranteeing minimal link quality loss. Reducing link establishment overhead leads to a higher spectral efficiency that is particularly important in mobile mmWave networks.

mmWave base stations in the sky: An experimental study of UAV-to-ground communication

We took a systems approach in studying how mmWave radio transmitters mounted on UAVs provide high throughput links under typical hovering conditions. Taking the IEEE 802.11ad protocol running on Terragraph sounder units, we studied the impact of signal fluctuations and suboptimal beam selection using a DJI M600 UAV testbed.

From the insights learned from these empirical studies, coupled with measured antenna radiation patterns, we experimentally validated the first stochastic, air-to-ground mmWave channel model using UAVs as transmitters. Our analytical model complements the classical path loss with additional losses expected in the mmWave channel during hovering, seamlessly merging antenna configuration with the system-level UAV characteristics.

Such characteristics include all types of motion during hovering, such as lateral displacement, roll, pitch, and yaw, their magnitude depending on availability of specialized hardware (e.g., real-time kinematic GPS). We then leveraged our analytical model to mitigate the hovering impact on the air-to-ground link by selecting a near-optimum beam.

4.8 Siradel and Deutsche Telekom

4.8.1 Test setup

The first collected measurements served as validation of the whole setup and process, including simulation comparisons. A maximum 1.3 dB difference was observed between the free-space theory and an LOS link measured in a clear open area. A perfect match was found between the measured and simulated angles of a clear reflected path, along with a 4 dB path loss difference that may be explained by non-calibrated wall material or antenna alignment mismatch.

Then two scenarios were measured for the channel characterization task. The first was located in a 35 m × 150 m street, bordered by two multi-floor office buildings much higher than the antennas. The fixed Tx was positioned at one end, while the Rx was moved to four positions along the street (Figure 67). The Tx – Rx direct. LOS link was parallel to the street axis; the Tx – Rx distance changed from 27.8 m to 118 m. Two parallel rows were measured, with Tx located at respectively 2.16 m from the closest building façade (sidewalk sub-scenario) and 13.3 m (middle-path sub-scenario).

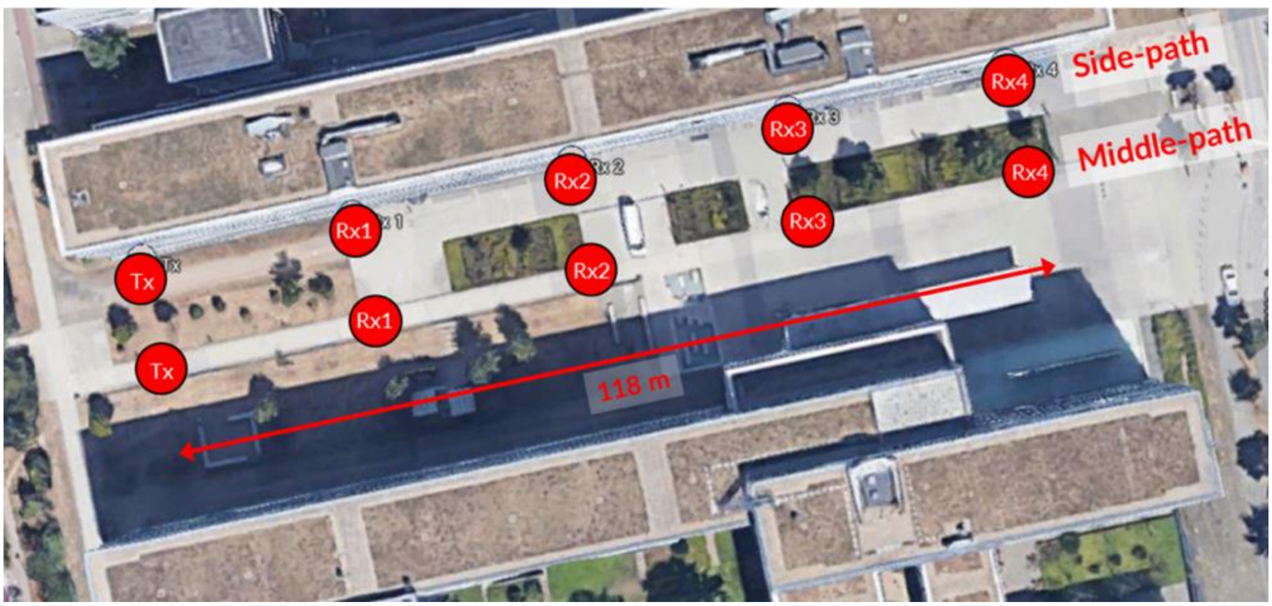

Figure 67 – Measurement positions in the urban canyon scenario

Figure 68 shows the antennas positioned on a trolley 3 meters aboveground. The antenna bore sights were approximately aligned (manually pointed toward each other). The façade was a metallic structure having large windows, but all were covered by a metallic shutter (sun protection) at the time of the measurements. A parking lot entrance near the middle of the north building presented a large gap in the façade. Some trees and bushes were present in the street between the buildings.

The second scenario took place along a residential street with three-story apartment buildings sparsely distributed on each side. Measurements were collected along one sidewalk. The fixed Tx was located at 7 m from the closest building wall, while the Rx was moved at seven positions at an average distance of 10 m each (Figure 69). Antennas were aligned as for the previous scenario.

Figure 68 – Equipment setup within the urban canyon environment

Figure 69 – Measurement positions in the residential scenario

Figure 70 – Equipment setup within the residential environment

A single pair of Tx and Rx positions in the residential scenario is shown in Figure 70. Many trees and bushes were present along the sidewalks or near the buildings. The façades are complex with concrete walls, large windows (possibly hidden by plastic shutters), and balconies. Many signposts and lampposts are in the measurement vicinity, along with the presence of parked cars. Antennas height is 3 m, so most of the interactions in the propagation environment (apart from the direct path) are due to the vegetation, lampposts, and the building façade.

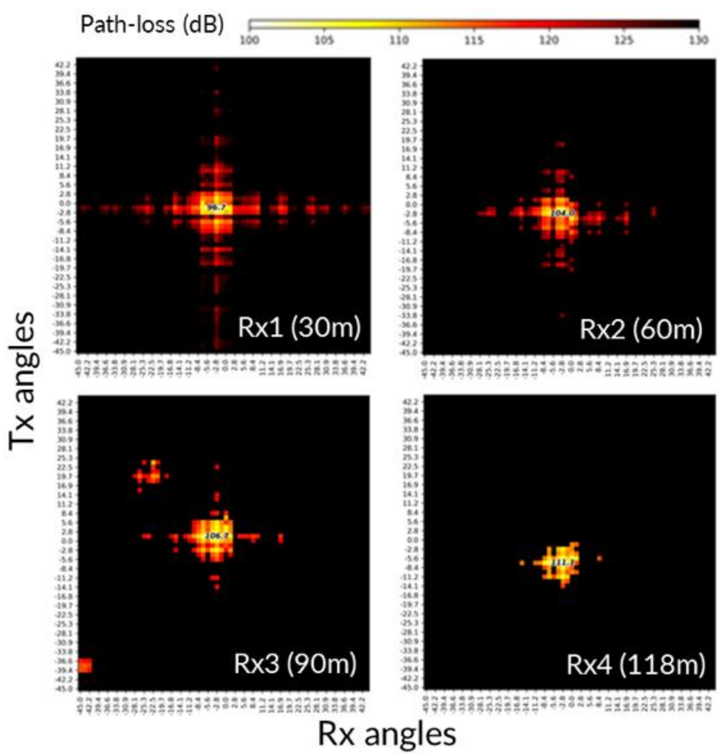

Figure 71 – Measured angular power response from the urban canyon scenario – middle-path

The measurements made directional received power and path loss results available. Due to angular equipment azimuth limitations along with its sensitivity, the dominant (and only) path for most combinations is direct. Figure 71 provides the measured path loss values for the four Rx positions of the middle-path, sub-scenario shown in Figure 67. With a clear LOS component, path loss increases with increased distance, there being a 14.4 dB difference between the first and the last Rx positions (separated by a distance of 90 m).

4.8.2 Ray-based model principles

The measurements described above were used to validate the ray-based simulations; further analysis of the in-street backhaul channel at 60 GHz was performed using the capabilities of the ray-based tool.

4.8.2.1 Deterministic prediction

Ray-based deterministic simulations were performed using the Volcano tool[6]. Ray-launching is considered to create multiple paths caused by various channel phenomena such as reflection and diffraction on various building façades and the ground. In-street objects, such as vegetation or urban fixtures, generate blockage or attenuation in addition to above-clutter diffraction.

The tool was adjusted and validated with various measurements at 60 GHz over the years in different scenarios. For this paper, backhaul pole-to-pole measurements were considered to validate the simulation framework, as well as in performing further analysis to understand the 60 GHz channel. A linear loss of 5 dB/m was used for calculating an average transmission loss through the tree foliage. Since Tx and Rx height was 3 m, there was no impact from cars (their roofs being lower), and no reflection from their roofs was considered.

4.8.2.2 LiDAR data use

The propagation model[5] uses highly detailed and accurate LiDAR map data. This enables consideration of actual trees and other in-street objects with their actual 3D shape. Blockage detection and estimated transmission depth is important at the investigated high frequency. For ease of LOS obstruction analysis, the VolcanoUrban tool also provides the possibility of illustrating the vertical profile of any link.

LiDAR point cloud data was collected for the scenarios presented in section 4.8.1. It was captured during the summer when leaves are present, and was obtained with a density and measurement protocol that guaranteed a precise 3D representation of most trees located along the street. The 60 GHz measurements were collected a few weeks after the LiDAR data, and with similar vegetation. Vegetation and other static objects such as lampposts were extracted from the point cloud data to complement the 3D building vectors.

4.8.3 60-GHz backhaul measurement and simulation analysis

Measurements for the residential scenario described in section 4.8.1 were used to validate the ray-based simulations in section 4.8.2 and, inversely, the simulated ray-paths enabled us to understand or confirm the physics of the observed channel. Further analysis was then conducted using a new Rx unit.

4.8.3.1 Residential scenario

Outdoor path loss is shown in Figure 72 in consideration of the LiDAR data and pole-to-pole backhaul measurements for the different Rx positions. Note the new virtual Rx positions that have been considered on the parallel side of the road to further evaluate the impact of street-side objects.

The path loss was calculated by considering the strongest path (or beam-to-beam value) obtained from the respective simulations and measurements. At positions closer than 40 m, measurements and simulations correlate well with expected performance. Due to issues such as antennas misalignment and accuracy of onsite GPS coordinates obtained during the measurements, we could expect a margin of error of up to ±6 dB. On average, the difference between the measurements and ray-based LiDAR simulations is 3.9 dB up to the receiver position 4 (40 m).

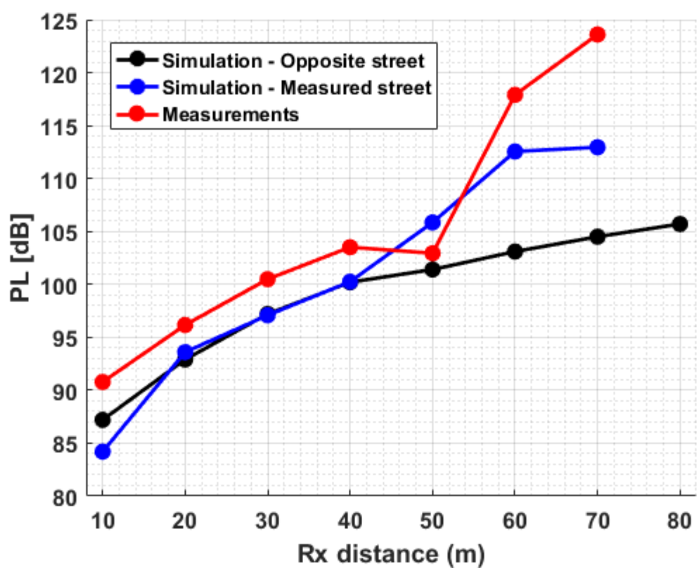

Figure 72 – Comparison between measured and simulated path loss in the residential scenario

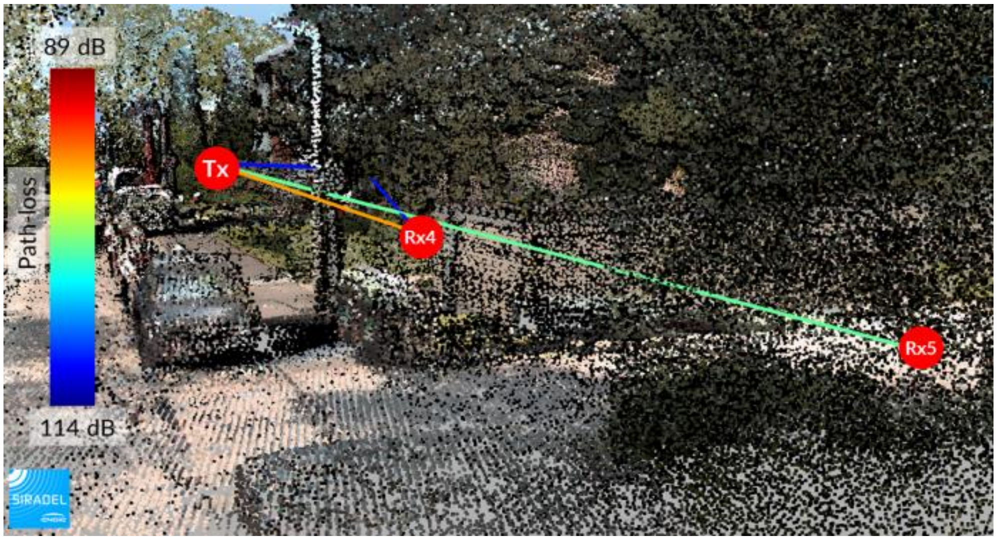

Figure 73 – Dominant simulated paths at two Rx positions in the residential scenario (side view)

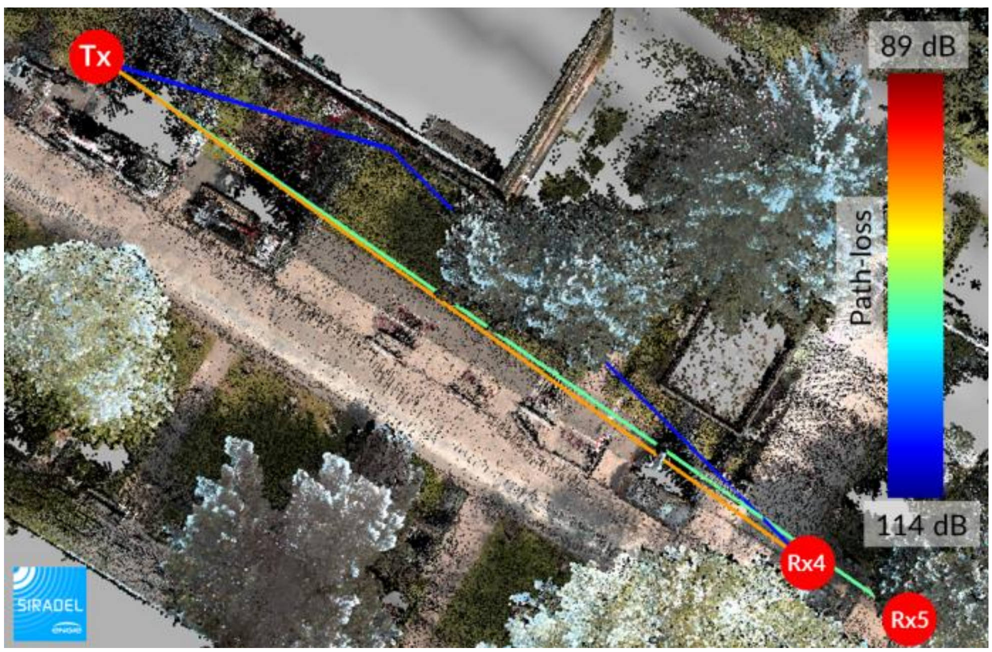

Figure 74 – Dominant simulated paths at two Rx positions in the residential scenario (top view)

A lamppost was located at 38.6 m from the Tx but didn't impact the direct LOS path at Rx position 4 (Figures 73 and 74). Rx positions greater than 40 m were impacted, as it obstructs the direct path. Another factor was transmission loss through a tree located at a distance of 53 m from the Tx position. The vertical profile at Rx position 6 includes the lamppost at 38.6 m and tree foliage from the LiDAR data (Figure 75). Direct path loss increased significantly due to these obstructions.

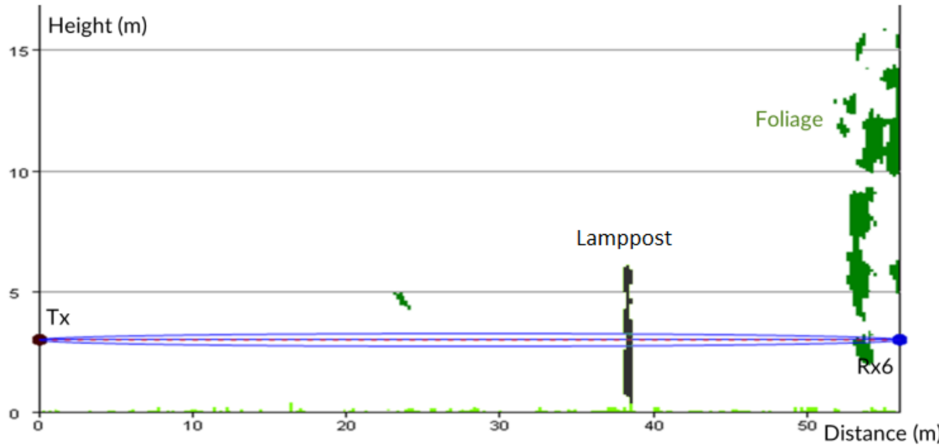

Figure 75 – Vertical profile along the path to Rx position 6 (deep green: vegetation; light green: lamppost)

For an operational, in-street backhaul deployment, a solution to the blockage or obstruction by in-street objects (such as lampposts and vegetation along the same sidewalk) is to consider a node on the parallel side of the street. Ray-based simulations were conducted in this alternative scenario to confirm the LOS situation is more likely (assuming the link passes above all vehicles driving along the road). The black curve in Figure 72 shows the resulting path loss, which continues to grow proportionally to log-distance beyond 40 meters.

4.8.3.2 Urban canyon scenario

In the urban canyon scenario, measurements were collected at eight Rx positions—four for each of the two cases: sidewalk and middle-path. Figure 76 shows the ray-based simulations for the Rx positions in the middle-path case. The LOS direct path is dominant for all four positions.

At short distances when the Rx is very close to the Tx, the angle of reflected ray arrival is large. Since the used channel sounder equipment only considers 45˚ angular resolution from the bore sight on either side, such reflections with large arrival angles were not represented in the measurements.

At larger distances, arrival angle is reduced but the path loss increases. In addition, the probability of increased path loss due to vegetation and other obstacles also increases, further reducing the received power. Such weak reflected paths are also impacted by building façade intricacies (e.g., glass doors with metallic frames), which haven't yet been considered in the classification of the LiDAR data. As a result, most of the paths are LOS direct path contributions with limited reflections.

For the urban canyon middle-path case, Figure 77 compares path loss of the measurements with the ray-based simulations obtained with the LiDAR data. Here, the ray-based simulation results remain within 2 dB of the measured path loss values. The slope of the measured path loss for the different positions is 0.16. Further perspectives could include consideration of larger distances and also different heights of the backhaul equipment. Such changes can be performed in the ray-based simulations setup to evaluate the impact. The comparison between the measurements and simulations for the sidewalk scenario will also be made in the near future.

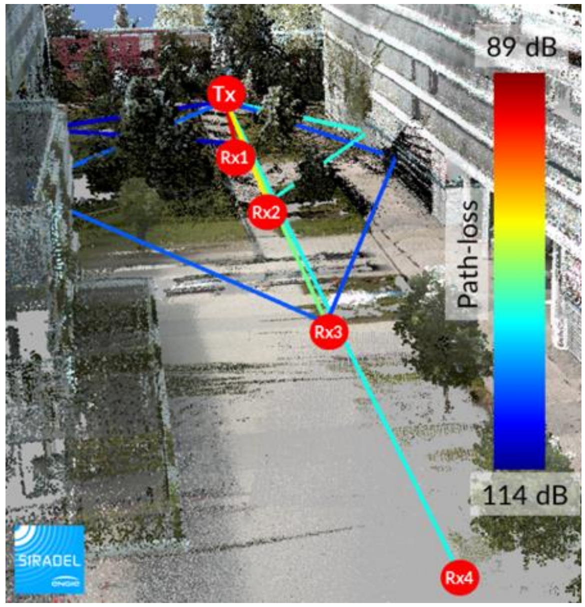

Figure 76 – Dominant simulated paths at four Rx positions in the urban canyon scenario (middle-path)

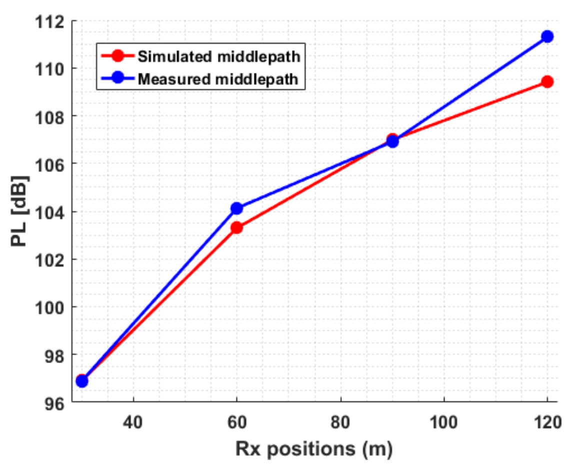

Figure 77 – Comparison between measured and simulated path-loss in the urban canyon scenario – middle-path

4.8.4 Conclusions and perspectives

Initial results of this ongoing work highlight the importance of using accurate map data at higher frequencies, along with accurate 3D positioning of measurement points. In-street objects such as lampposts and vegetation can have a significant impact on the links. In the residential scenario, the receivers were positioned along a street having obstruction from vegetation and lampposts. This led to high path loss values at a distance of about 70 m from the Tx. Measurement and simulation results remain within 10 dB and are highly sensitive to accurate positioning information that is difficult to obtain onsite.

Further investigations on the impact of obstructing lampposts are yet to be performed.

The urban canyon scenario provides results within 2 dB from the measurements due to presence of strong LOS links and limited environmental reflections (partly due to trees and partly to the limited angular range of the measurement equipment). The absence of a rich scattering environment in this particular urban canyon scenario was an interesting finding that wasn't expected; it's to be considered for future evaluations and deployments.

The presented work remains ongoing to achieve a complete characterization of the measured scenarios.

4.8.5 References

[6] https://www.siradel.com/solutions/software/volcano-5g/

4.9 The Ohio State University

4.9.1 Test scope

4.9.1.1 Indoor channel reciprocity measurements

We started our investigation into mmWave band channel reciprocity by conducting indoor experiments. In time-division duplexing (TDD), reciprocity enables channel estimation in uplink via downlink pilots.

4.9.1.2 Outdoor football field measurements

We ran several experiments in a football field for different distance separations between Tx and Rx to assess propagation characteristics over a long distance, as well as to compare measured path losses and calculated free space path losses for several locations.

4.9.1.3 Outdoor measurements to estimate blockage impact

In live sounding mode, channel sounders measure SNR, path loss, and estimated PHY rate every few seconds. We used this mode while conducting experiments on the top floor of a parking garage and in a field to measure the effect of a blockage passing through the LOS path between the Tx and Rx.

4.9.1.4 Outdoor rural area measurements

We ran several outdoor experiments in the South Central Agricultural Laboratory (SCAL) fields in Nebraska, aiming to evaluate propagation characteristics in a rural area. With motivation provided by the previous measurement campaign, we also conducted experiments to see if there might be viable NLOS paths that can contribute to path diversity in a field.

4.9.2 Test setup

4.9.2.1 Indoor channel reciprocity measurements

The channel sounders were positioned four meters apart and attached to tripods set on top of two tables (Figure 78). Then two beam sweeps were performed with identical channel sounder settings and positions: one with Node 1 transmitting and Node 2 receiving, and the other with Node 2 transmitting and Node 1 receiving. An impulse response was observed for both beam sweeps for chosen beam pair.

When transmitting from Node 1 to Node 2, the Tx beam angle was −16.8°, with the Node 2 beam angle at 4.2°. A 0° angle corresponds to the normal direction with respect to the channel sounder face surface. When transmitting from Node 2 to Node 1, the beam angles were set to 4.2° and -16.8°, respectively.

Figure 78 – Indoor measurements were taken in an office environment

Table 8 – Channel sounder parameters for indoor measurements

Parameter	Settings
Antenna mask (Tx & Rx)	0xFFF, 0xFFF, 0xFFF
Tx gain index	15
Averaging (n_stat)	1
Antenna height (Tx & Rx)	1.5 m

4.9.2.2 Outdoor football field measurements

Figure 79 – Outdoor experiments were conducted in a football field by placing Rx at four locations (red circles)

For these experiments, the Tx and Rx were mounted on tripod at a height of 1.5 m. We placed the Rx at four locations (Figure 79) while keeping the Tx stationary. There was always a strong LOS path since there was no obstacle between them during the measurements.

Full beam sweeps were performed for each receiver location. The results were used to calculate the difference between the FSPL and measured path loss for disparate Tx/Rx distance separations and to characterize the multipath field components.

Table 9 – Channel sounder parameters for football field measurements

Parameter	Settings
Antenna mask (Tx & Rx)	0xFFF, 0xFFF, 0xFFF
Tx gain index	25
Averaging (n_stat)	1
Antenna height (Tx & Rx)	1.5 m

4.9.2.3 Outdoor measurements for estimating blockage impact

Figure 80 – Outdoor experiments were conducted on the top floor of a parking garage

This measurement campaign was to evaluate the effect of an obstacle (vehicle) between the Tx and Rx in an outdoor environment. The first measurement was run on the top floor of a parking garage with 10 m separation between the sounders (Figure 80). An initial beam sweep was run to find the approximate transmit and receive beam angle pair that would result in the least path loss. This pair was then used in the live sounding mode, during which 1) a sedan drove slowly between the channel sounders twice, then 2) a pedestrian walked once between the sounders. Each time path loss, SNR, and the estimated data rate was measured.

Table 10 – Channel sounder parameters for parking garage measurements

Parameter	Settings
Antenna mask (Tx & Rx)	0xFFF, 0xFFF, 0xFFF
Tx gain index	25
Averaging (n_stat)	1
Antenna height (Tx & Rx)	1 m

The second measurement was conducted in a SCAL field in Nebraska. Here, the Tx was mounted on a pole 40 m from the truck-mounted Rx (Figure 81). Height alignment was checked using a laser pointer. We again performed live sounding using the best beam pair for a stationary Tx and Rx, during which a tractor (Figure 82) moved between the sounders. Its effect in path loss, SNR, and data rate was measured.

Table 11 – Channel sounder parameters for field measurements

Parameter	Settings
Antenna mask (Tx & Rx)	0xFFF, 0xFFF, 0xFFF
Tx gain index	25
Averaging (n_stat)	1
Antenna height (Tx & Rx)	2 m

Figure 81 – Tx and Rx setup for the field measurements

Figure 82 – Tractor movement between sounders

4.9.2.4 Outdoor field measurements

In contrast to urban areas, rural environments don't contain many objects (e.g., buildings, vehicles) that influence radio frequency signal propagation. We therefore have an LOS path between Tx and Rx most of the time. Despite this, partial LOS path obstruction—most typically tree foliage or a truck—can still be a problem. The links can therefore be broken under certain situations due to user mobility or environmental obstacles.

In this campaign we aimed to characterize propagation in a field having a long-distance measurement, then analyze viable NLOS paths in the event an LOS path is obstructed. To this end, we placed the Tx and Rx 150 m apart (Figure 83). The setup was the same as with the previous measurement (Figure 81, Table 11). We also obtained measurements near metal silos in the field (Figure 84) to compare the direct path with reflected path power.

Figure 83 – Field experiment setup (150 m)

Figure 84 – Outdoor experiment near metal silos

4.9.3 Results

4.9.3.1 Indoor channel reciprocity measurements

Figure 85 shows two measured channel impulse responses CIRs that correspond to a specific beam pair we evaluated. At left is the measurement with Node 1 transmitting and Node 2 receiving, with the right-side measurement corresponding with Node 2 transmitting and Node 1 receiving. Comparing the two plots reveals a high degree of reciprocity. The three magnitude peaks indicate that the multipath signals arrive at the receiver with approximately the same delay and attenuation in both cases. Thus, the results show that channel reciprocity holds at 60 GHz in an indoor environment.

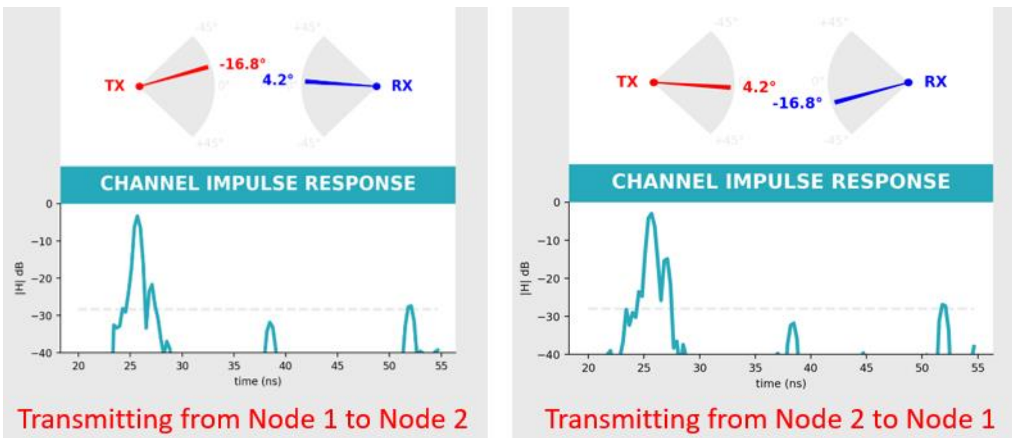

Figure 85 – CIRs with different Tx/Rx sounder roles

4.9.3.2 Outdoor football field measurements

Figure 86 shows path loss heatmaps at four locations. We observed that the metal field light poles are the main reflection sources. Short distances exhibit a more cross-like form, where the main Tx beam overlaps a set of Rx beams. The reflected paths are less observable at 90- and 125 m separation.

Table 12 compares the measured path losses and calculated FSPL at four locations. As expected, measured path loss results follow a decreasing trend, with a deviation of 3 to 6.5 dB from the calculated FSPL.

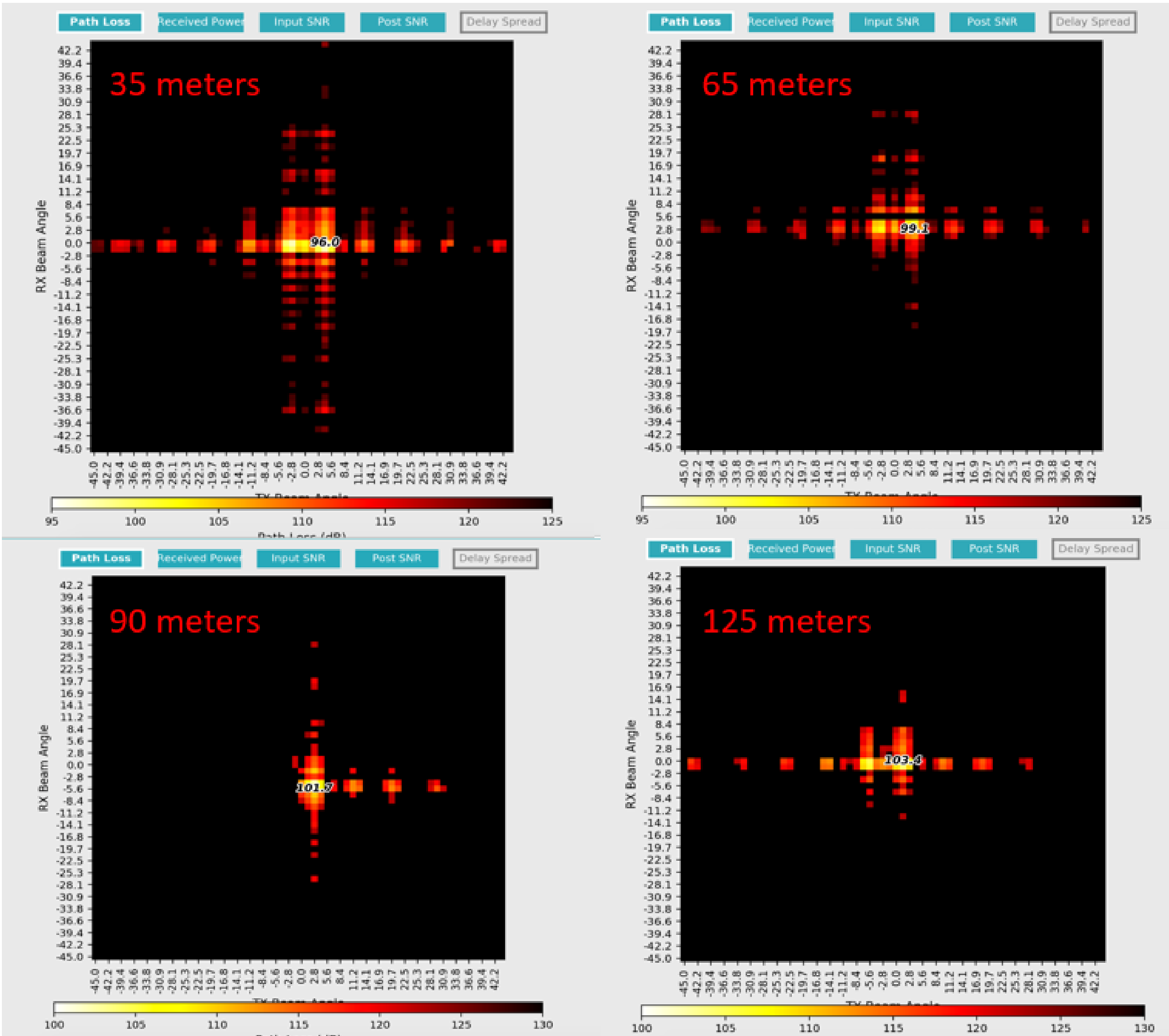

Figure 86 – Path loss heatmaps for four locations

Table 12 – Measured path loss and calculated FSPL for four Rx locations

Distance	Measured Path Loss	FSPL
35 m	96 dB	98.88 dB
65 m	99.1 dB	104 dB
90 m	101.7 dB	107.1 dB
125 m	103.4 dB	109.9 dB

4.9.3.3 Outdoor measurements for estimating blockage impact

Figure 87 shows the result of the live channel sounding for the parking garage scenario. With no obstruction between the sounders, path loss remained steady at about 88 dB and SNR was always greater than 15 dB. SNR decreased dramatically each of the three times the LOS path was blocked. Both times the sedan passed between the sounders, SNR dropped around 15 dB and path loss increased to about 120 dB. When the pedestrian walked between the sounders, SNR dropped to about 9 dB and path loss increased to about 108 dB. As expected, the sedan caused a greater path loss increase than did the pedestrian.

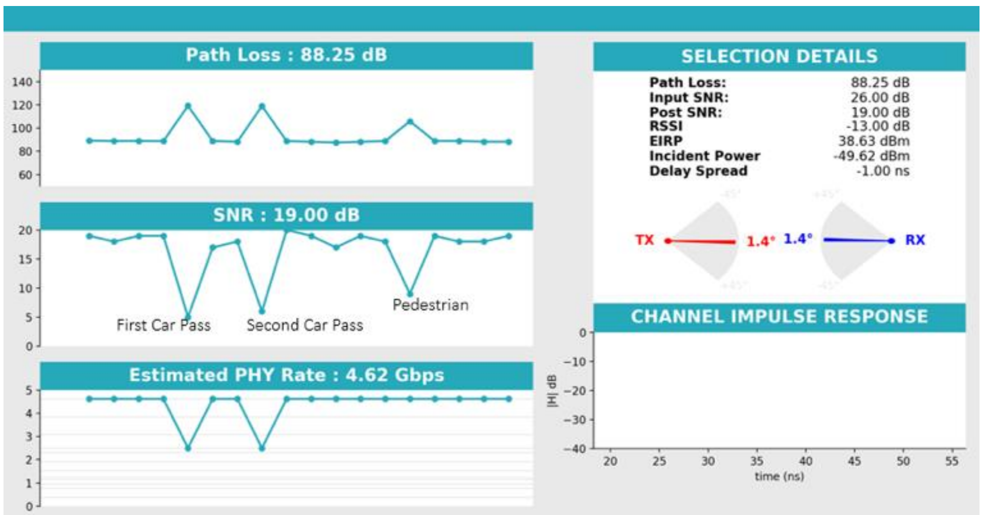

Figure 87 – Live sounding results of the parking garage experiments

For the field experiments we increased Tx – Rx separation to 40 meters from 10 meters and the sounders were placed 1 m higher than the parking garage scenario. We again observed an SNR decrease around 5 dB and a 10 dB increase in path loss (Figure 88) while a tractor moved between the sounders. As expected, increased distance and height decreased blockage impact.

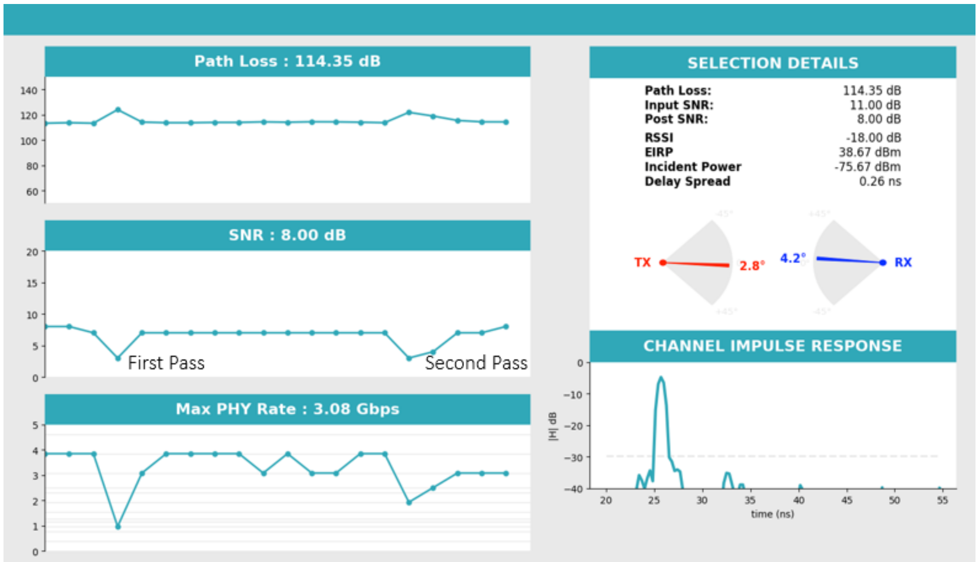

Figure 88 – Live sounding results of the field experiments

4.9.3.4 Field measurements

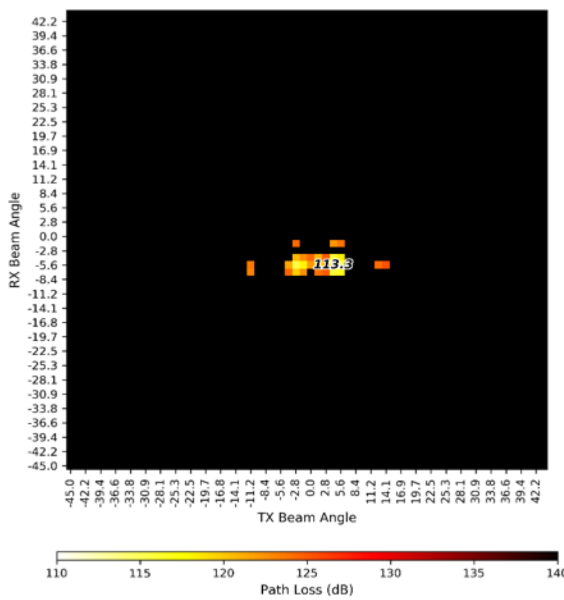

Figure 89 – Path loss heatmap in a field

The measurement was achieved for the Figure 83 scenario. In contrast to urban environments, there were no significant reflections in the field. Measured path loss was 2 dB above the FSPL (Figure 89). Lack of NLOS paths might cause problems when there is no LOS between the sounders, or the LOS path is blocked. To overcome this, artificial reflectors could be placed in such fields to create NLOS paths between the Tx and Rx.

We can also exploit existing field objects to enable NLOS paths. In the measurements taken near metal silos, we observed there is a strong reflection from them. The reflected path power is almost equal (1 dB below) to the direct path (Figure 90). Therefore, we can keep communications active by using such NLOS links where the LOS is cut by foliage or other obstacle (e.g., a truck, as in the previous measurements).

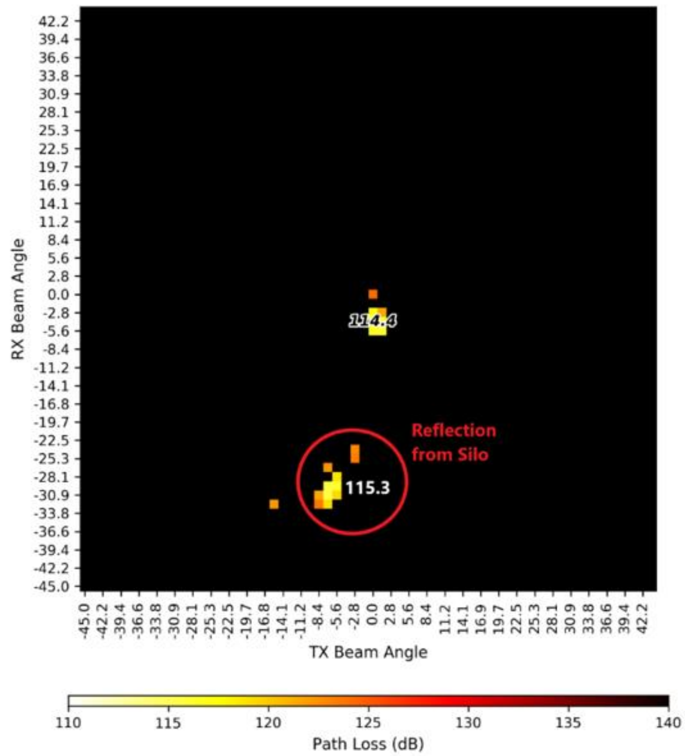

Figure 90 – Path Loss heatmap near metal silos

4.10 Technische Universität Berlin – TUB

The TKN-TUB research group has many years of experience in wireless communications. The current research interests are in architectures and protocols of next-generation wireless communication networks (e.g., mmWave), as well as in protocol engineering having impact on performance and QoS aspects. Therefore, it's of paramount interest for the group to have realistic models for the wireless (interference) channel.

In summary, the group performs experimental measurements, then analyzes the data to learn the relationship between parameters and observed higher-level metrics (e.g., bit or frame errors) so as to create digital models that can be used within time-discrete network simulators.

4.10.1 Test scope

In this work we analyzed selected aspects of 60 GHz (mmWave) channel propagation. We started with a simple experiment to analyze how well mmWave can penetrate materials common to typical indoor office environments[7] We then wanted to characterize the impact of beam width on SNR.

Thereafter, we analyzed mmWave in a multipath environment to see whether the CIR provides enough information to draw conclusions about the environment. Lastly, we performed mmWave link-level measurements to understand 1) the impact of multipath on packet error rate (PER) and 2) the relationship between receive power and SNR on PER.

4.10.2 Test setup

We ran experiments using a pair of Terragraph sounders. Results were collected using the channel sounder package and later processed using Matlab/Python tools. Parameters such as SNR, receive power, path loss, PER, and CIR were obtained from captured measurements results and analyzed. If not otherwise mentioned, a default configuration for the beam width (2.8°) and MCS 0 were used. The distances between the TG nodes and/or obstacles were obtained using a laser rangefinder.

4.10.3 Results

We conducted six experiments, each having a different objective.

Experiment 1: (LOS blockage)

Here we investigated the impact of LOS path blockage of an mmWave radio link. Tx and Rx were placed at a distance of 2 m from each other and with a clear LOS path. During the experiment placed some sheets of photocopying paper (A4, 80 gr) between the two nodes (Figure 91). We divide 500 papers into 8 stacks, add one stack up each time, and measure the SNR and path loss values.

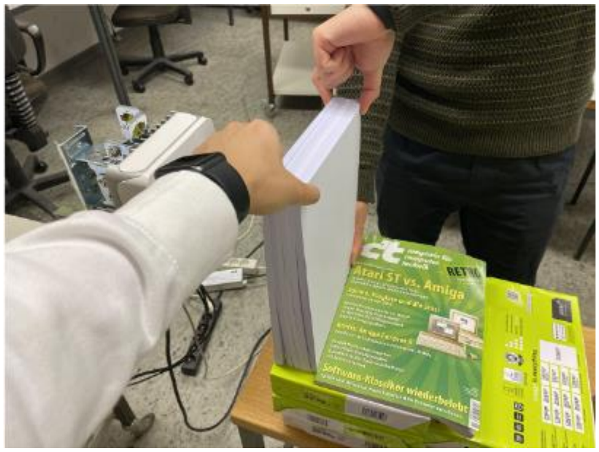

Figure 91 – Experiment 1: Blocking the LOS path with photocopying paper

Result 1

The following figures show the relationship between the number of sheets of paper and SNR (Figure 92) and path loss (Figure 93) values. The more sheets of paper block the LOS path the more SNR drops and path loss increases. From the results, we conclude that path loss grows logarithmically (linearly in dB units) for each additional sheet, where path loss increased by 0.05dB. (100 sheets of paper has a thickness of 1 cm.)

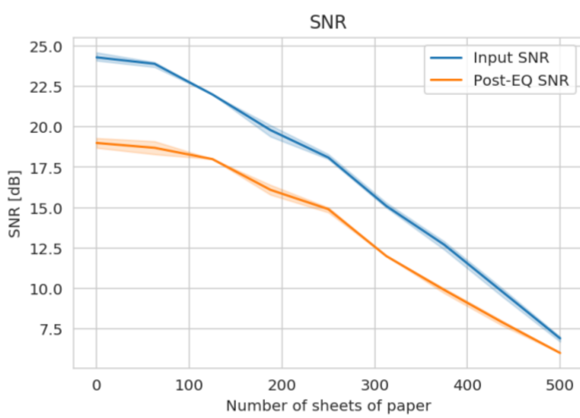

Figure 92 – EXP 1: Relationship between number of sheets of paper and SNR

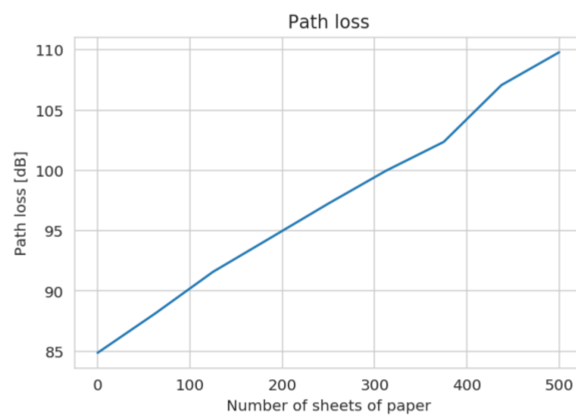

Figure 93 – EXP 1: Relationship between number of sheets of paper and path loss

Experiment 2 – Beam width

In this experiment, we analyzed the impact of mmWave beam width on SNR. The Tx and Rx nodes were placed at a distance of 2 m from one another with a clear LOS path.

Result 2

Figure 94 shows the relationship between beam width and SNR. Here, using the widest beam width resulted in a severe SNR drop—around 20 dB. Since the nodes are calibrated for only three width settings—102°, 8.5°, and 2.8°—we saw a large gap between the medium and widest setting and were unable to interpolate the in-between results.

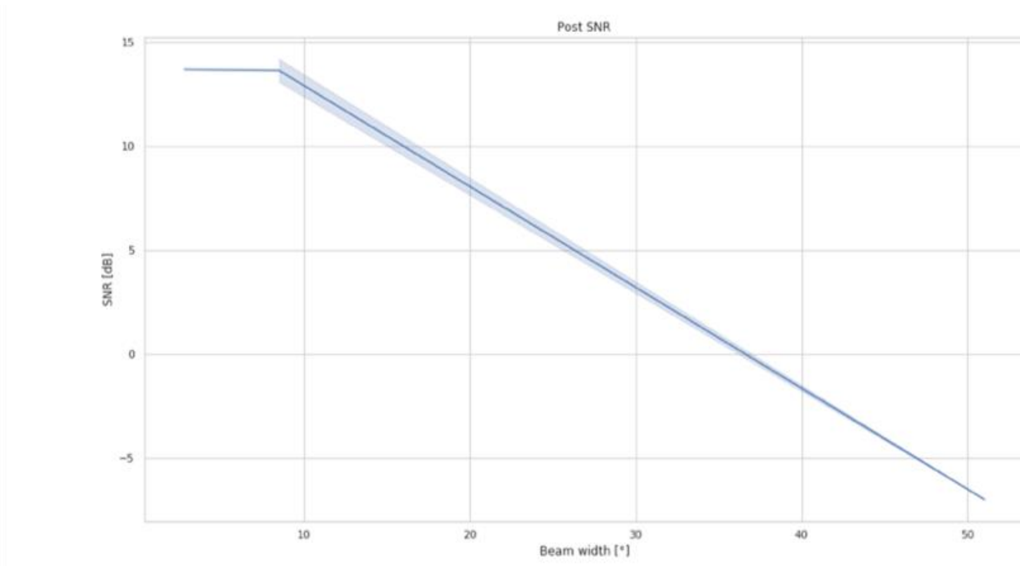

Figure 94 – EXP 2: Relationship between beam width and SNR

Experiment 3 – CSI & multipath

For this experiment we analyzed mmWave link characteristics in a multipath environment by examining the CIR collected by the nodes (Figure 95). In this setup the Tx pencil beam (width of 2.8°) was aligned with the Rx (0° beam angle), with reflections occurring over the sidelobes.

Based on the measured distances:

- direct path length between nodes
- reflection path length (Tx-mirror-Rx, Figure 95)

The difference between the two can be calculated as 4.59 m−3.27 m = 1.32 m. Given such a configuration, the expected multipath reflection delay relative to the LOS path is:

path difference [m] / speed of light = 1.32 m / c = 4.4 ns

Figure 95 – EXP 3: Experiment setup for multipath propagation

Result 3

Figure 96 shows the measured CIR. The first peak is the impulse response from the direct path (LOS) between Tx and Rx, while the second represents the impulse response from the mirrored reflection. The third peak (some reflection off the left wall) can be ignored. Perfectly fitting our prediction, the observed signal drop was 13 dB with a 4.4 ns delay.

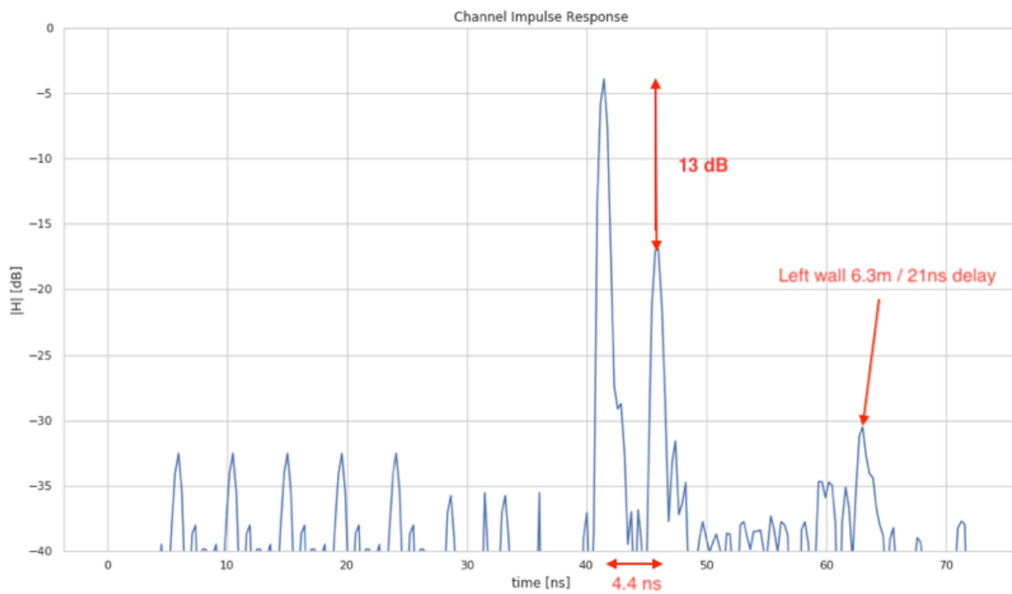

Figure 96 – EXP 3: Channel Impulse Response (CIR) from multipath environment

Experiment 4 – Wooden tunnel

In this experiment, we wanted to understand the impact of multipath reflections when communicating through a wooden tunnel (Figure 97).

Figure 97 – EXP 4: Short range LOS inside a wooden tunnel

Result 4

Due to multiple reflections inside the tunnel, as well as reflection from the plastic node enclosures, we saw four significant peaks in the CIR (Figure 98). We were able to estimate the difference between peaks in terms of delay and difference in power.

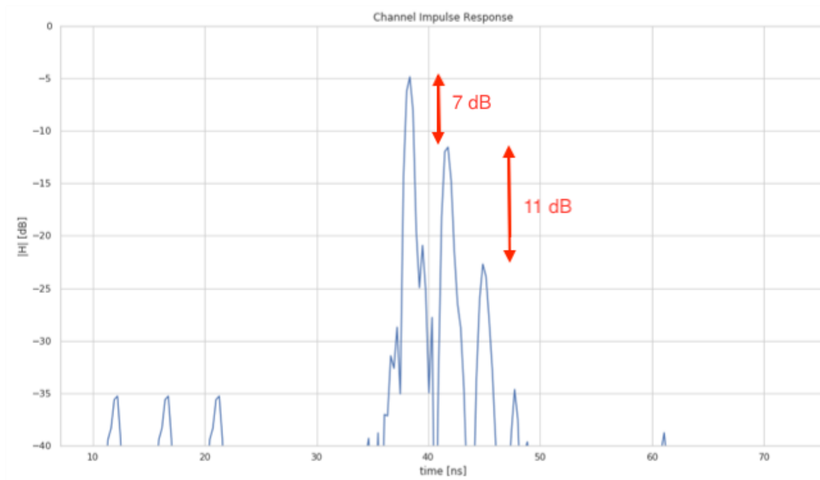

Figure 98 – EXP 4: CIR from multipath inside a wooden tunnel

Experiment 5: (mirror bounce)

Here we wanted to understand the impact of multiple reflections using mirrors (Figure 99).

Figure 99 – EXP 5: Short-range LOS with mirrors to create multiple reflections

Result 5

Figure 100 shows the results. From the CIR we could estimate the distance between the first and second peaks. The Tx signal reflects off the mirror back to the Rx, then back to the Tx over a mirror reflection. The results show the second peak has a relative delay to the first of around 12 ns, which corresponds to a 3.6 m path length—matching our measured values.

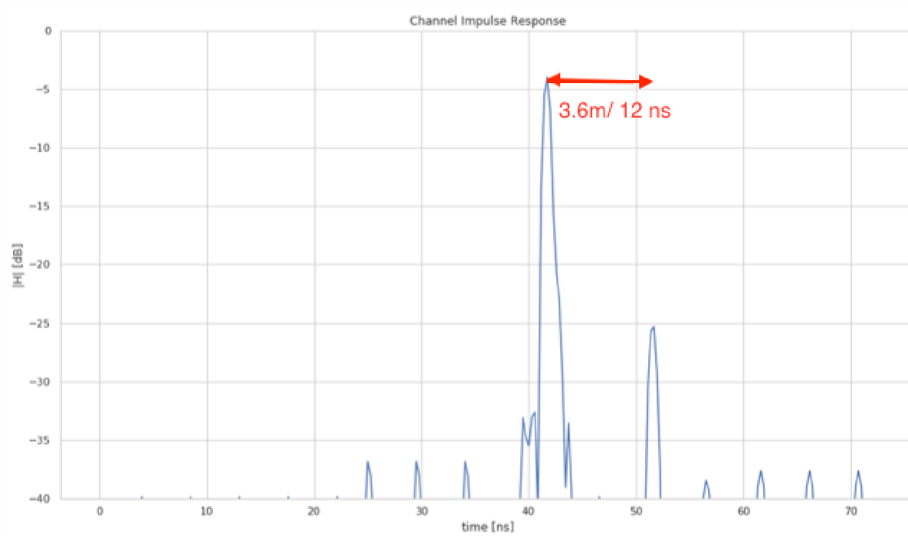

Figure 100 – EXP 5: Channel impulse response

Experiment 6 – Packet error rate

This time we wanted to study the relationship between the receive power and SNR on the packet error rate (PER). Therefore, we created an indoor, office-like environment with a P2P mmWave link having clear LOS and a Tx – Rx distance of 4.7 m (Figure 101). MCS 1 (BPSK ½) was selected for the packet transmission.

Figure 101 – EXP 6: Indoor P2P mmWave link with LOS

Result 6

The scatterplot (Figure 102) shows only a very weak correlation between PER and receive power. There is a wide transition period with many outliers, similar to analyzing the relationship between PER and STF SNR. However, post-processing SNR shows a good correlation to PER with a transition period of just 2dB and only a few outliers—making it a good predictor.

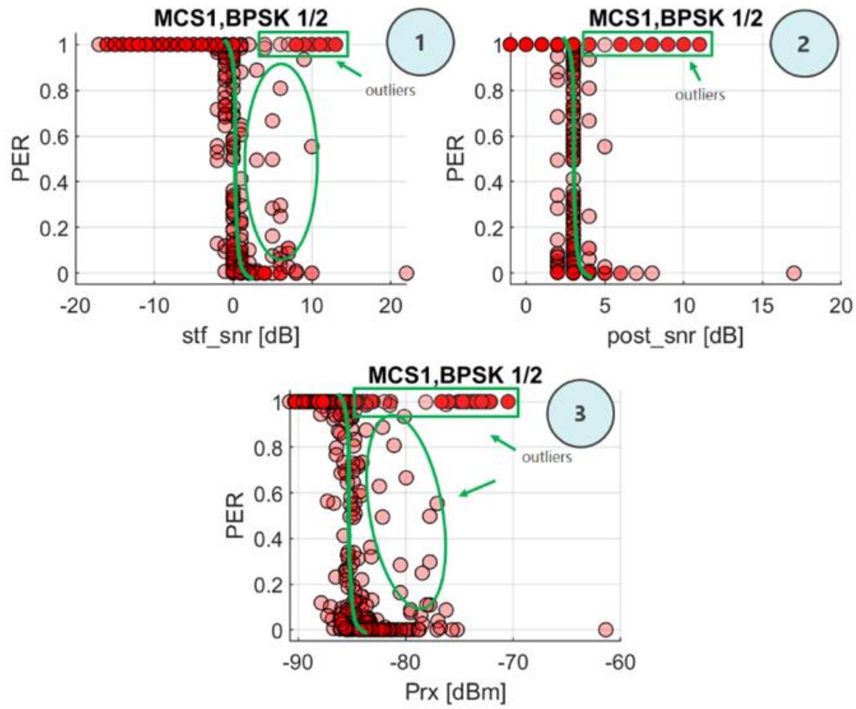

Figure 102 – EXP 6: PER vs. 1) STF SNR, 2) post SNR, 3) receive power

4.10.4 Findings

For this project, the main contents and contribution were as follows:

- In contrast to common belief, mmWave signals can penetrate materials such as paper (wood). Our results reveal that 500 sheets of paper (5 cm thickness) placed in LOS path attenuate the signal by 25 dB.
- The characteristics of an mmWave multipath environment—i.e., number of multipath components (reflections) and their relative difference in path length and signal strength—can be fully captured with channel impulse response (CIR).
- Results from link-level, indoor measurements reveal there is only a weak correlation between receive power and packet error rate (PER). But post-SNR is a good predictor for PER and hence can be used for closed-loop MCS selection algorithms in practical systems.

4.10.5 References

[7] Statement made by Neville Ray, chief technology officer of T-Mobile US: "Millimeter wave (mmWave) spectrum has great potential in terms of speed and capacity, but it doesn't travel far from the cell site and doesn't penetrate materials at all," https://www.t-mobile.com/news/network/the-5g-status-quo-is-clearly-not-good-enough

5 Conclusions and Next Steps

The Channel Sounder Program enabled participants to measure effective propagation and channel response of V-band signals in a variety of settings: indoor, outdoor, suburban, urban, and agricultural. A range of propagation conditions were investigated: in clear LOS, blocked LOS, through foliage, bounced, in traffic, mobile, aerial, and over some weather conditions.

Features of the Channel Sounder Kits allow for measurements of CIR and beam scan path loss. This program contributes to the body of work of V-band channel measurements and modeling.

V-band in LOS conditions

- Indoor, urban, suburban, agriculture settings
- Path loss scales according to model prediction
- V-band radios can effectively mitigate multipath in a rich scattering environment

V-band in OLOS/NLOS conditions

- NLOS path loss is favorable in many cases
- Might take advantage of opportunistic NLOS
- Provides alternate paths in event of fading/ LOS path obstruction

V-band simulation and network planning

- We showed a workflow of LiDAR ➔ signal prediction ➔ network planning
- We showed how to derive physical modeling, such as how dielectric constant of materials and foliage can be used for signal prediction

V-band and mobility

- Vehicle static and dynamic behavior was considered
- Aerial platforms and mmWave

Potential future efforts include

- Study of propagation properties for specific use cases, such as mobile backhaul (MBH) and small cell backhaul (SCBH)
- Long-term availability performance of links with different geometries (e.g., unblocked, foliage-blocked, bounced)
- Effects of street-level dynamics, such as cars, trucks, pedestrians on link performance
- Effects of polarizations choices
- Integrated analysis of propagation and radio beam shape optimization

- Effects of frequency diversity on V-band sub-bands

6 General References and Related Publications

Other related mmWave channel sounder works published in industry forums:

- ETSI Industry Specification Group on Millimeter Wave Transmission
  https://www.etsi.org/committee/1426-mwt
- ETSI V-band propagation modeling
  https://www.etsi.org/images/files/ETSIWhitePapers/etsi_wp10_field_proven_experience_of_mwt_20150923.pdf
- ETSI V-band interference & SRD
  https://www.etsi.org/deliver/etsi_gr/mWT/001_099/010/01.01.01_60/gr_mWT010v010101p.pdf
- ETSI V-band street-level interference analysis
  https://www.etsi.org/deliver/etsi_gs/mWT/001_099/004/01.01.01_60/gs_mWT004v010101p.pdf
- An Experimental mmWave Channel Model for UAV-to-UAV Communications (Northeastern University)
  https://arxiv.org/abs/2007.11869
  Authors: Michele Polese, Lorenzo Bertizzolo, Leonardo Bonati, Abhimanyu Gosain, Tommaso Melodia